

**Prediction of Capillary Pressure for Arabian
Carbonate Reservoirs using Artificial Intelligence**

BY

Yasser Ridha BuSaleh

A Thesis Presented to the
DEANSHIP OF GRADUATE STUDIES

KING FAHD UNIVERSITY OF PETROLEUM & MINERALS

DHAHRAN, SAUDI ARABIA

1963 ١٣٨٣

In Partial Fulfillment of the
Requirements for the Degree of

MASTER OF SCIENCE

In

PETROLEUM ENGINEERING

December 2017

KING FAHD UNIVERSITY OF PETROLEUM & MINERALS
DHAHRAN 31261, SAUDI ARABIA

DEANSHIP OF GRADUATE STUDIES

This thesis, written by **Mr. Yasser Ridha BuSaleh** under the direction of his thesis advisor and approval by his thesis committee, has been presented to and accepted by the Dean of Graduate Studies, in partial fulfillment of the requirements for the degree of **MASTER OF SCIENCE IN PETROLEUM ENGINEERING**.

Thesis Committee



Dr. Abdulazeez Abdulraheem (Thesis Advisor)



Dr. Taha Okasha (Member)



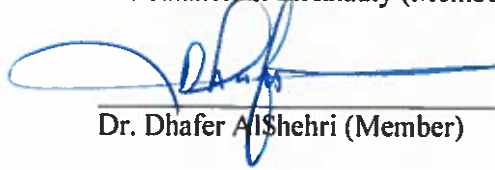
Dr. Md. Rafiul Hassan (Member)



Dr. Salaheldin ElKatatny (Member)



Dr. Dhafer AlShehri
(Department Chairman)



Dr. Dhafer AlShehri (Member)



Dr. Salam A. Zummo
(Dean of Graduate Studies)



Date

21/12/17

DEDICATION

To my parents who made me the man I am today.

*To my wife who supported me and provided all the
encouragement, dedication and patience.*

ACKNOWLEDGEMENT

I would first like to thank my thesis advisor Dr. Abdulazeez Abdulraheem. The door to Dr. Abdulazeez's office was always open whenever I ran into a trouble spot or had a question about my research or writing. He consistently allowed this paper to be my own work, but steered me in the right direction whenever he thought I needed it.

I would also like to thank the experts who were involved in the problem and the solution of this research project: Dr. Taha Okasha and Dr. Md. Rafiul Hassan. Without their passionate participation and input, this research project could not have been successfully conducted.

I would also like to extend my sincere gratitude to the rest of the thesis committee for providing support, guidance and technical advice throughout my thesis.

Table of Contents

ACKNOWLEDGEMENT	iv
Table of Contents	v
List of Figures	vii
List of Tables	xvii
Thesis Abstract.....	xviii
ملخص الرسالة	xx
CHAPTER 1	1
Introduction.....	1
CHAPTER 2	6
Literature review.....	6
2.1 Laboratory methods	6
2.2 Mathematical models	9
2.3 Artificial Intelligence approach	11
CHAPTER 3	14
Scope of the Problem and Approach to the Solution	14
3.1 Statement of the problem	14
3.2 Objective	14
3.3 Advantages.....	14
3.4 Approach.....	15
CHAPTER 4	19
Artificial Intelligence	19
Applied techniques.....	20
CHAPTER 5	26
Results and Discussion	26
5.1 Data acquisition	26
5.2 Data processing and filtering	26
5.3 Number of data points.....	27
5.4 Input parameters.....	27
5.5 Target parameter	28
5.6 Data statistics	28
5.7 Artificial Intelliengence Models	29
5.8 Statistical results	30
5.9 Graphical results	38
5.10 Nearest Neighbor Curve Prediction (NNCP).....	51

5.11 Data Classification	53
5.12 J-function Approach.....	55
5.13 Discussion of Results from NNCP and J-function approach.....	62
CHAPTER 6	111
Conclusions and Recommendations	111
6.1 Conclusions.....	111
6.2 Recommendations.....	111
References.....	113
APPENDIX-A.....	118
APPENDIX-B.....	123
B1. Artificial neural network	124
B2. Fuzzy logic	142
B3. Fuzzy logic type-2	148
B4. Support vector machine.....	151
B5. Functional Network.....	154

List of Figures

Figure 1: Capillary tube	2
Figure 2: Capillary pressure curve and saturation height column	3
Figure 3: Capillary pressure, water saturation, and permeability	4
Figure 4: A typical artificial neural network.....	20
Figure 5: Example of fuzzy logic.....	22
Figure 6: Example of fuzzy logic type 2.....	24
Figure 7: Example of dicision tree.....	24
Figure 8: An example of support vector machine.....	25
Figure 9: Different Modalities of Capillary Pressure	27
Figure 10: Standard Deviation Comparison of capillary pressure values.....	36
Figure 11: Mean Absolute Error Comparison of capillary pressure values.....	36
Figure 12: Root Mean Square Error Comparison of capillary pressure values.	37
Figure 13: Coefficient of Determination Comparison of capillary pressure values.	37
Figure 14: Predicted vs. measured values using ANN – trainlm 2-layer alogrithm (Training)....	38
Figure 15: Predicted vs. measured values using ANN – trainlm 2-layer algorithm (Testing).	39
Figure 16: A sample of uni-modal data using ANN - trainlm 2-layer algorithm in semi-log scale plot	39
Figure 17: A sample of uni-modal data using ANN - trainlm 2-layer algorithm in cartesian scale plot	40
Figure 18: Predicted vs. measured values using ANN – trainlm 2-layer algorithm (Training)....	41
Figure 19: Predicted vs. measured values using ANN – trainlm 2-layer algorithm (Testing).	41
Figure 20: A sample of bi-modal sata using ANN - trainlm 2-layer algorithm in log-log scale plot	42
Figure 21: A sample of bi-modal sata using ANN - trainlm 2-layer algorithm in cartesian scale plot	42
Figure 22: Predicted vs. measured values using ANN – trainlm 2-layer algorithm (Training)....	43
Figure 23: Predicted vs. measured values using ANN – trainlm 2-layer algorithm (Testing).	44
Figure 24: Predicted vs. measured values using Decision tree algorithm (Training).	45
Figure 25: Predicted vs. measured values using Decision tree algorithm (Testing).....	45
Figure 26: A sample of uni-modal sata using decision tree algorithm in log-log scale plot	46

Figure 27: A sample of uni-modal sata using decision tree algorithm in cartesian scale plot.....	46
Figure 28: Predicted vs. measured values using Decision tree algorithm (Training).....	47
Figure 29: Predicted vs. measured values using Decision tree algorithm (Testing).....	48
Figure 30: A sample of bi-modal sata using decision tree algorithm in log-log scale plot	48
Figure 31: A sample of bi-modal sata using decision tree algorithm in cartesian scale plot.....	49
Figure 32: Predicted vs. measured values using Decision tree alogrithm (Training).....	50
Figure 33: Predicted vs. measured values using Decision tree alogrithm (Testing).....	50
Figure 34. Capillary pressure curve prediction based on the nearest datapoint.....	52
Figure 35: Flow Zone Units for Uni-modal group.....	53
Figure 36: Flow Zone Units for Bi-modal group.....	54
Figure 37: J-function values for uni-modal class # 1 samples.....	56
Figure 38: J-function values for uni-modal class # 2 samples.....	57
Figure 39: J-function values for uni-modal class # 3 samples.....	57
Figure 40: J-function curves based on ranges of FZI for uni-modal data.....	58
Figure 41: J-function values for bi-modal class # 1 samples.....	59
Figure 42: J-function values for bi-modal class # 2 samples.....	59
Figure 43: J-function values for bi-modal class # 3 samples.....	60
Figure 44: J-function values for bi-modal class # 4 samples.....	60
Figure 45: J-function values for bi-modal class # 5 samples.....	61
Figure 46: J-function curves based on ranges of FZI for bi-modal data.....	61
Figure 47: Comparison of NNCP, the average of the closest three curves and J-function to predict the capillary pressure with the laboratory data for testing sample # 1 in class 1	62
Figure 48: Comparison of NNCP, the average of the closest three curves, and J-function to predict the capillary pressure with the laboratory data for testing sample # 2 in class 1	63
Figure 49: Comparison of NNCP, the average of the closest three curves, and J-function to predict the capillary pressure with the laboratory data for testing sample # 1 in class 2	64

Figure 50: Comparison of NNCP, the average of the closest three curves, and J-function to predict the capillary pressure with the laboratory data for testing sample # 2 in class 2 64

Figure 51: Comparison of NNCP, the average of the closest three curves, and J-function to predict the capillary pressure with the laboratory data for testing sample # 3 in class 2 65

Figure 52: Comparison of NNCP, the average of the closest three curves, and J-function to predict the capillary pressure with the laboratory data for testing sample # 4 in class 2 66

Figure 53: Comparison of NNCP, the average of the closest three curves, and J-function to predict the capillary pressure with the laboratory data for testing sample # 5 in class 2 67

Figure 54: Comparison of NNCP, the average of the closest three curves, and J-function to predict the capillary pressure with the laboratory data for testing sample # 6 in class 2 67

Figure 55: Comparison of NNCP, the average of the closest three curves, and J-function to predict the capillary pressure with the laboratory data for testing sample # 1 in class 3 69

Figure 56: Comparison of NNCP, the average of the closest three curves, and J-function to predict the capillary pressure with the laboratory data for testing sample # 2 in class 3 70

Figure 57: Comparison of NNCP, the average of the closest three curves, and J-function to predict the capillary pressure with the laboratory data for testing sample # 3 in class 3 71

Figure 58: Comparison of NNCP, the average of the closest three curves, and J-function to predict the capillary pressure with the laboratory data for testing sample # 4 in class 3 71

Figure 59: Comparison of NNCP, the average of the closest three curves, and J-function to predict the capillary pressure with the laboratory data for testing sample # 5 in class 3 72

Figure 60: Comparison of NNCP, the average of the closest three curves, and J-function to predict the capillary pressure with the laboratory data for testing sample # 6 in class 3	73
Figure 61: Comparison of NNCP, the average of the closest three curves, and J-function to predict the capillary pressure with the laboratory data for testing sample # 7 in class 3	74
Figure 62: Comparison of NNCP, the average of the closest three curves, and J-function to predict the capillary pressure with the laboratory data for testing sample # 8 in class 3	75
Figure 63: Comparison of NNCP, the average of the closest three curves, and J-function to predict the capillary pressure with the laboratory data for testing sample # 9 in class 3	76
Figure 64: Comparison of NNCP, the average of the closest three curves, and J-function to predict the capillary pressure with the laboratory data for testing sample # 10 in class 3.....	77
Figure 65: Comparison of NNCP, the average of the closest three curves to predict the capillary pressure compared to laboratory data for testing sample # 1 in class 1.....	78
Figure 66: Comparison of NNCP, the average of the closest three curves to predict the capillary pressure compared to laboratory data for testing sample # 2 in class 1.....	79
Figure 67: Comparison of NNCP, the average of the closest three curves to predict the capillary pressure compared to laboratory data for testing sample # 3 in class 1.....	80
Figure 68: Comparison of NNCP, the average of the closest three curves to predict the capillary pressure compared to laboratory data for testing sample # 4 in class 1.....	81
Figure 69: Comparison of NNCP, the average of the closest three curves to predict the capillary pressure compared to laboratory data for testing sample # 5 in class 1.....	82
Figure 70: Comparison of NNCP, the average of the closest three curves to predict the capillary pressure compared to laboratory data for testing sample # 1 in class 2.....	83
Figure 71: Comparison of NNCP, the average of the closest three curves to predict the capillary pressure compared to laboratory data for testing sample # 2 in class 2.....	84
Figure 72: Comparison of NNCP, the average of the closest three curves to predict the capillary pressure compared to laboratory data for testing sample # 3 in class 2.....	84

Figure 73: Comparison of NNCP, the average of the closest three curves to predict the capillary pressure compared to laboratory data for testing sample # 4 in class 2..... 85

Figure 74: Comparison of NNCP, the average of the closest three curves to predict the capillary pressure compared to laboratory data for testing sample # 5 in class 2..... 85

Figure 75: Comparison of NNCP, the average of the closest three curves to predict the capillary pressure compared to laboratory data for testing sample # 6 in class 2..... 86

Figure 76: Comparison of NNCP, the average of the closest three curves to predict the capillary pressure compared to laboratory data for testing sample # 7 in class 2..... 87

Figure 77: Comparison of NNCP, the average of the closest three curves to predict the capillary pressure compared to laboratory data for testing sample # 8 in class 2..... 87

Figure 78: Comparison of NNCP, the average of the closest three curves to predict the capillary pressure compared to laboratory data for testing sample # 9 in class 2..... 88

Figure 79: Comparison of NNCP, the average of the closest three curves to predict the capillary pressure compared to laboratory data for testing sample # 1 in class 3..... 89

Figure 80: Comparison of NNCP, the average of the closest three curves to predict the capillary pressure compared to laboratory data for testing sample # 2 in class 3..... 90

Figure 81: Comparison of NNCP, the average of the closest three curves to predict the capillary pressure compared to laboratory data for testing sample # 3 in class 3..... 91

Figure 82: Comparison of NNCP, the average of the closest three curves to predict the capillary pressure compared to laboratory data for testing sample # 4 in class 3..... 91

Figure 83: Comparison of NNCP, the average of the closest three curves to predict the capillary pressure compared to laboratory data for testing sample # 5 in class 3..... 92

Figure 84: Comparison of NNCP, the average of the closest three curves to predict the capillary pressure compared to laboratory data for testing sample # 6 in class 3..... 93

Figure 85: Comparison of NNCP, the average of the closest three curves to predict the capillary pressure compared to laboratory data for testing sample # 7 in class 3..... 93

Figure 86: Comparison of NNCP, the average of the closest three curves to predict the capillary pressure compared to laboratory data for testing sample # 8 in class 3..... 94

Figure 87: Comparison of NNCP, the average of the closest three curves to predict the capillary pressure compared to laboratory data for testing sample # 9 in class 3..... 95

Figure 88: Comparison of NNCP, the average of the closest three curves to predict the capillary pressure compared to laboratory data for testing sample # 10 in class 3..... 95

Figure 89: Comparison of NNCP, the average of the closest three curves to predict the capillary pressure compared to laboratory data for testing sample # 11 in class 3..... 96

Figure 90: Comparison of NNCP, the average of the closest three curves to predict the capillary pressure compared to laboratory data for testing sample # 1 in class 4..... 97

Figure 91: Comparison of NNCP, the average of the closest three curves to predict the capillary pressure compared to laboratory data for testing sample # 2 in class 4..... 98

Figure 92: Comparison of NNCP, the average of the closest three curves to predict the capillary pressure compared to laboratory data for testing sample # 3 in class 4..... 98

Figure 93: Comparison of NNCP, the average of the closest three curves to predict the capillary pressure compared to laboratory data for testing sample # 4 in class 4..... 99

Figure 94: Comparison of NNCP, the average of the closest three curves to predict the capillary pressure compared to laboratory data for testing sample # 5 in class 4..... 99

Figure 95: Comparison of NNCP, the average of the closest three curves to predict the capillary pressure compared to laboratory data for testing sample # 6 in class 4..... 100

Figure 96: Comparison of NNCP, the average of the closest three curves to predict the capillary pressure compared to laboratory data for testing sample # 7 in class 4..... 101

Figure 97: Comparison of NNCP, the average of the closest three curves to predict the capillary pressure compared to laboratory data for testing sample # 8 in class 4..... 101

Figure 98: Comparison of NNCP, the average of the closest three curves to predict the capillary pressure compared to laboratory data for testing sample # 1 in class 5..... 103

Figure 99: Comparison of NNCP, the average of the closest three curves to predict the capillary pressure compared to laboratory data for testing sample # 2 in class 5..... 104

Figure 100: Comparison of NNCP, the average of the closest three curves to predict the capillary pressure compared to laboratory data for testing sample # 3 in class 5..... 104

Figure 101: Comparison of NNCP, the average of the closest three curves to predict the capillary pressure compared to laboratory data for testing sample # 4 in class 5..... 105

Figure 102: Comparison of NNCP, the average of the closest three curves to predict the capillary pressure compared to laboratory data for testing sample # 5 in class 5..... 106

Figure 103: Comparison of NNCP, the average of the closest three curves to predict the capillary pressure compared to laboratory data for testing sample # 6 in class 5.....	106
Figure 104: Comparison of NNCP, the average of the closest three curves to predict the capillary pressure compared to laboratory data for testing sample # 7 in class 5.....	107
Figure 105: Comparison of NNCP, the average of the closest three curves to predict the capillary pressure compared to laboratory data for testing sample # 8 in class 5.....	108
Figure 106: Comparison of NNCP, the average of the closest three curves to predict the capillary pressure compared to laboratory data for testing sample # 9 in class 5.....	108
Figure 107: Comparison of NNCP, the average of the closest three curves to predict the capillary pressure compared to laboratory data for testing sample # 10 in class 5.....	109
Figure 108: Comparison of NNCP, the average of the closest three curves to predict the capillary pressure compared to laboratory data for testing sample # 11 in class 5.....	110
Figure 109: Predicted vs. measured values using ANN – trainb algorithm (Training).....	124
Figure 110. Predicted vs. measured values using ANN – trainb algorithm (Testing).....	125
Figure 111. Predicted vs. measured values using ANN – trainbfg algorithm (Training).....	125
Figure 112. Predicted vs. measured values using ANN – trainbfg algorithm (Testing).....	126
Figure 113. Predicted vs. measured values using ANN – traingd algorithm (Training).....	126
Figure 114. Predicted vs. measured values using ANN – traingd algorithm (Testing).....	127
Figure 115. Predicted vs. measured values using ANN – traingdx algorithm (Training).....	127
Figure 116. Predicted vs. measured values using ANN – traingdx algorithm (Testing).....	128
Figure 117. Predicted vs. measured values using ANN – trainlm algorithm (Training).....	128
Figure 118. Predicted vs. measured values using ANN – trainlm algorithm (Testing).....	129
Figure 119. Predicted vs. measured values using ANN – trainoss algorithm (Training).....	129
Figure 120. Predicted vs. measured values using ANN – trainoss algorithm (Testing).....	130
Figure 121. Predicted vs. measured values using ANN – trainb algorithm (Training).....	130
Figure 122. Predicted vs. measured values using ANN – trainb algorithm (Testing).....	130
Figure 123. Predicted vs. measured values using ANN – trainbfg algorithm (Training).....	131
Figure 124. Predicted vs. measured values using ANN – trainbfg algorithm (Testing).....	131
Figure 125. Predicted vs. measured values using ANN – traingd algorithm (Training).....	132
Figure 126. Predicted vs. measured values using ANN – traingd algorithm (Testing).....	132
Figure 127. Predicted vs. measured values using ANN – traingdx algorithm (Training).....	133

Figure 128. Predicted vs. measured values using ANN – traingdx alogrithm (Testing).	133
Figure 129. Predicted vs. measured values using ANN – trainlm alogrithm (Training).	134
Figure 130. Predicted vs. measured values using ANN – trainlm alogrithm (Testing).	134
Figure 131. Predicted vs. measured values using ANN – trainoss alogrithm (Training).	135
Figure 132. Predicted vs. measured values using ANN – trainoss alogrithm (Testing).	135
Figure 133. Predicted vs. measured values using ANN – trainb alogrithm (Training).	136
Figure 134. Predicted vs. measured values using ANN – trainb alogrithm (Testing).	136
Figure 135. Predicted vs. measured values using ANN – trainbfg alogrithm (Training).	137
Figure 136. Predicted vs. measured values using ANN – trainbfg alogrithm (Testing).	137
Figure 137. Predicted vs. measured values using ANN – traingd alogrithm (Training).	138
Figure 138. Predicted vs. measured values using ANN – traingd alogrithm (Testing).	138
Figure 139. Predicted vs. measured values using ANN – traingdx alogrithm (Training).	139
Figure 140. Predicted vs. measured values using ANN – traingdx alogrithm (Testing).	139
Figure 141. Predicted vs. measured values using ANN – trainlm alogrithm (Training).	140
Figure 142. Predicted vs. measured values using ANN – trainlm alogrithm (Testing).	140
Figure 143. Predicted vs. measured values using ANN – trainoss alogrithm (Training).	141
Figure 144. Predicted vs. measured values using ANN – trainoss alogrithm (Testing).	141
Figure 145. Predicted vs. measured values using Fuzzy Logic – Grid Partitioning alogrithm (Training).	142
Figure 146. Predicted vs. measured values using Fuzzy Logic – Grid Partitioning alogrithm (Testing).	142
Figure 147. Predicted vs. measured values using Fuzzy Logic – Cluster Radius alogrithm (Training).	143
Figure 148. Predicted vs. measured values using Fuzzy Logic – Cluster Radius alogrithm (Testing).	143
Figure 149.1 Predicted vs. measured values using Fuzzy Logic – Grid Partitioning alogrithm (Training).	144
Figure 150. Predicted vs. measured values using Fuzzy Logic – Grid Partitioning alogrithm (Testing).	144
Figure 151. Predicted vs. measured values using Fuzzy Logic – Cluster Radius alogrithm (Training).	145

Figure 152. Predicted vs. measured values using Fuzzy Logic – Cluster Radius algorithm (Testing).....	145
Figure 153: Predicted vs. measured values using Fuzzy Logic – Grid Partitioning algorithm (Training).....	146
Figure 154. Predicted vs. measured values using Fuzzy Logic – Grid Partitioning algorithm (Testing).....	146
Figure 155. Predicted vs. measured values using Fuzzy Logic – Cluster Radius algorithm (Training).....	147
Figure 156. Predicted vs. measured values using Fuzzy Logic – Cluster Radius algorithm (Testing).....	147
Figure 157. Predicted vs. measured values using Fuzzy Logic type-2 algorithm (Training)....	148
Figure 158. Predicted vs. measured values using Fuzzy Logic type-2 algorithm (Testing).....	148
Figure 159. Predicted vs. measured values using Fuzzy Logic type-2 algorithm (Training)....	149
Figure 160. Predicted vs. measured values using Fuzzy Logic type-2 algorithm (Testing).....	149
Figure 161. Predicted vs. measured values using Fuzzy Logic type-2 algorithm (Training)....	150
Figure 162. Predicted vs. measured values using Fuzzy Logic type-2 algorithm (Testing).....	150
Figure 163. Predicted vs. measured values using support vector machine algorithm (Training).	151
Figure 164. Predicted vs. measured values using support vector machine algorithm (Testing).	151
Figure 165. Predicted vs. measured values using support vector machine algorithm (Training).	152
Figure 166. Predicted vs. measured values using support vector machine algorithm (Testing).	152
Figure 167. Predicted vs. measured values using support vector machine algorithm (Training).	153
Figure 168. Predicted vs. measured values using support vector machine algorithm (Testing).	153
Figure 169. Predicted vs. measured values using functional network algorithm (Training)....	154
Figure 170. Predicted vs. measured values using functional network algorithm (Testing).....	154
Figure 171. Predicted vs. measured values using functional network algorithm (Training)....	155

Figure 172. Predicted vs. measured values using functional network algorithm (Testing)..... 155
Figure 173. Predicted vs. measured values using functional network algorithm (Training)..... 156
Figure 174. Predicted vs. measured values using functional network algorithm (Testing)..... 156

List of Tables

Table 1: Error data in predictions for Ali Abedini’s ANN model.	11
Table 2: uni-modal statistics	28
Table 3: bi-modal statistics	28
Table 4: combined modals statistics	29
Table 5: uni-modal statistical analysis	30
Table 6: bi-modal statistical analysis	32
Table 7: combined modals statistical analysis	34
Table 8: Number of core samples in each flow zone.....	54
Table 9: FZI range of each J-function group for uni-modal data	55
Table 10: FZI range of each J-function group for bi-modal data	55
Table 11: Average error of NNCP and J-function methods versus laboratory data for class 163	
Table 12: Average error of NNCP and J-function methods versus laboratory data for class 268	
Table 13: Average error of NNCP and J-function methods versus laboratory data for class 377	
Table 14: Average error of NNCP method versus laboratory data for class 1	82
Table 15: Average error of NNCP method versus laboratory data for class 2	88
Table 16: Average error of NNCP method versus laboratory data for class 3	96
Table 17: Average error of NNCP method versus laboratory data for class 4	102
Table 18: Average error of NNCP method versus laboratory data for class 5	110

Thesis Abstract

NAME OF STUDENT : Yasser Ridha BuSaleh
TITLE : Prediction of Capillary Pressure for Arabian Oil Carbonate Reservoirs using Artificial Intelligence
MAJOR FIELD : Petroleum Engineering
DATE OF DEGREE : December 2017

Capillary pressure data is one of the most critical parameters used in reservoir characterization and initialization stage of simulation models. Many reservoirs do not have enough data for a comprehensive evaluation. This method utilizes a small core dataset to derive models that can be used to predict capillary pressure in reservoirs that lack these measurements.

Several types of Artificial Intelligence (AI) techniques were utilized to predict capillary pressure in carbonate oil reservoirs with complex morphologies. To develop AI models that predict capillary pressure, a training dataset is used in this study that comprises of mercury injection drainage capillary pressure data. The training data included a set of 70% of 202 core samples that included porosity, permeability, and grain density measurements from conventional core analysis tests. Models were developed using this data to predict capillary pressure vs. saturation curves. Using an error estimation routine, a comparison between the predicted results and laboratory measurements was plotted and tabulated to show the validity of this analysis. The model was tested against a new dataset, the remaining 30% of the 202 core samples, that was not included in the training phase. This process was performed on uni-modal, bi-modal, and combined modal datasets. The analysis of the AI models used in this study showed that AI has promising potential to solve this complicated problem.

The proposed approach has three advantages: (i) it saves time and money; (ii) it does not require core samples for new spots in the same area; and (iii) it uses the available results to their maximum potential from previously destroyed core samples. While previous work did not address the prevalent bimodality of the carbonate rock, this study addresses specifically the AI application to the different rock modals using Thomeer methodology.

ملخص الرسالة

اسم الطالب	:	ياسر رضا بوصالح
عنوان الرسالة	:	التنبؤ بالضغط الاسموزي للصخور الكربونية العربية باستخدام الذكاء الاصطناعي
التخصص	:	هندسة البترول
تاريخ التخرج	:	ربيع أول 1439 هـ

ضغط الشعيرات الأسموزية هي واحدة من أهم المعالم المستخدمة في توصيف المكامن ومرحلة التهيئة من نماذج المحاكاة. في السابق، لم يكن لدينا بيانات كافية لإجراء تقييم شامل للعديد من الخزانات النفطية.

استخدمت في هذه الدراسة عدة أنواع من تقنيات الذكاء الاصطناعي للتنبؤ عن ضغط الشعيرات الأسموزية في مكامن النفط الكربونية المتعددة الأشكال والمعقدة التضاريس. لتطوير نماذج التنبؤ على الضغط الشعري الأسموزي، يتم استخدام مجموعة تدريب للبيانات التي تضم بيانات اختبار حقن الزئبق في العينة الصخرية لحساب ضغط الشعيرات الأسموزية في المعمل. في هذه الدراسة، تضمنت بيانات التدريب مجموعة من 70% من 202 عينة شملت قياسات المسامية والنفاذية وكثافة الحبيبات الترايبية من اختبارات التحليل الأساسية التقليدية. وقد وضعت نماذج استخدام هذه البيانات للتنبؤ عن ضغط الشعيرات الأسموزية باستخدام طريقة تقليص الخطأ، تم استخدام المقارنة بين النتائج المتوقعة والقياسات العملية لإظهار صحة هذا التحليل من خلال الجداول والرسوم البيانية. تم اختبار النموذج على مجموعة بيانات جديدة، 30% المتبقية من 202 عينة، التي لم تكن مدرجة في مرحلة التدريب. تم تنفيذ هذه العملية على المنحنيات الأحادية، المنحنيات الثنائية، والجمع بين مجموعات جميع المنحنيات في سجل البيانات. تحليل نماذج تقنيات الذكاء الاصطناعي للتنبؤ عن ضغط الشعيرات الأسموزية في مكامن النفط الكربونية المستخدمة في هذه الدراسة، أظهرت أن لديها إمكانات واعدة لحل هذه المسألة المعقدة. ومع ذلك، لا يزال هناك مجال لتطوير طرق أخرى لحساب الضغط الشعري الأسموزي.

هذه الطريقة تستخدم البيانات الأساسية من مجموعة صغيرة لاستخلاص النماذج التي يمكن استخدامها للتنبؤ عن ضغط الشعيرات الأسموزية في الخزانات النفطية التي تفتقر إلى هذه القياسات. هذا النهج المقترح لديه ثلاث مزايا: يوفر الوقت والمال، لا تتطلب عينات للبع الجديدة في نفس المنطقة، ويستخدم النتائج المتوفرة إلى أقصى إمكاناتها من عينات دُمرت سابقاً. بينما الأعمال السابقة

لم تتناول تعدد المنحنيات السائدة في الصخور الكربونية من خلال استخدام مؤشر تدفق المنطقة ومؤشر جودة الصخور، فإن هذه الدراسة أخذت في عين الاعتبار تعدد المنحنيات السائدة من خلال منهج "ثمير".

درجة ماجستير العلوم
جامعة الملك فهد للبترول والمعادن
الظهران – المملكة العربية السعودية
التاريخ: ربيع أول 1439 هـ

CHAPTER 1

Introduction

When two immiscible different fluids in a tube contact each other, a curvature shape will occur on their touching surfaces due to the pressure difference between them because of their different interfacial tensions. This pressure difference is called **Capillary Pressure**.

Capillary Pressure is one of the most important properties of reservoir rocks due to its strong effect in controlling reservoir fluids distribution when two or more immiscible fluids co-exist on pore spaces. Late 1950's, reservoir simulation engineers started incorporating the capillary pressure curves into their models to account for this effect which makes a clear difference in the results. Misuse of capillary pressure in reservoir simulation models can result in wrong water cut ratios and hydrocarbon recovery. As a result, capital investments might be jeopardized.

Initially when oil reservoirs started forming, water was filling all reservoir pore spaces, and then oil (non-wetting phase) started to migrate from source rock into the reservoir creating a process called **drainage**. During oil production, water (wetting phase) comes back again to fill oil-filled pore spaces creating a process called **imbibition**.

Capillary pressure curves can be obtained from core samples using one of several laboratory measurements such as mercury injection, centrifuge, and porous plate methods. There are also some mathematical models to normalize and evaluate capillary pressure such as Leverett J-function, Thomeer model, and Brooks and Corey model.

Regardless of which method is used to obtain capillary pressure, the basic physical equation given as:

$$P_c = \frac{2\sigma \cos \theta}{r_c} \dots\dots\dots(1)$$

which express the relationship between capillary pressure (P_c), pore throat radius (r_c), interfacial tension between fluids (σ), and fluid contact angle with the surface of the tube (θ). To calculate it for two fluids in contact, this equation is used:

$$P_c = P_{f1} - P_{f2} = (\rho_{f1} - \rho_{f2})gh \dots\dots\dots(2)$$

To use the above equation (2) with field units:

$$P_c = \left(\frac{h}{144}\right) \Delta\rho \dots\dots\dots(3)$$

Where:

- ρ = fluid density, lb/ft³
- g = gravity acceleration, ft/s²
- h = hight of the heavier fluid in the tube, ft

The details of the above parameters are illustrated in figure (1).

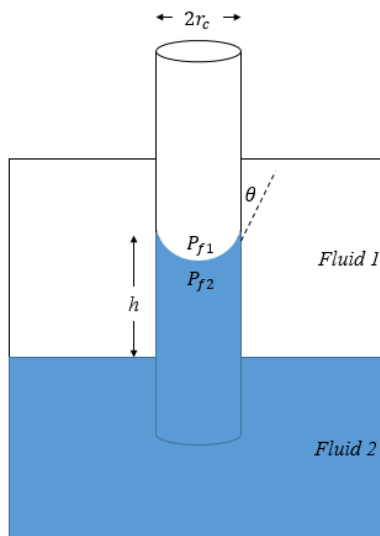


Figure 1: Capillary tube

A typical capillary pressure curve vs. saturation is shown in figure (2). This figure shows the drainage and imbibition curves. It also shows the end point of the drainage curve which is the connate water saturation (S_{wc}) which is the water saturation in the pore spaces that could not be drained by oil during the drainage process. Another important point is the end point of the imbibition curve which is the irreducible oil saturation (S_{oi}) which is the minimum oil saturation in the pore spaces that could not be flushed by water during the imbibition process.

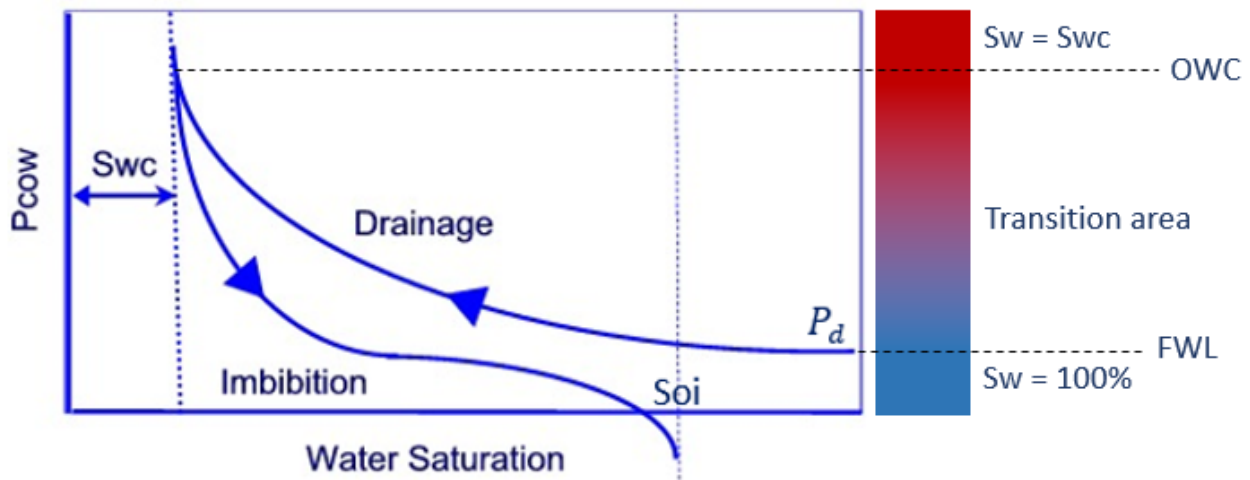


Figure 2: Capillary pressure curve and saturation height column

Another important parameter needs to be mentioned here is the displacement pressure (P_d). This is the first point of the drainage curve at which water saturation is less than 100%. This is the minimum required pressure for the oil to drain the water.

The capillary pressure can be used to calculate the water height in the reservoir at any point (Figure 2). The point at which water saturation is 100% is called the **Free Water Level (FWL)** and at which the water saturation is equal to the connate water saturation is the **Oil-Water Contact** level (OWC). The area in between is a transition zone where a mix of oil and water can be found.

Comparison between different capillary pressure curves gives an idea about the reservoir rock properties. A major property is the permeability which therefore provides an information about the thickness of the transition zone. As figure (3) illustrates, the higher the curve, the less the permeability and the lower the curve, the higher the permeability.

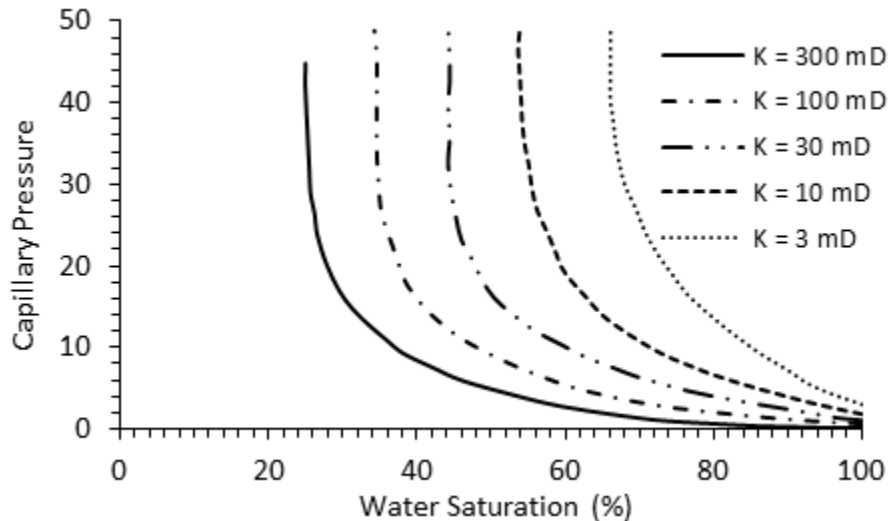


Figure 3: Capillary pressure, water saturation, and permeability

Another comparison can be made is between different oil APIs. The higher the API, the lower the density. The lower the density, the higher the density difference between oil and water. The higher the density difference, the lower the transition zone and vice versa.

Utilization of Artificial Intelligence (AI) techniques to solve large scale problems has been used in several industries such as medical, mechanical and petroleum engineering. It has gained a wide acceptance as it showed very good results that could not be easily achieved by classical physics or engineering concepts. This study focuses on developing new models for several AI techniques to predict the capillary pressure. These models are:

- Artificial neural network (ANN)
- Fuzzy logic (FL)
- Fuzzy logic type-2 (FL-2)
- Decision tree (DT)
- Support vector machine (SVM)
- Functional network (FN)
- Nearest Neighbor Curve Prediction (NNCP)

This thesis is comprised of six chapters. Chapter 2 describes the approaches of capillary pressure determination and evaluation and the use of Artificial Intelligence in the petroleum industry. Scope of the problem and the solution are presented in Chapter 3. In Chapter 4, the basic concepts of the AI techniques used in this study are described. The results and discussion of analysis are discussed in detail in chapter 5, and finally, in Chapter 6, the conclusions and recommendations are stated.

CHAPTER 2

Literature review

Due to the importance of capillary pressure in reservoir engineering studies, several attempts were made to calculate it using laboratory methods and mathematical models. Below is a brief of the commonly used laboratory methods and mathematical models in addition to the review of a paper discussing applying Artificial Intelligence in the field of capillary pressure.

2.1 Laboratory methods

Mercury injection method

In this method, rock samples must be cleaned and dried before placing it in an evacuated chamber (Dr. Paul Glover Notes). Two tests can be carried out here:

- Pressure-controlled Porosimetry: mercury is injected at several pressure increments and then cumulative mercury volumes are measured.
- Volume-controlled Porosimetry: mercury is introduced at fixed volumetric rates and then pressures are recorded. This procedure is preferred because it gives more information about pore structure (Pedro et. al. 1994).

The following basic formula shows the relationship between capillary pressure, contact angle, interfacial tension and pore throat radius. This formula is the basis of this method and is also used to convert between different fluid systems.

$$P_c = \frac{2\sigma \cos \theta}{r_c} \dots\dots\dots(4)$$

P_c = capillary pressure measured, psi.

σ = Interfacial tension, dyne/cm.

θ = contact angle, degrees.

r_c = radius of pore throats, cm.

To convert from air-mercury to brine-hydrocarbon, the following conversion is used.

$$P_{c(\text{brine-hydrocarbon})} = P_{c(\text{air-mercury})} \frac{\sigma_{(\text{brine-hydrocarbon})} \cos \theta_{(\text{brine-hydrocarbon})}}{\sigma_{(\text{air-mercury})} \cos \theta_{(\text{air-mercury})}} \dots\dots\dots(5)$$

$P_{c(\text{brine-hydrocarbon})}$ = capillary pressure in the brine-hydrocarbon system of the reservoir, psi.

$P_{c(\text{air-mercury})}$ = capillary pressure of the air-mercury system, psi.

$\sigma_{(\text{brine-hydrocarbon})}$ = interfacial tension of brine-hydrocarbon, dyne/cm.

$\sigma_{(\text{air-mercury})}$ = interfacial tension of air-mercury, dyne/cm.

$\theta_{(\text{brine-hydrocarbon})}$ = contact angle of brine-hydrocarbon-solid, degrees.

$\theta_{(\text{air-mercury})}$ = contact angle of air-mercury-solid, degree.

Although this method is commonly used, there are some limitations and disadvantages:

1. The tested sample can't be used again in any test because it gets destructed.
2. Low implied connate water saturation can occur due to the collapse coating minerals covering grains surfaces and the fact that the core sample has to be dried before use.
3. Mercury vapor is toxic which requires special safety precautions.
4. It takes time and money to make this test.
5. Any fault with the test can result in losing the money, time, results and the sample itself.

Centrifuge method

A brine-saturated sample is placed inside a holder in the centrifuge machine where it is surrounded by lighter fluid (oil). When the centrifuge machine is started with a low revolution per minute (RPM), the brine is expelled gradually into a measuring tube. Recorded RPMs and water amounts are converted to drainage capillary pressure versus saturation. The following equation is used to calculate P_c from RPM (Dr. Paul Glover Notes).

$$P_c = 7.9 \times 10^{-8} \text{ RPM}^2 (\rho_1 - \rho_2)(r_b^2 - r_t^2) \dots\dots\dots(6)$$

P_c = capillary pressure measured, psi.

RPM = number of revolutions per minute.

ρ_1 and ρ_2 = densities of the phases used in the experiment, g/cm³.

r_b and r_t = bottom (b) and top (t) radii of the rotation of the core, respectively, cm.

7.9×10^{-8} = conversion factor.

The main disadvantage of this method is that at low pressures, overstated saturation gradient will occur due to applied capillary pressure gradient.

Porous plate method

The sample in this method should be fully saturated with brine. This sample is placed on a porous desk, with a special membrane in between, that has uniform small pores with entry pressure greater than the maximum capillary pressure of the sample. During the drainage test, the pressure of the displacing fluid, e.g. oil, is increased in small steps. The volume of the brine getting out of the sample is monitored and measured during each step until each step reaches equilibrium. Then produced brine and pressure steps are used to draw the drainage capillary pressure.

The main advantages of this method that overcome the limitations of the mercury injection method are:

1. The ability to mimic reservoir fluids.
2. The ability to conduct the test on sleeved cores.

On the other hand, the only limitation of this method is that obtaining the highest capillary pressure depends on the maximum entry pressure of the membrane.

2.2 Mathematical models

Leverett J-function model

Leverett and his coworkers (1940) developed the following equation after evaluating gas/water capillary pressure data for unconsolidated sands.

$$j(S_w) = \frac{P_{c_{gw}}}{\sigma_{gw}} \sqrt{\frac{k}{\phi}} \dots\dots\dots(7)$$

$j(S_w)$ = Leverett J-function, dimensionless.

S_w = saturation increments, fraction.

$P_{c_{gw}}$ = capillary pressure between gas and water, psi.

σ_{gw} = surface tension between gas (air in this case) and water, dyne/cm.

ϕ = porosity, in fraction.

k = permeability, mD.

This dimensionless model covers for drainage and imbibition phenomena and is called the J-function. This model serves well in developing a common curve of P_c , however it has two limitations when providing more details:

1. The value of the permeability depends on the direction of choice, either k_x or k_y which are different in their values. Thus, P_c value will be different for each direction.
2. This model does not account for rock type difference. Therefore, classification of rock samples has to be done prior to developing P_c .

Thomeer model

Thomeer (1960) developed the following model which depends on the bulk mercury saturation, threshold pressure, displacement pressure and pore geometric factor (G). Bulk mercury saturation is more appropriate for irregular shape samples.

$$\frac{(V_b)_{P_c}}{(V_b)_{P_\infty}} = e^{-G/\left(\log\left(\frac{P_c}{P_d}\right)\right)} \dots\dots\dots(8)$$

where

$(V_b)_{P_c}$ = fractional bulk volume occupied by mercury at P_c .

$(V_b)_{P_\infty}$ = fractional bulk volume occupied at infinite pressure.

G = pore geometric factor.

P_c = capillary pressure, psi.

P_d = extrapolated displacement pressure, psi.

Brooks and Corey model

Brooks and Corey (1964) suggested that the residual oil saturation is a major factor that affects the capillary pressure. The saturatoin has a range from 8 to 40%. Pore size distribution and threshold pressure also contribute to the magnitude of capillary pressure.

$$P_c = P_{ct} \left(\frac{1-S_{or}}{S_o-S_{or}}\right)^{1/\lambda} \dots\dots\dots(9)$$

where

P_c = capillary pressure, psi.

P_{ct} = threshold (entry) pressure, psi.

S_{or} = residual oil saturation in fraction.

S_o = oil saturation in fraction.

λ = pore size distribution.

This model has the advantage of accounting for the difference in threshold pressure coefficients in different porous media which captures the barrier effect.

2.3 Artificial Intelligence approach

Artificial Intelligence (AI) has proved to be highly efficient in solving different petroleum engineering problems. However, limited number of papers were published discussing the use of AI in prediction of capillary pressure. Here is a review of a few papers that have dealt with the use of AI to predict capillary pressure data.

Ali Abedini et. al. (2013) used data of 37 core samples from a Middle Eastern oil reservoir including porosity (ϕ), permeability (k), normalized porosity (ϕ_z), rock quality index (RQI) and flow zone indicator (FZI) to predict the capillary pressure of each saturation point. Capillary pressure curves of all 37 core samples were drawn and classified by different rock index values. Two Artificial Neural Network (ANN) models were developed using feed-forward back-propagation method with one hidden layer. The first model predicts the rock index and the second one predicts the capillary pressure by inclusion of the rock index and water saturation as inputs into the second model. Data of 16 core samples were used in the training phase, 8 in the validation phase and 13 in the testing phase. The statistical results of the second model are shown in the table below.

Table 1: Error data in predictions for Ali Abedini’s ANN model.

	Mean square Error	Average relative error	Average absolute relative error	Standard deviation
Training	0.12	-0.21	0.10	0.11
Validation	0.11	-0.13	0.18	0.16
Testing	0.16	-0.10	0.15	0.12

The limitation in this study is that the author used cores from different rock types which makes it

difficult for the ANN model to be trained especially that the number of samples is too low. In addition, the publication does not contain plots of predicted vs. measured capillary pressure; therefore, their work is not described properly and can not be evaluated.

Hasan Nooruddin et. al. (2013) used a dataset of more than 200 core samples collected from mercury injection tests in addition to their corresponding air porosities and uncorrected air permeabilities. The data used from the mercury injection test were: porosity, displacement pressure, Purcell integration, Swanson, Winland, Dastidar and Pittman parameters. In the feed-forward neural network model to predict permeability from mercury injection capillary pressure data, they used 70% of the data for the training phase, 15% for the validation phase and 15% for the testing phase. Comparing the output against the mathematical models of Purcell, Winland, Swanson, Pittman and Dastidar et. al., they found that the absolute relative error (ARE) was 0.93% using AI while for Winland, the ARE was 31.5%. Similar observation was noticed when other error measurements were used such as average absolute relative error (AARE), root mean square (R^2), standard deviation (SD), and relative mean square error (RMSE).

They also discussed the use of Thomeer parameters, air porosity and grain density to predict corrected air permeability using AI (2014). Thomeer parameters were shape factor, permeability, capillary pressure, entry pressure, percent bulk volume of macro-pores, percent bulk volume occupied by mercury, and percent bulk volume occupied by mercury at infinite capillary pressure. 80% of the data was used for training and 20% was used for validation and testing. The comparison was between actual permeability and predicted permeability using different AI techniques, namely; functional network (FN), support vector machine (SVR), feed-forward neural network (FFNN), generalized regression neural network (GRNN), radial basis function network (RBFN) and adaptive network fuzzy inference system (ANFIS). The best AI model was FFNN based on

Least Average Relative Error (LARE), Absolute Average Relative Error (AARE), Standard Deviation (SD) and coefficient of Determination (R^2).

CHAPTER 3

Scope of the Problem and Approach to the Solution

3.1 Statement of the problem

In a typical laboratory test, expensive rock samples extracted from reservoirs have to be destroyed after completion of capillary pressure test by mercury injection method. In addition, the cost of rock sample extraction from the well during drilling operation, cost of laboratory test including labor and laboratory machines, and time spent on the preparation for the test, the test itself and the analysis of the outcome to obtain the results makes the whole process very expensive. Therefore, the need for an economical and quick tool to provide such an essential information for new spots/cores across the reservoir has been increasing especially that important impromptu decisions are highly expected be made.

3.2 Objective

The objective of this study is to develop a model using artificial intelligence to predict drainage capillary pressure for Arabian carbonate reservoirs from conventional core analysis data. The conventional core analysis test is done fast and provides essential information about the core sample. This study covers a wide range of parameters that directly affect capillary pressure such as porosity, permeability, grain density, and wetting phase saturation. It will also address the identification of rock modality i.e. uni-modal and bi-modal, identify rock types based on flow units methods, and then the prediction of capillary pressure curves of each rock type.

3.3 Advantages

Successful implementation of this study will result in the following advantages:

1. Saving time and money of coring, transportation, testing, ...etc.

2. Preservation of original core samples so it does not need to be destroyed. This makes it available for future studies.
3. Less error than mathematical models which until now are not able to directly obtain capillary pressure curves.

3.4 Approach

The following approach were used to achieve the objective of the study:

1. Collect mercury injection capillary pressure data for carbonate core samples of Arabian carbonate reservoirs. More than one sample was collected from the same well at different depths. The benefit of this is the samples are assured to be distinct from each other and the whole dataset covers a wide range of values for the different parameters.
2. Quality-check all collected data and remove outliers. It is important to have a wide range of values for all parameters to cover a wide range of the capillary pressures and rock sample. However, curves that seem to be a straight line that do not fall under uni-modal or bi-modal should be eliminated for this study. In addition, core samples that contain fractures should also be eliminated from this study.

All data of each parameter should have the same unit. In other words,

- a. All saturation values and porosity values should be in fraction not in percentage.
- b. All permeability values should be in millidarcy not in Darcy.
- c. All grain density values should be in gm/cc.
- d. Similarly, all capillary pressure values should be in psi.

This is to make sure that interpreted data is not used wrongly.

Another quality check is making sure that only drainage capillary pressure values are used and imbibition values are not included in this study.

Finally, it is very important to make sure that each value of saturation corresponds to one value of capillary pressure. In other words, since MS Excel rounds the fraction values to the nearest double digit or triple digit value, it is important to omit repeated values of saturation that correspond to multiple capillary pressure values. Otherwise, the results of the artificial intelligence models are not going to be promising.

3. Classify the data into different modalities. Capillary pressure curves should either uni-modal or bi-modal behavior. Each core sample should fall either under uni-modal class or bi-modal class. This is essential to make sure each class with similar behavior is studied separately.
4. Classify the data into different rock types based on the unit flow zone. This is done based on the Rock Quality Index (RQI) and Flow Zone Indicator (FZI) method. This is done using the following steps:

- a. Calculate the normalized porosity, φ_z , using equation (10)

$$\varphi_z = \frac{\varphi}{1-\varphi} \dots\dots\dots(10)$$

- b. Calculate the Rock Quality Index, RQI , using equation (11)

$$RQI = \sqrt{\frac{k}{\varphi}} \dots\dots\dots(11)$$

- c. Calculate the Flow Zone indicator, FZI , using equation (12)

$$FZI = \frac{RQI}{\varphi_z} \dots\dots\dots(12)$$

- d. Plot φ_z vs. RQI on a log-log scale. Then draw unit lines with slope of (1) to cover the most points possible. Draw as many lines as needed. Each line represents a flow unit. Points falling on these lines are grouped and called “core samples of that flow unit”

5. Based on the above classification techniques, different sets are going to be generated to make sure that core samples with similar behavior are studied together.
6. 70% of the data in each set is going to be used for training and 30% is going to be used for testing while applying different artificial intelligence methods.
7. Evaluate the best artificial intelligence method graphically and statistically. In order to identify the best method, results need to be compared with laboratory data. Graphical comparison was used by plotting cross plots of the measured capillary pressure vs. the predicted capillary pressure for each method one for the training stage and one for the testing stage. Furthermore, the best models need to be tested by plotting both the measured and the predicted capillary pressure curves vs. saturation. This extra step ensures the validity of the artificial intelligence model. In addition, statistical comparison using statistical measures of the error is very important:

- a. Standard Deviation (SD): is a value used to quantify the degree of difference of the dataset values. If the value of the standard deviation is low, this indicates that the data points are close to the mean of this dataset. However, if the value of the standard deviation is high, this indicates that the data points are spread out over a wide range. Equation (13) is used to calculate the value of the standard deviation.

$$SD = \frac{1}{N} \sum_{i=1}^N (x_i - \mu)^2 \dots \dots \dots (13)$$

Where:

N = the number of points in the dataset.

i = is a counter indicating the index number of the data point in the dataset.

x = is the value of the data point in the dataset.

μ = the mean of the dataset

- b. Mean Absolute Error (MAE): is a value that indicates how close the prediction is to the measured value. Absolute value of the error is used since predicted values could be lower or higher than the measured value. The interest here is to measure how close the predicted value is to the measured one. Then, an average of the whole points indicates the average of the error for the whole dataset. Equation (14) is used to calculate the Mean Absolute Error.

$$MAE = \frac{\sum_{i=1}^N |y_i - x_i|}{N} \dots\dots\dots(14)$$

Where:

y = the measured value

x = the predicted value

N = the number of values

- c. Root Mean Square Error (RMSE): is a common statistical comparison measure that provides a general predictive measure of the residuals which punishes the large residuals. A residual is individual difference between the measured and the predicted value. Equation (15) is used to calculate the Root Mean Square Error.

$$RMSE = \sqrt{\frac{\sum_{i=1}^N (x_i - y_i)^2}{N}} \dots\dots\dots(15)$$

- d. Coefficient of Determination, R^2 : is a very common statistical comparison measure that shows how accurate the model is. If the value of the R^2 is 0, then the model cannot predict the measured value. However, if the R^2 is 1, then the model can predict the measured value with no error. If the value of R^2 is between 0 and 1, then the model can predict the measured value with partial error. Equation (16) can be used to calculate the Coefficient of Determination.

$$R^2 = \frac{\sum_{i=1}^N (\hat{y}_i - \bar{y})^2}{\sum_{i=1}^N (y_i - \bar{y})^2} \dots\dots\dots(16)$$

\hat{y}_i = the regression value

y_i = the value of the dataset

\bar{y} = the average of the dataset

CHAPTER 4

Artificial Intelligence

The utilization of AI techniques to solve large scale problems has been used in different applications, including petroleum engineering. It has gained a wide acceptance as it showed excellence in solving different problems, showing very good results that could not be easily achieved by using classical physics or engineering concepts alone.

Joost N. Kok et al. defines AI in several ways. One of which is:

“An area of study in the field of computer science. Artificial intelligence is concerned with the development of computers able to engage in human-like thought processes such as learning, reasoning and self-correction”

This study focuses on developing new models for several AI techniques to predict the capillary pressure.

Applied techniques

The following AI techniques were applied in this study. One of the reasons behind selecting these techniques is because of the nature of the problem. i.e. four input parameters and one output parameter. In addition, for each core sample, three input parameters are fixed (grain density, porosity, and permeability) and one input parameter is changing (saturation) along with the output parameter (capillary pressure).

1. **Artificial Neural Network (ANN):** is a computational model similar to the biological neural network structure and functions. It consists of an input layer of neurons, hidden neurons and output neurons. When a neuron learns from the flow of information through the network, signals travel from the input layer to the output layer. The structure of the ANN changes to adapt to this information. At the input layer, between the input parameter values are presented and sent to the hidden layer. At the hidden layer, weight and bias are adjusted to produce an output as close as possible to the observed output data. Figure (4) shows a typical artificial neural network. The main advantage of ANN is that it can learn from observing datasets to adjust the weights and biases.

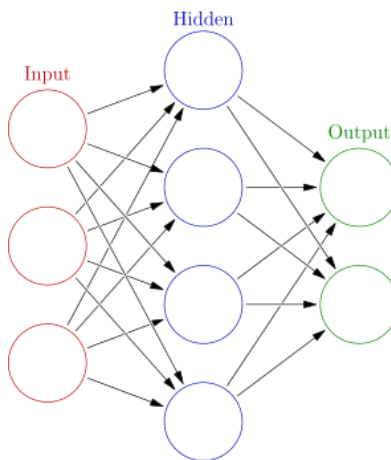


Figure 4: A typical artificial neural network

There are several algorithms of this technique. The following are the ones used in this study:

Trainlm: This is the most commonly used algorithm and it produces very good results. It is recommended to be used as a first choice although it requires more computer memory than other algorithms. It is named after Levenberg-Marquardt who came up with a mathematical optimization technique to solve non-linear least square curve fitting problems. *Trainlm* uses Levenberg-Marquardt approach to update weights and biases during the learning process.

Trainbr: This algorithm uses the Bayesian Regularization to update weight and bias during the learning process.

Trainscg: This algorithm is useful for transfer functions that have derivative functions. It is based on supervised learning approach and uses scaled conjugate gradient method to update weights and biases during the learning process.

Trainoss: This algorithm uses one-step secant method to update weights and biases during the learning process. The process works on finding the root of a function by using the roots of the lines.

Traingd: For proposed functions that have derivatives, this algorithm can be employed for efficient results. It uses gradient descent backpropagation with momentum method to update weights and biases during the learning process.

Traingdx: This is another algorithm that is good for transfer functions that have derivative functions. It combines adaptive learning rate with momentum training.

The above algorithms have standard parameters that can be changed manually, automatically, or kept at their default values. These parameters are: maximum number of

epochs to train, performance goal, learning rate, ratio to increase learning rate, ratio to decrease learning rate, maximum validation failures, maximum performance increase, momentum constant, minimum performance gradient, epochs between displays, generate command-line output, show training GUI, and maximum time to train in seconds. Training of the algorithm stops when one of the following conditions is met:

- Maximum number of epochs is reached.
- Maximum amount of time is exceeded.
- Performance is minimized to the goal.
- Performance gradient falls below minimum.
- Validation performance has increased to more than the maximum.

2. **Fuzzy Logic:** As the name suggests, it is a model that is based on logic operations to make decisions. The output is in the form of (0) and (1). (1) means the truth and (0) means the false, and in between is the degree of membership (partial truth) where fuzzy logic operates. A typical example of this technique is what figure (5) shows. A distance of 4 meters has a membership of 0.7 for the function representing “small” and of 0.2 for the function representing “medium.” This means the distance of 4 meters is more “small” than “medium” with a ratio of (0.7:0.2).

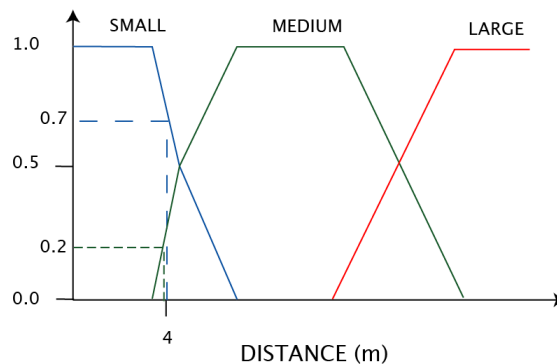


Figure 5: Example of fuzzy logic

Fuzzy logic programming involves the following steps:

- a. Fuzzify the input values to fuzzy membership functions.
- b. Execute the user-selected rules to compute fuzzy output functions.
- c. De-fuzzify the output to obtain real values.

There are two types of this technique:

Cluster radius: This is a clustering technique used to specify the group to which each data point belongs. Originally, the fuzzy logic tool starts with a random cluster center which is generally incorrect. Then the tool starts to give a membership degree for each data point. As the cluster centers are updated with every iteration, the membership degrees are also updated. This process goes on until a minimum distance is achieved between the datapoints and the centers of their assigned clusters.

Grid partitioning: This approach generates membership functions for input data by regularly partitioning the input variable range and creates a single output Sugeno fuzzy system. The fuzzy rule contains one rule for each input membership function.

3. **Fuzzy Logic type-2:** It generalizes the fuzzy logic by adding an uncertainty parameter to the input itself. This uncertainty parameter is added to the system because of the difficulty of assigning exact membership grades due to noise in the input data. This technique is

similar to the fuzzy logic technique in terms of the overall approach. It includes a fuzzifier, a rule base with an inference engine, and an output processor.

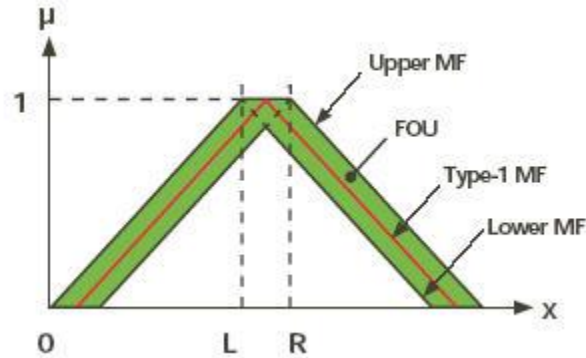


Figure 6: Example of fuzzy logic type 2

As shown in figure (6), the red line represents the exact membership assignment for the input data while the green area is the uncertainty added to the data.

4. **Decision Tree:** It is a model that predicts the output based on a branching series of Boolean tests, like a tree. This model uses the target as a specific fact to predict the output in a generalized form. Each decision point of the tree has the nodes, actions, and choices as components, and paths as rules. These components transfer from one node to another until the target is reached.

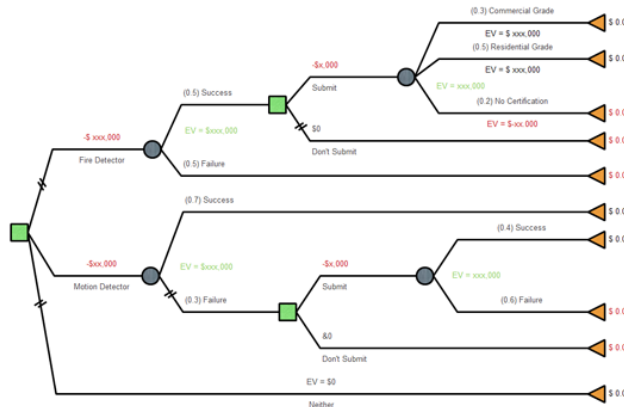


Figure 7: Example of decision tree

Figure (7) shows a typical example of the decision tree. Squares represent decision nodes, circles represent chance nodes, and triangles represent end nodes.

5. **Support Vector Machine (SVM):** SVM engages in supervised learning by modifying certain parameters in the models to develop a non-probabilistic classifier. Figure (8) shows a simple example of the scatter in the dataset in a two-dimensional space and the linear regression line, in red, created by this technique.

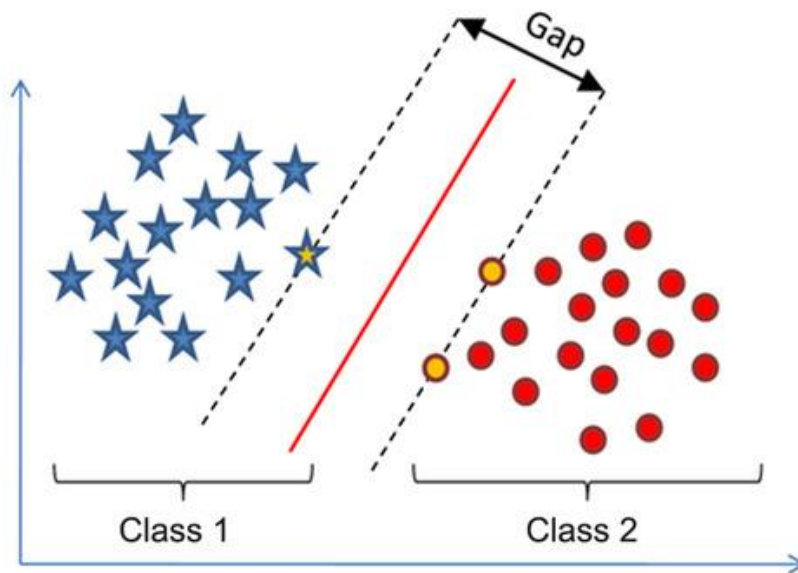


Figure 8: An example of support vector machine

6. **Functional Network (FN):** This approach provides a linear combination of the inputs and neuron (coefficient) parameters. The transfer functions in these networks linked with neurons are not fixed. They are learned from the data. Moreover, there is no need to include weights to links among the neurons since their effect is taken care of by the neural functions.
7. **Nearest Neighbor Curve Prediction:** This technique will be discussed later in details as it is a new technique.

CHAPTER 5

Results and Discussion

5.1 Data acquisition

The most common laboratory technique used in the industry to evaluate capillary pressure is the mercury injection test (MICP). All available data of the core samples used in this study for a specific oil carbonate reservoir were obtained using MICP.

5.2 Data processing and filtering

The workflow involved the following steps:

1. All available mercury injection test data were fitted to Thomeer parameters.
2. Imbibition data was removed and only drainage data was kept.
3. All units for data columns were unified to field units as follows:
 - a. Porosity, fraction
 - b. Permeability, mD
 - c. Grain density, lb/ft³
 - d. Saturation, fraction
 - e. Capillary pressure, psig
4. The available data for each core sample are porosity, permeability, grain density and at least 50 points of different capillary pressures and their corresponding saturations.
5. Based on Thomeer concept, data were classified based on modality. Out of the total samples, 66 were found to exhibit uni-modal behavior while the remaining 136 were found to exhibit bi-modal behavior. Figure (9) shows the difference between the two types of behavior, namely, uni-modal and bi-modal.

6. The classification of these datasets was saved in a separate sheet. At the end of this data preparation phase, three datasets were prepared:
- For uni-modal data,
 - For bi-modal data, and
 - For both modals combined together.

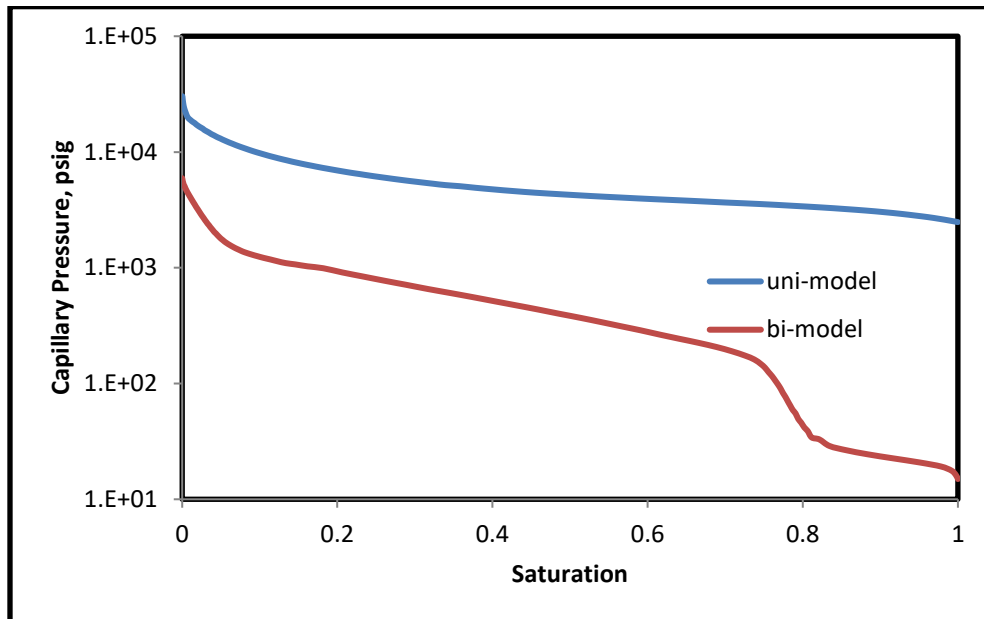


Figure 9: Different Modalities of Capillary Pressure

5.3 Number of data points

As mentioned earlier, data of 202 core samples was obtained in the laboratory using mercury injection test. Each one's capillary pressure vs. saturation curve is made of at least 50 points. Appendix-A shows a sample of the data.

5.4 Input parameters

The input parameters are the porosity, permeability, grain density, and wetting phase saturation.

5.5 Target parameter

The target parameter is the capillary pressure. The capillary pressure values range from zero to 60,000 psi in the database used in this study.

5.6 Data statistics

Tables (2-4) show the statistics of the used datasets after classification. The correlation coefficient values show that there is a relationship between the input parameters and the target parameter.

Relationship might not be linear among these parameters; non-linear relationship might exist.

Table 2: Uni-modal statistics

Parameter	Capillary Pressure	Grain Density	Permeability	Porosity	Saturation
Correlation Coefficient with respect to P_c	1	-0.234	0.139	0.021	0.238
Minimum	0.511	2.439	0.001	0.003	0
Maximum	59909	2.834	1192	0.322	1
Mean	4453	2.744	178	0.142	0.824
Median	1768	2.747	4.536	0.147	0.971
Standard Deviation	8509	0.063	312	0.072	0.294
Skewness	3.965	-2.098	1.923	0.172	-1.817
Kurtosis	17.478	8.417	2.905	-0.518	1.889

Table 3: Bi-modal statistics

Parameter	Capillary Pressure	Grain Density	Permeability	Porosity	Saturation
Correlation Coefficient with respect to P_c	1	-0.195	0.057	-0.170	0.330
Minimum	0.812	2.469	0.114	0.026	0
Maximum	58736	2.884	2900	0.288	1
Mean	4076	2.726	356	0.172	0.734
Median	1218	2.726	160	0.191	0.912
Standard Deviation	8638	0.047	517	0.070	0.324
Skewness	3.971	0.057	2.548	-0.477	-1.069
Kurtosis	17.367	3.848	8.063	-0.892	-0.268

Table 4: Combined modal statistics

Parameter	Capillary Pressure	Grain Density	Permeability	Porosity	Saturation
Correlation Coefficient with respect to P_c	1	-0.201	0.066	-0.119	0.306
Minimum	0.511	2.439	0.001	0.003	0
Maximum	59909	2.884	2900	0.322	1
Mean	4180	2.731	307	0.164	0.759
Median	1378	2.728	80	0.177	0.939
Standard Deviation	8604	0.053	476	0.072	0.318
Skewness	3.967	-0.832	2.673	-0.291	-1.237
Kurtosis	17.375	5.867	9.347	-0.935	0.112

5.7 Artificial Intelligence Models

All models were employed with a focus on proper prediction of capillary pressure. Some of them had to be tweaked to produce better results. Here are the parameters that needed to be modified for each AI model.

1. **Artificial neural network (ANN):** Regardless of which model of ANN is used, the main parameters that can be tweaked are the number of layers, number of neurons and the stratification of data.
2. **Fuzzy logic:** In the Matlab programming code, grid partitioning is referred to as “genfis1” and cluster radius as “genfin2”. The main parameters to modify here for the first type are number of membership functions and membership type. In the other type, the radius of cluster is the parameter to be tuned.
3. **Fuzzy logic type-2:** In this approach, the degree of uncertainty about the input parameters is incorporated into the program.
4. **Decision tree:** This type of AI tool is a function of the maximum number of branch node splits to generate a deep or shallow tree.

5. **Support vector machine:** In this approach, a number of parameters can be adjusted, viz., kernel option, kernel type, C, lambda, epsilon and verbose.
6. **Functional network:** The model here works by choosing a specific function type.
7. **Nearest Neighbor Curve Prediction (NNCP):** This technique depends on the distance between the input parameters in a multi-dimensional space. Since a curve is defined by a number of points, a normalized curve is being generated and used for the training of this model. The parameter tuned is the number of points used for the normalized capillary pressure vs. saturation during the normalization process.

5.8 Statistical results

As mentioned above, three different datasets were used which were classified according to uni-modal or bi-modal behavior. Tables 5-7 show the statistical comparison for the first six methods for each dataset.

Method No. 7, Nearest Neighbor Curve Prediction, is not compared with the rest of the methods in these tables. It will be discussed in detail in a separate section.

Table 5: Uni-modal statistical analysis.

Statistical Parameter	Standard Deviation		Mean Absolute Error		Root Mean Squared Error		Coefficient of Determination	
	Training	Testing	Training	Testing	Training	Testing	Training	Testing
ANN - trainbr	3153	34922	1349	10189	3152	35648	0.90	0.60
ANN - trainlm	3576	35357	1453	16291	3576	36583	0.87	0.55
ANN - trainscg	7968	6149	4704	3169	7970	6158	0.33	0.02
ANN - trainoss	7793	3889	4333	2496	7794	3981	0.36	0.42
Decision Tree	353	4567	110	2145	353	4604	1.00	0.35

Support Vector Machine	4453	4928	1079	2460	4529	5119	0.85	0.03
Fuzzy Logic – Grid Partitioning	5704	5630	2864	2851	5703	5628	0.56	0.54
Fuzzy Logic – Cluster Radius	6569	6354	3092	3008	6568	6352	0.42	0.41

Statistical comparison in Table-5 for the six AI models for a uni-modal dataset shows that the **Decision Tree** model has the least Standard Deviation (SD) among all techniques, in training and testing at **353** and **4567**, respectively (figure 10).

The lowest Mean Absolute Error (MAE) for the **Decision Tree** model in training and testing at **110** and **2145**, respectively. While the highest was for **trainscg** in training and **trainlm** in testing at **4704** and **16291**, respectively (figure 11).

The lowest Root Mean Square Error (RMSE) was for the **Decision Tree** model in training and **trainoss** for testing at **353** and **3981**, respectively. Similar to the MAE, the highest RMSE was for **trainscg** in training and **trainlm** in testing at **7970** and **36583**, respectively (figure 12).

The highest Coefficient of Determination (R^2) for training was from the **Decision Tree** model at **1.00**, but for the testing was for **trainbr** at **0.6**. The **Decision tree** was not good for the testing, which suggests that the model was memorizing the input. The **trainbr** for training model shows **0.9**, which suggests that this is an acceptable model (figure 13).

On the other hand, **trainscg**, **trainoss**, **fuzzy logic using cluster radius**, and **fuzzy logic using grid partitioning** produced the worst results in the training and testing with MAE of **4704**, **4333**, **3092**, and **2864** in the training, respectively, and **3169**, **2496**, **3008** and **2851** in the testing,

respectively. Their coefficient of determination in the training was **0.33**, **0.36**, **0.42** and **0.56** respectively and in the testing was **0.02**, **0.42**, **0.41**, and **0.54**, respectively.

Support vector machine yielded a coefficient of determination of **0.85** in training but **0.03** in testing and its standard deviation was **4453** in training and **4928** in testing. This implies that the model had memorized the training data. RMSE also proves this point where it showed an RMSE value of **4529** in training and **5119** in testing.

Table 6: Bi-modal statistical analysis

Statistical Parameter Set	Standard Deviation		Mean Absolute Error		Root Mean Squared Error		Coefficient of Determination	
	Training	Testing	Training	Testing	Training	Testing	Training	Testing
ANN - trainbr	4360	2633	1869	1278	4360	2633	0.81	0.50
ANN - trainlm	3857	3207	1717	1993	3857	3216	0.85	0.43
ANN - trainscg	6832	2948	3594	2116	6833	3056	0.54	0.39
ANN - trainoss	5826	2631	2745	1766	5827	2689	0.67	0.44
Decision Tree	767	5041	113	1523	767	5049	0.99	0.27
Support Vector Machine	4735	2589	1255	1950	4830	2630	0.84	0.00
Fuzzy Logic – Grid Partitioning	5511	5557	2811	2825	5510	5556	0.59	0.59
Fuzzy Logic – Cluster Radius	5198	5256	2378	2389	5198	5255	0.64	0.64

Table 6 summarizes the statistical comparison between the six different AI models for bi-modal dataset. Similar to Table 5, Table 6 shows that the **Decision Tree** training run model has the least

SD among all techniques at **767**, but the **Support Vector Machine** has the least for testing at **2589** (figure 10).

MAE for the **Decision Tree** model in training and testing was **113** and **1523**, respectively. While the highest was for **trainscg** in training and **Fuzzy Logic – Grid Partitioning** in testing at **3594** and **2825**, respectively (figure 11).

The lowest RMSE was for the **Decision Tree** model in training, and the **Support Vector Machine** for testing at **767** and **2630**, respectively. The highest RMSE was for **trainscg** in training and the **Decision Tree** in testing at **6833** and **5049**, respectively (figure 12).

The R^2 for training was from the **Decision Tree** model at **0.99** but for the testing was for **Fuzzy Logic – Cluster Radius** at **0.64**. The **Decision tree** was not good for the testing, which suggests that the model was memorizing the output. The **trainbr** for training and testing model shows **0.81** and **0.5**, respectively, which suggests that this is an acceptable model (figure 13).

On the other hand, **trainscg**, **trainoss**, **fuzzy logic – culter radius** and **fuzzy logic – grid partitioning** produced the worst results in the training and testing with MAE of **3594**, **2745**, **2378**, and **2811** in the training respectively and **2116**, **1766**, **2389** and **2825** in the testing respectively. Their coefficient of determination in the training was **0.54**, **0.67**, **0.64** and **0.59** respectively and in the testing was **0.39**, **0.44**, **0.64**, and **0.59** respectively.

Support vector machine's coefficient of determination was **0.84** in training but **0.00** in testing and its standard deviation was **4735** in training and **2589** in testing which means the the model was force fitted on the training data. RMSE also proves this point where it showed **4830** in training and **2630** in testing.

Table 7: Combined modals statistical analysis

Statistical Parameter	Standard Deviation		Mean Absolute Error		Root Mean Squared Error		Coefficient of Determination	
	Training	Testing	Training	Testing	Training	Testing	Training	Testing
ANN - trainbr	4754	2029	2243	1118	4754	2052	0.78	0.59
ANN - trainlm	4360	5204	2011	1739	4360	5248	0.81	0.31
ANN - trainscg	5828	3452	2732	1709	5828	3533	0.67	0.32
ANN - trainoss	5437	3615	2533	1733	5437	3742	0.71	0.39
Decision Tree	476	3609	96	1362	476	3648	1.00	0.41
Support Vector Machine	Model did not work							
Fuzzy Logic – Grid Partitioning	5809	5907	2992	3014	5809	5906	0.54	0.53
Fuzzy Logic – Cluster Radius	6068	6177	3002	3025	6068	6177	0.50	0.49

Statistical comparison in Table-7 between used AI models for combined-modal dataset shows that the **Decision Tree** model has the least Standard Deviation (SD), among all techniques, at **476** for training, but **trainbr** shows the least for testing at **2029** (figure 10).

The lowest Mean Absolute Error (MAE) for the **Decision Tree** model in training and testing at **96** and **1362**, respectively. While the highest was for **Fuzzy Logic – Cluster Radius** in training and testing at **3002** and **3025**, respectively (figure 11).

The lowest Root Mean Square Error (RMSE) was for the **Decision Tree** model in training and **trainoss** for testing at **476** and **2052**, respectively. Similar to the bi-modal dataset, the highest RMSE was for **Fuzzy Logic – Cluster Radius** in training and at **6068** and **6177**, respectively (figure 12).

The highest Coefficient of Determination (R^2) for training was from the **Decision Tree** model at **1.0**, but for the testing was for **trainbr** at **0.59**. The Decision tree was not good for the testing, which suggests that the model was memorizing the output. The **trainbr** for training model shows **0.78** for the training, which suggests that this is an acceptable model (figure 13).

On the other hand, **trainscg**, **trainoss**, **fuzzy logic – culter radius** and **fuzzy logic – grid partitioning** produced the worst results in the training and testing with MAE of **5828**, **5437**, **6068**, and **5809** in the training respectively and **3452**, **3615**, **6177** and **5907** in the testing respectively. Their coefficient of determination in the training was **0.67**, **0.71**, **0.50** and **0.54** respectively and in the testing was **0.32**, **0.39**, **0.49**, and **0.53** respectively.

Support vector machine model did not finish running which suggest that it could not reach to a conversion point to produce results. This happen when the model cannot find a solution for the data.

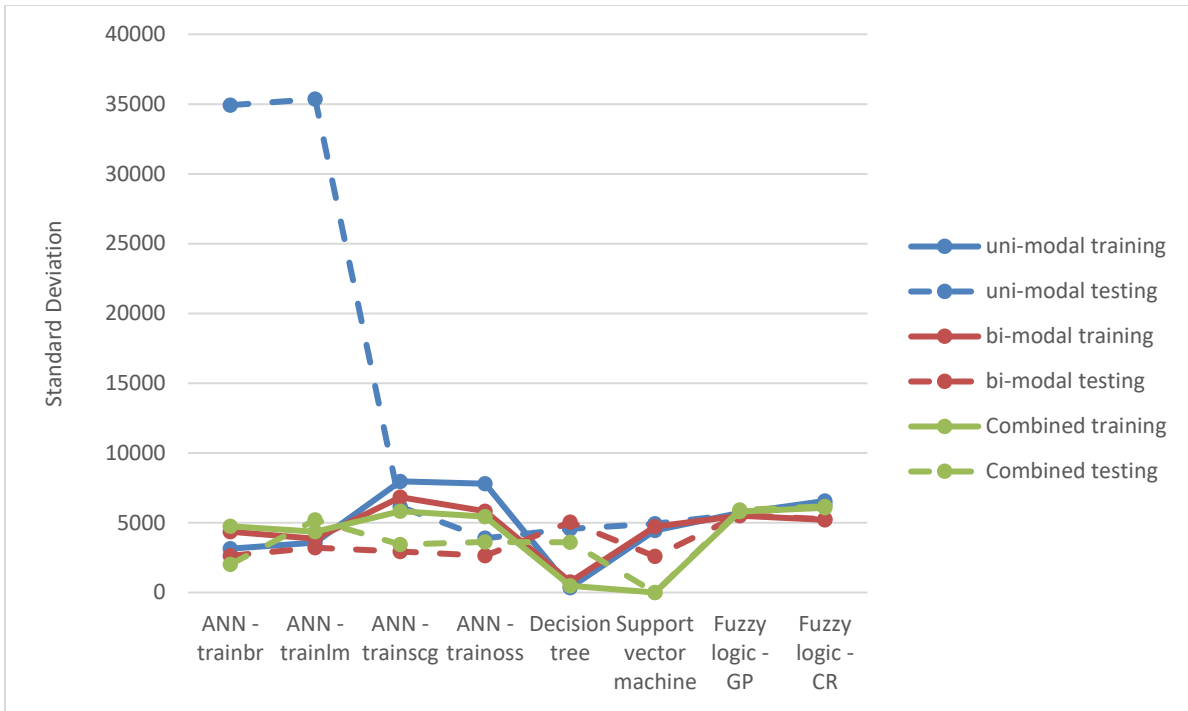


Figure 10: Standard Deviation Comparison of capillary pressure values.

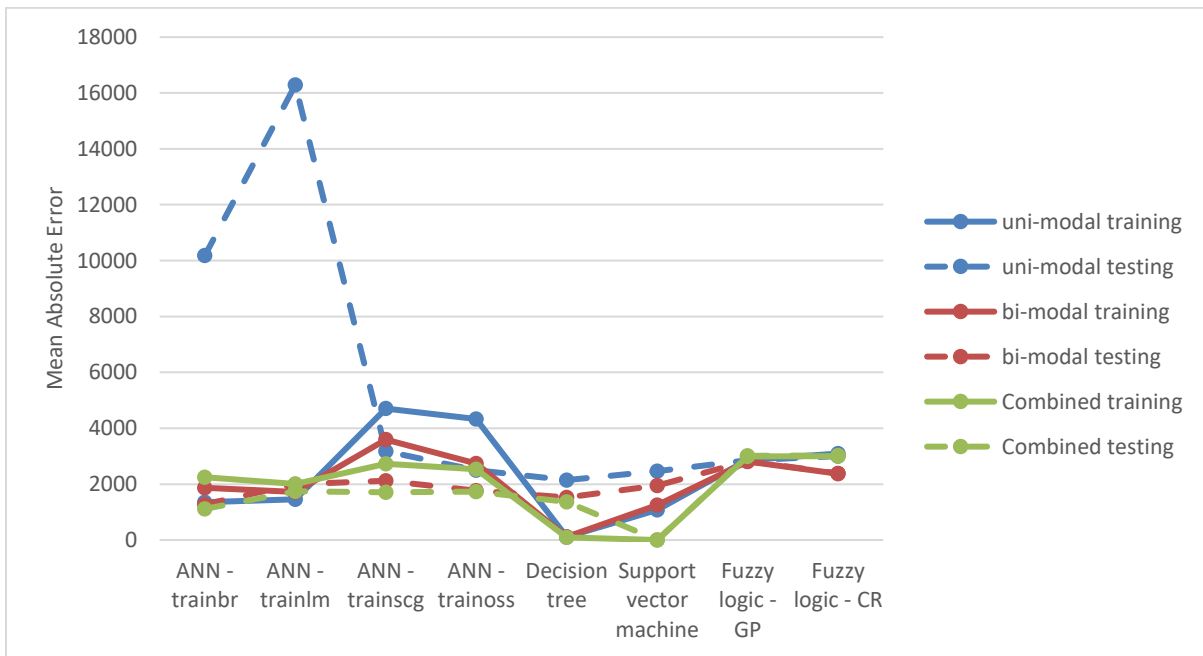


Figure 11: Mean Absolute Error Comparison of capillary pressure values.

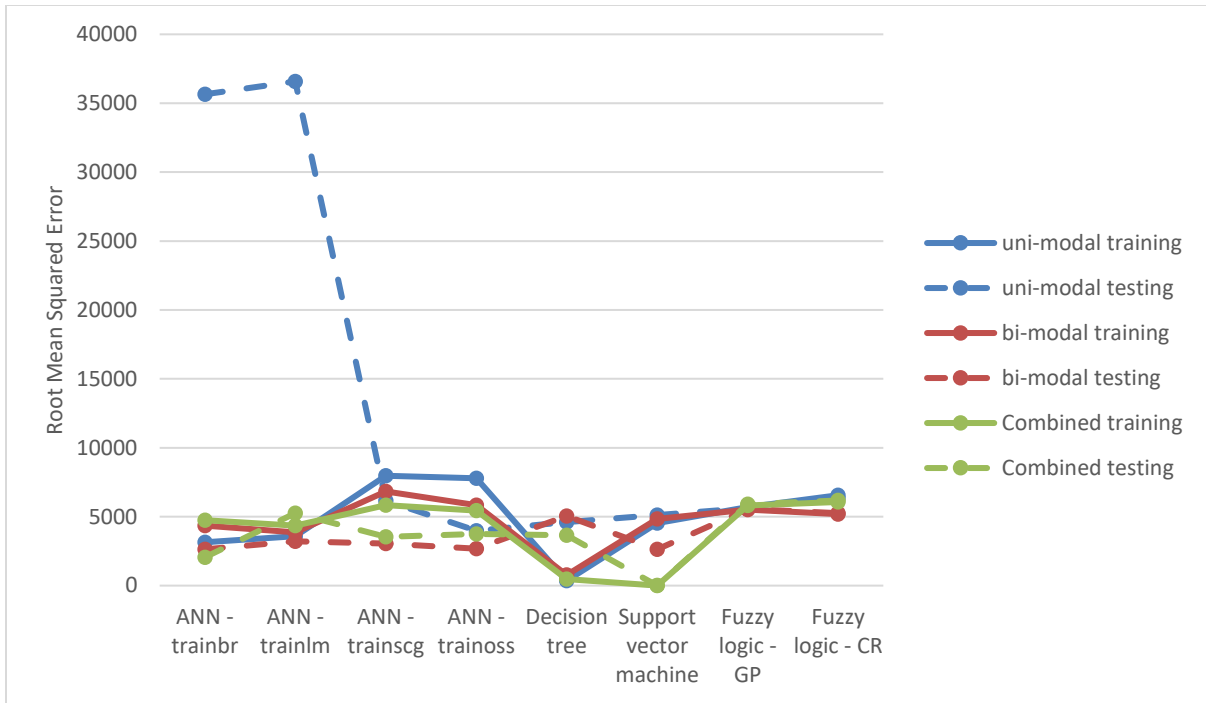


Figure 12: Root Mean Square Error Comparison of capillary pressure values.

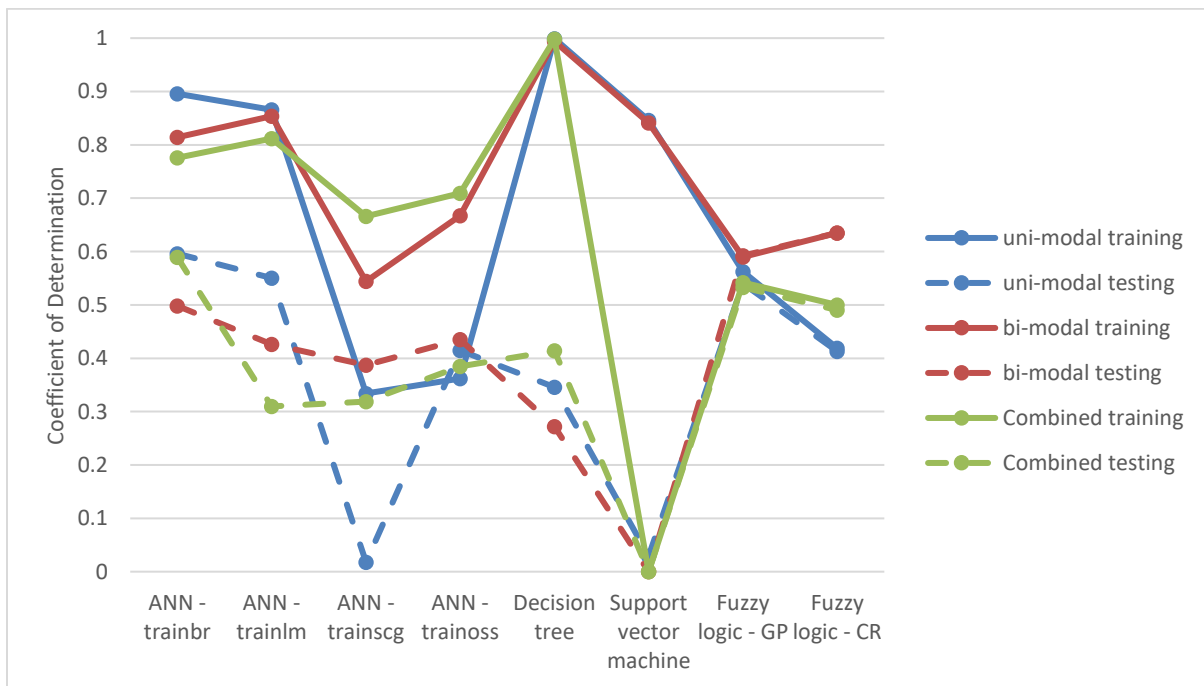


Figure 13: Coefficient of Determination Comparison of capillary pressure values.

5.9 Graphical results

Since each technique has its own algorithm of solving problems, not all of them show the same answer. Some of them showed excellent results while some others showed poor results. ANN training with 2-layers showed excellent results in training and testing for uni-modal, bi-modal and combined modals.

Figures (14-15) show a crossplot of the measured vs. predicted capillary pressure in training and testing for uni-modal data. The accuracy of this model was 85% in training and 55% in testing.

Figure (16) shows laboratory capillary pressure vs. saturation and predicted capillary pressure vs. saturation in a log-log scale plot. It shows how inaccurate the prediction was for this testing sample. However, in figure (17), where the same results are plotted in a cartesian scale plot, the curves look close to each other. However, the predicted plot is not behaving in a uni-modal behavior.

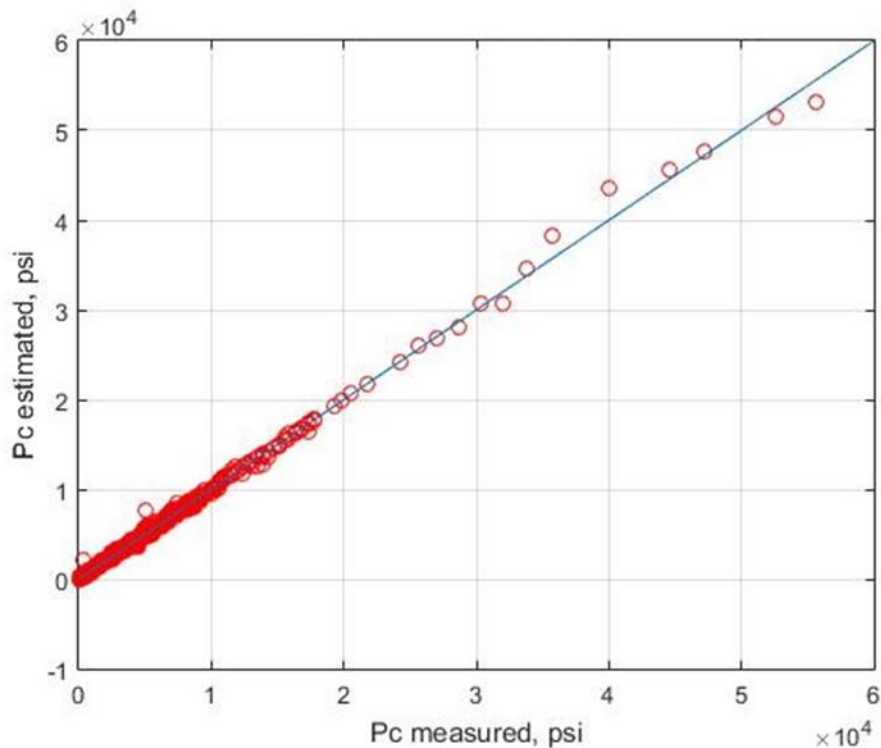


Figure 14: Predicted vs. measured values using ANN – trainlm 2-layer algorithm (Training).

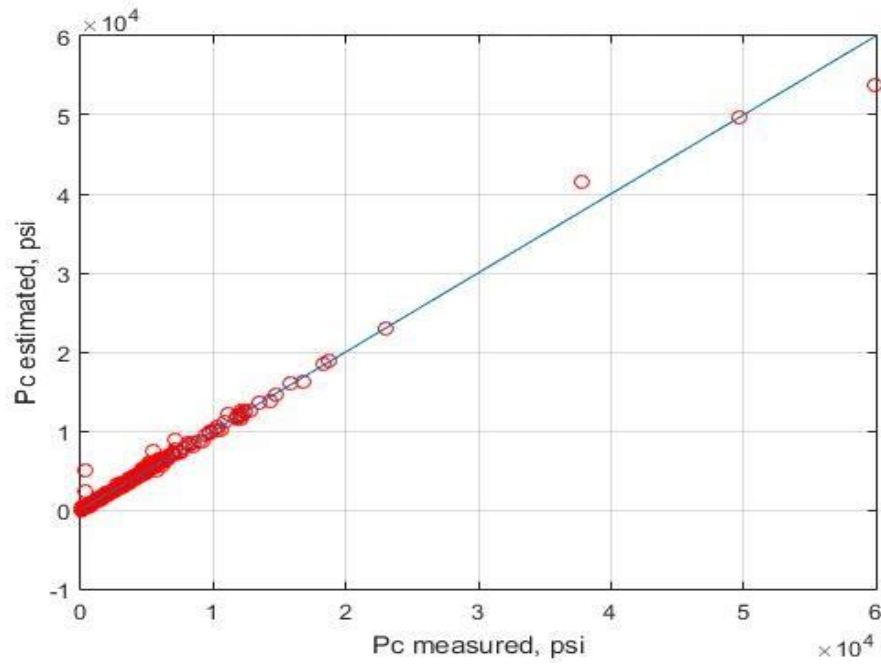


Figure 15: Predicted vs. measured values using ANN – trainlm 2-layer algorithm (Testing).

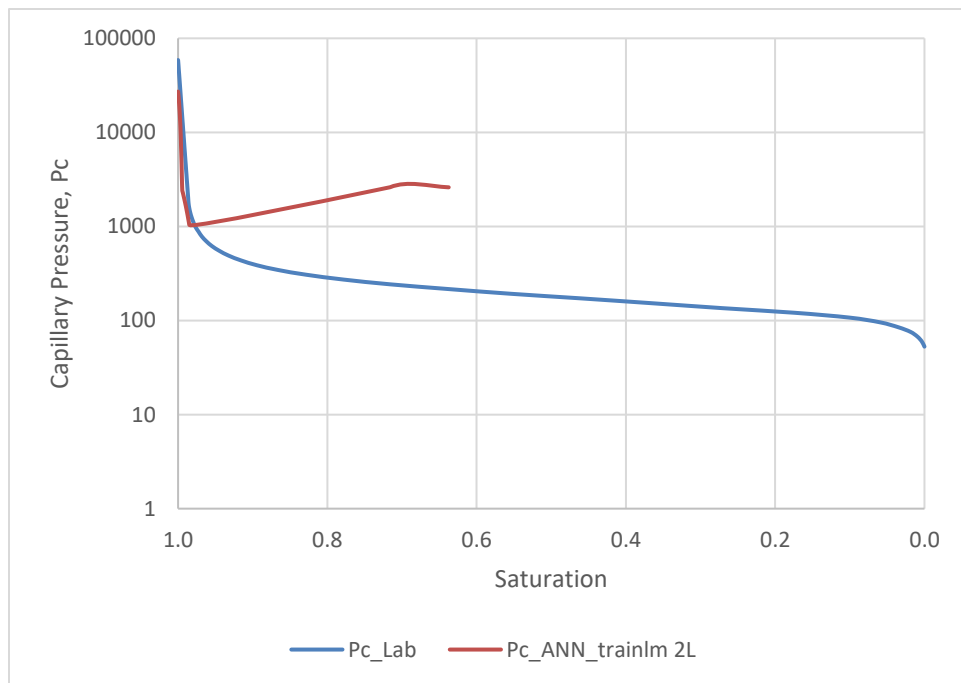


Figure 16: A sample of uni-modal data using ANN - trainlm 2-layer algorithm in semi-log scale plot

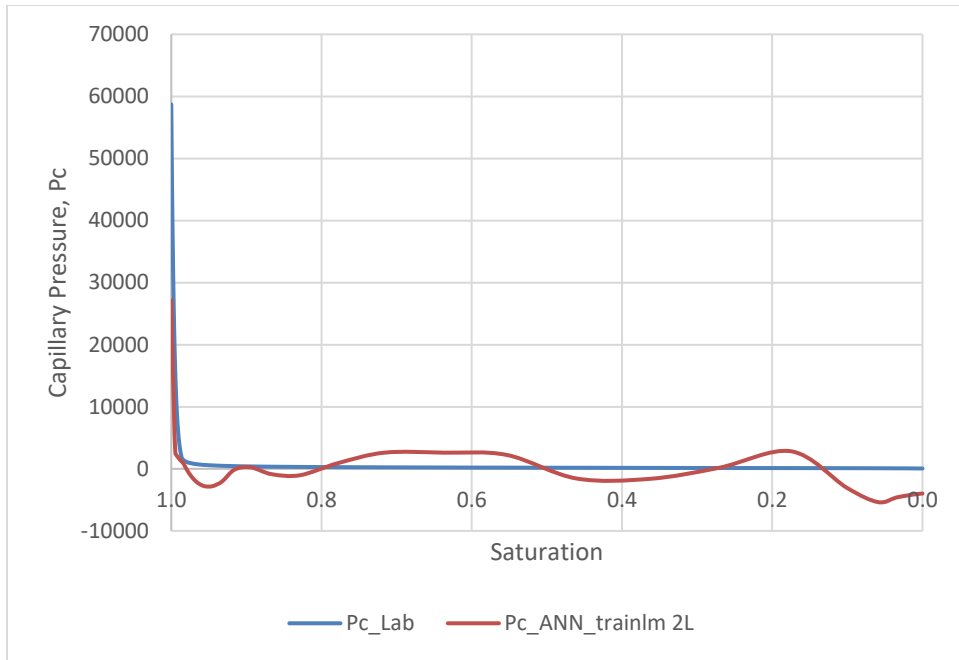


Figure 17: A sample of uni-modal data using ANN - trainlm 2-layer algorithm in cartesian scale plot

Figures (18-19) show a crossplot of the measured vs. predicted capillary pressure in training and testing for bi-modal data. The accuracy of this model was 85% in training and 43% in testing. Figure (20) shows laboratory capillary pressure vs. saturation and predicted capillary pressure vs. saturation in a semi-log scale plot. It shows how inaccurate the prediction was for this testing sample. However, in figure (21), where the same results are plotted in a cartesian scale plot, the curves look close to each other. However, the predicted plot is not behaving in a bi-modal behavior.

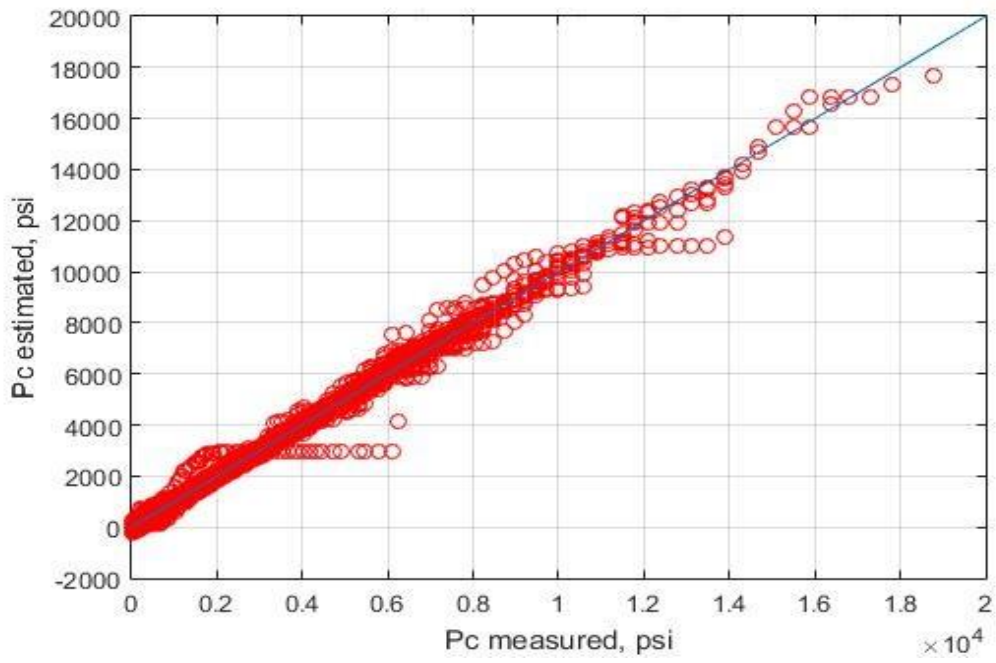


Figure 18: Predicted vs. measured values using ANN – trainlm 2-layer algorithm (Training).

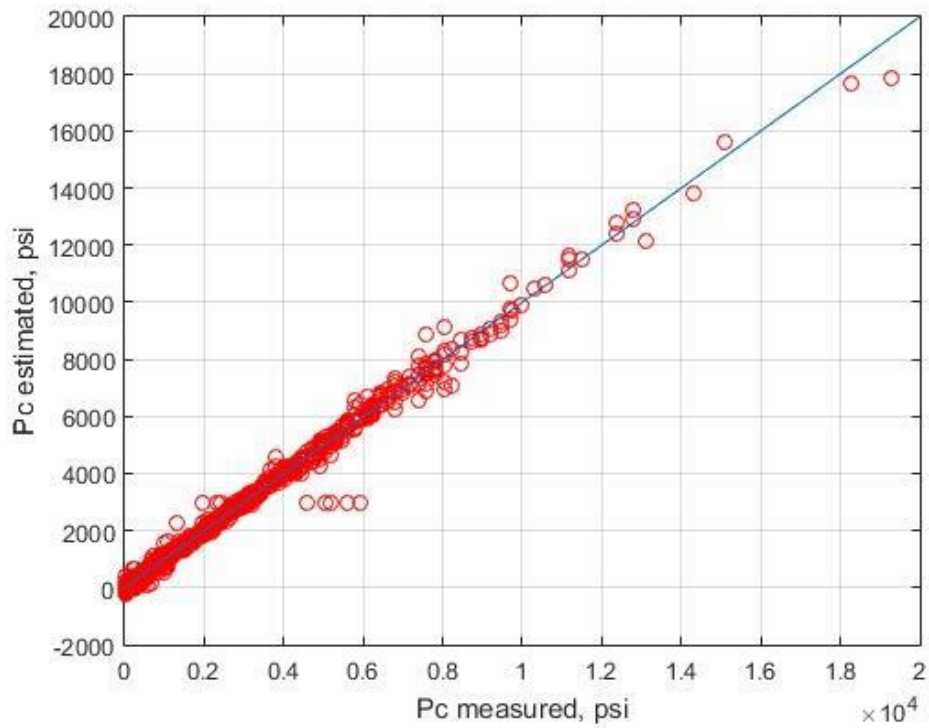


Figure 19: Predicted vs. measured values using ANN – trainlm 2-layer algorithm (Testing).

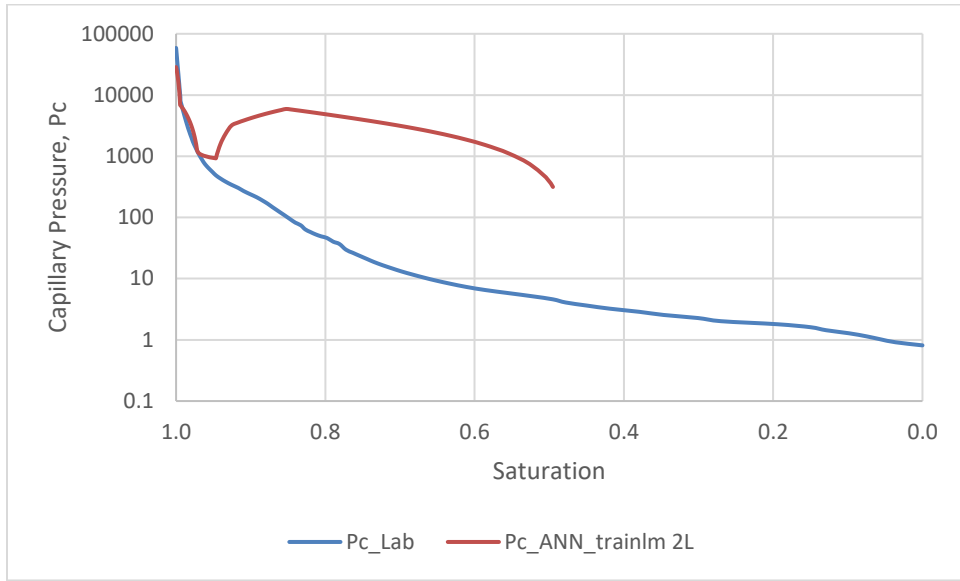


Figure 20: A sample of bi-modal sata using ANN - trainlm 2-layer algorithm in log-log scale plot

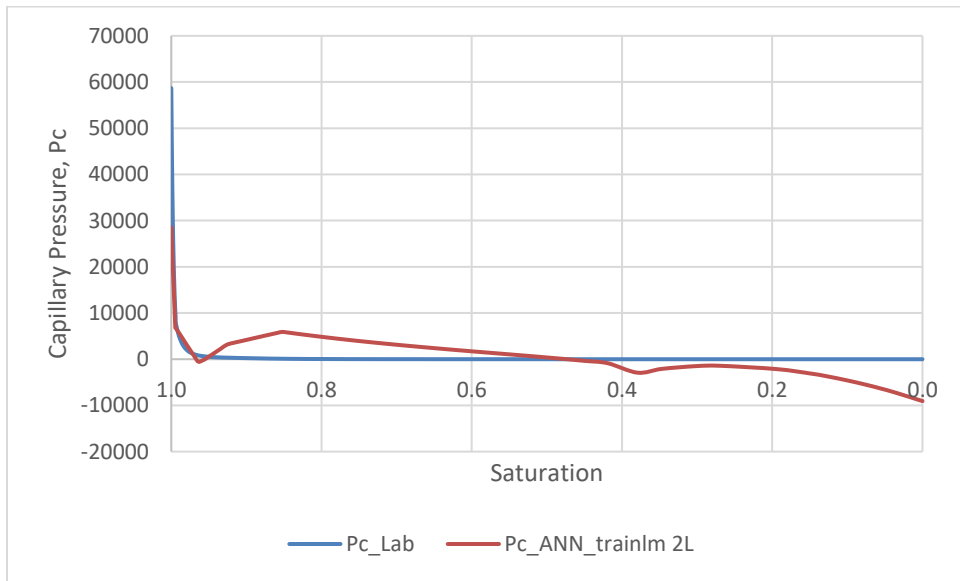


Figure 21: A sample of bi-modal sata using ANN - trainlm 2-layer algorithm in cartesian scale plot

Figures (22-23) show a crossplot of the measured vs. predicted capillary pressure in training and testing for combined modals data. The accuracy of this model was 81% in training and 31% in testing.

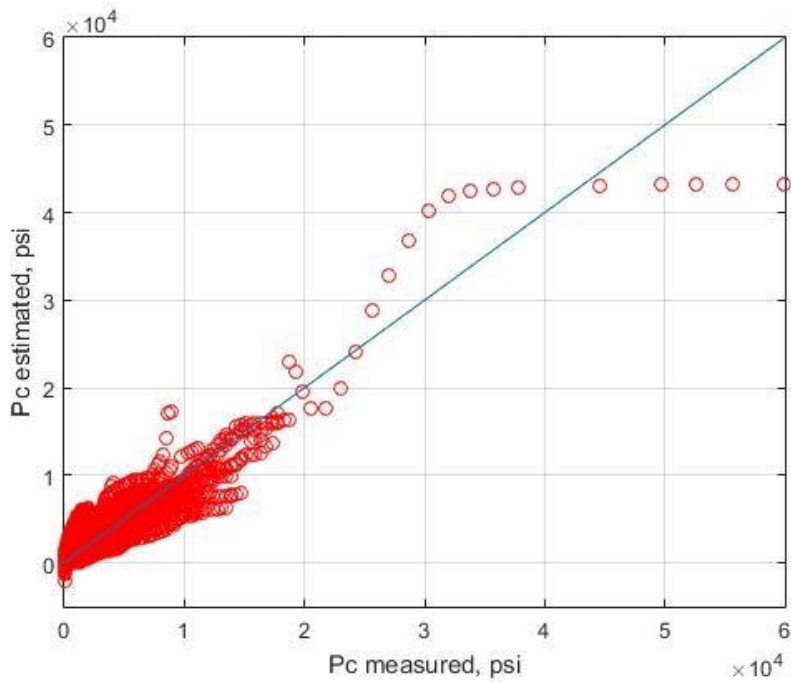


Figure 22: Predicted vs. measured values using ANN – trainlm 2-layer algorithm (Training).

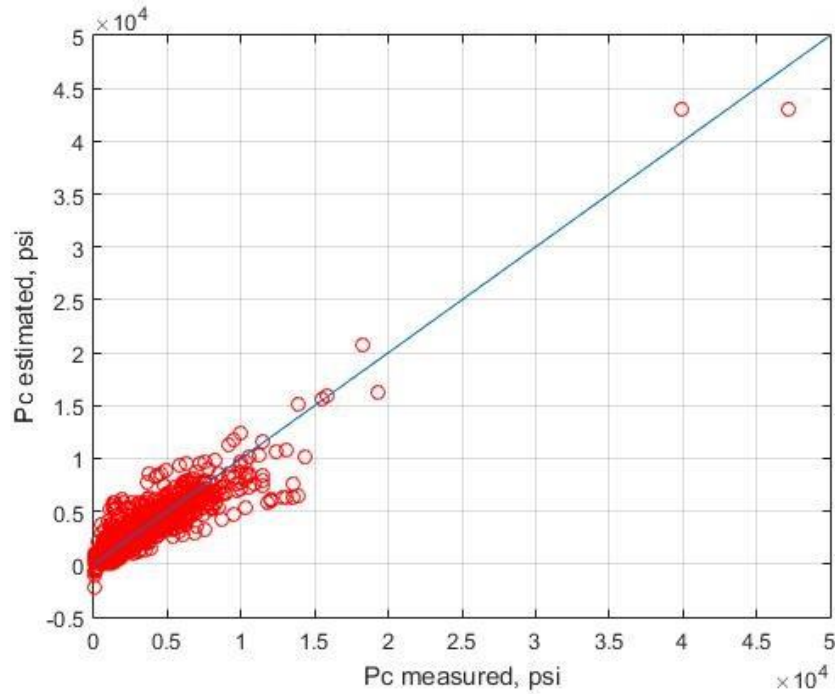


Figure 23: Predicted vs. measured values using ANN – trainlm 2-layer algorithm (Testing).

Figures (24-25) show a crossplot of the measured vs. predicted capillary pressure in training and testing for uni-modal data. The accuracy of this model was 100% in training and 35% in testing using decision tree technique. Figure (26) shows laboratory capillary pressure vs. saturation and predicted capillary pressure vs. saturation in a log-log scale plot. It shows how inaccurate but very close the prediction was for this testing sample. However, in figure (27), where the same results are plotted in a cartesian scale plot, the curves look close to each other. However, the predicted plot is not behaving in a uni-modal behavior.

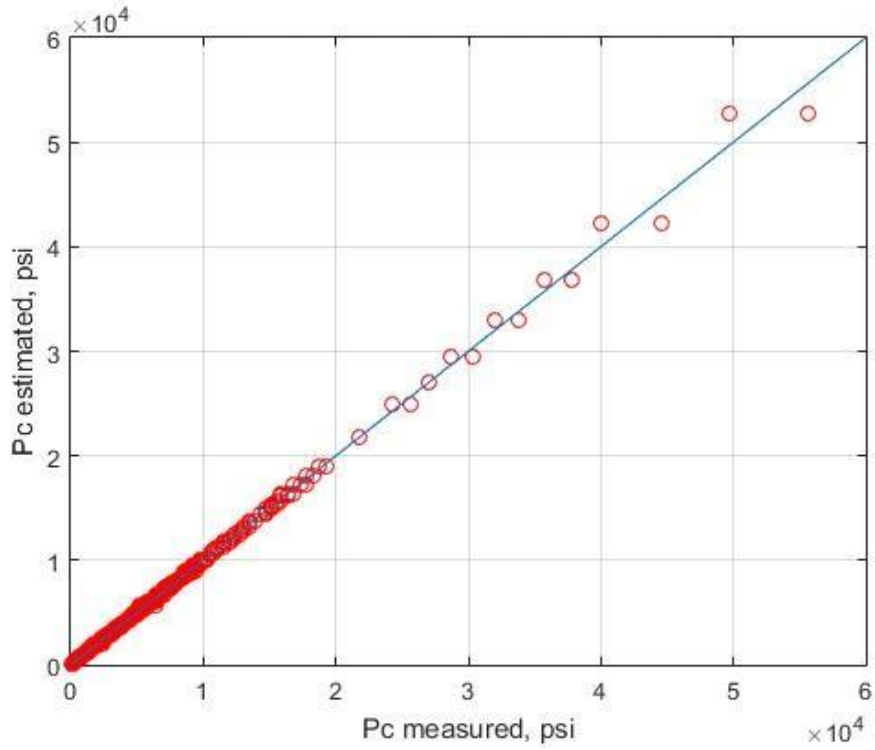


Figure 24: Predicted vs. measured values using Decision tree algorithm (Training).

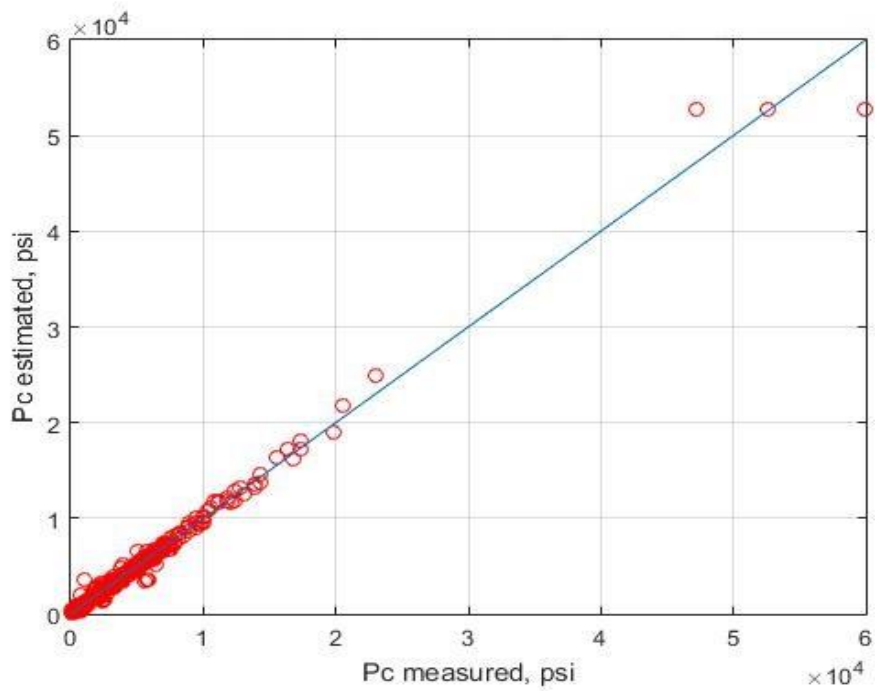


Figure 25: Predicted vs. measured values using Decision tree algorithm (Testing).

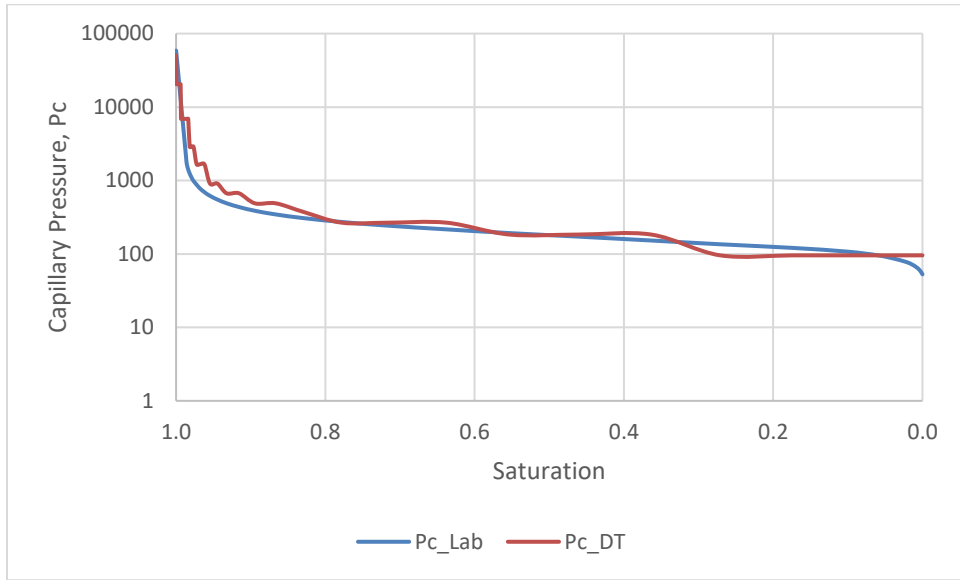


Figure 26: A sample of uni-modal sata using decision tree algorithm in log-log scale plot

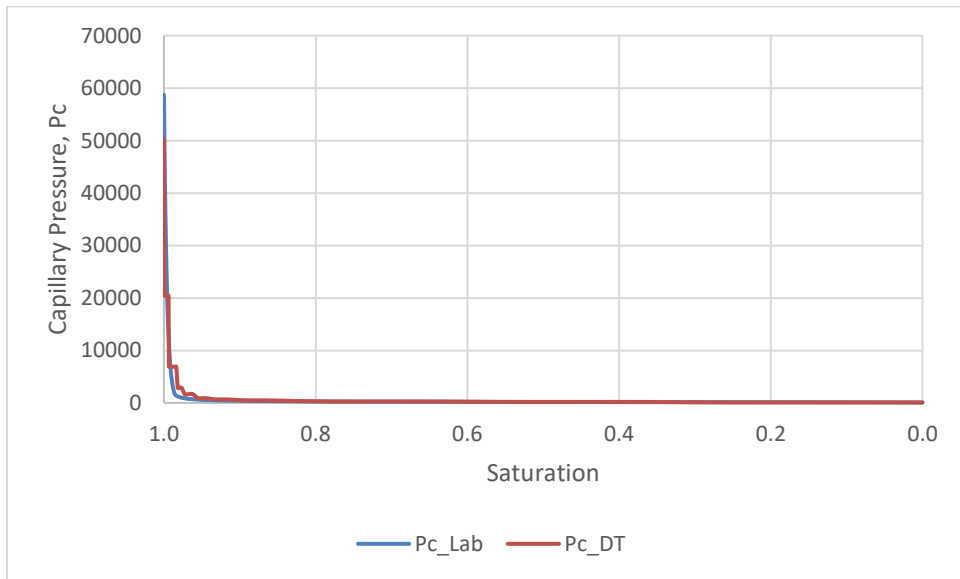


Figure 27: A sample of uni-modal sata using decision tree algorithm in cartesian scale plot

Figures (28-29) show a crossplot of the measured vs. predicted capillary pressure in training and testing for bi-modal data the accuracy of this model was 99% in training and 27% in testing using decision tree technique. Figure (30) shows laboratory capillary pressure vs. saturation and predicted capillary pressure vs. saturation in a log-log scale plot. It shows how inaccurate the prediction was for this testing sample. However, in figure (31), where the same results are plotted in a cartesian scale plot, the curves look close to each other. However, the predicted plot is not behaving in a bi-modal behavior.

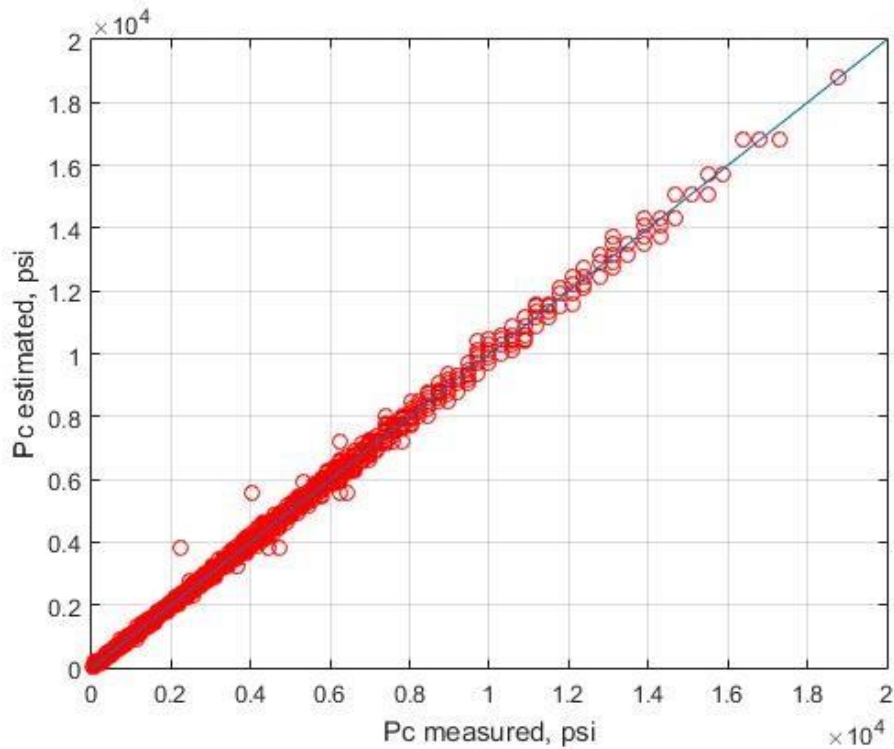


Figure 28: Predicted vs. measured values using Decision tree algorithm (Training).

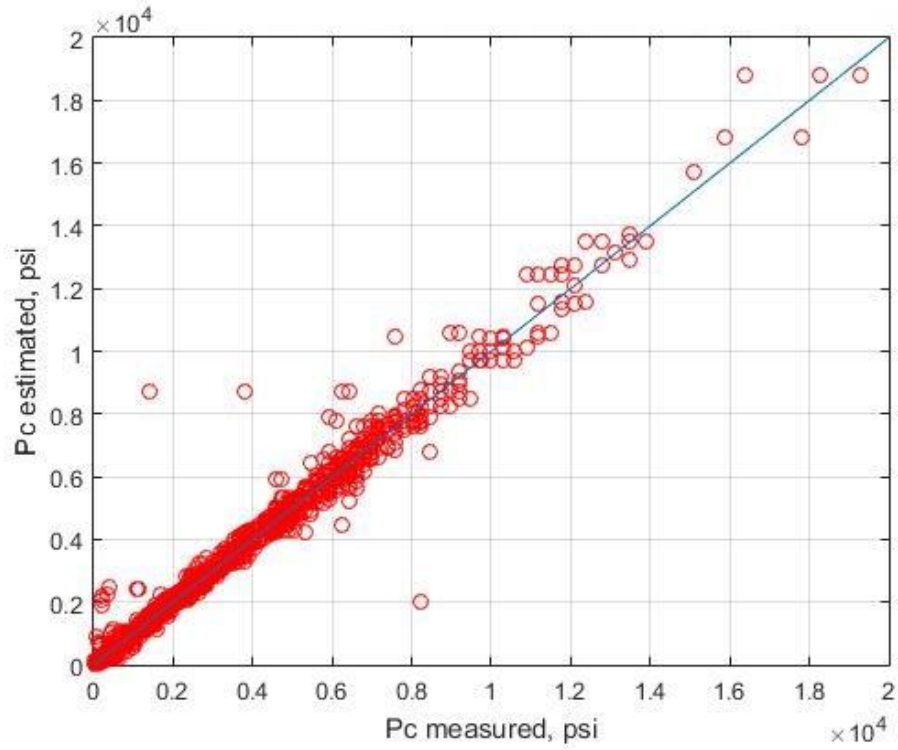


Figure 29: Predicted vs. measured values using Decision tree algorithm (Testing).

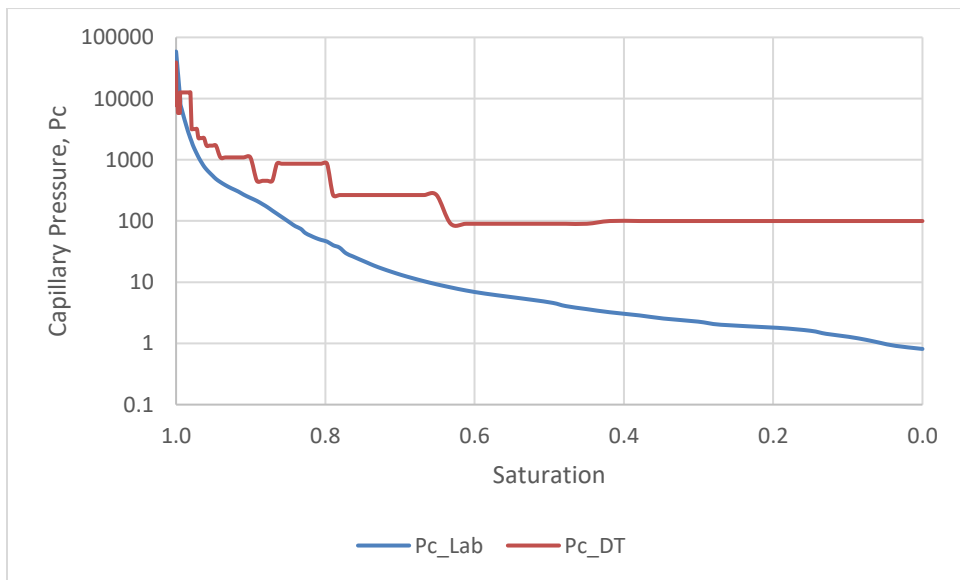


Figure 30: A sample of bi-modal sata using decision tree algorithm in log-log scale plot

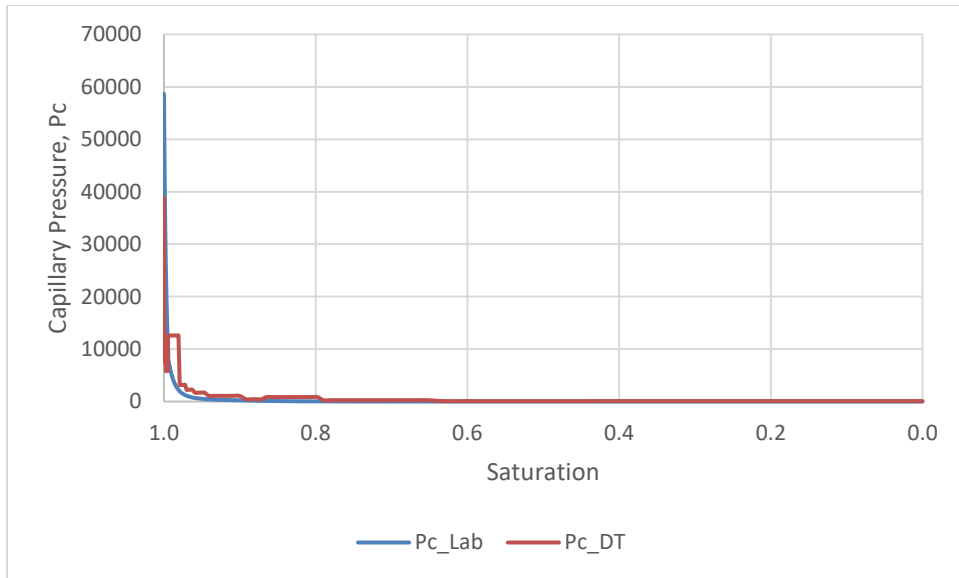


Figure 31: A sample of bi-modal sata using decision tree algorithm in cartesian scale plot

Figures (32-33) show a crossplot of the measured vs. predicted capillary pressure in training and testing for combined modals data the accuracy of this model was 100% in training and 41% in testing using decision tree technique.

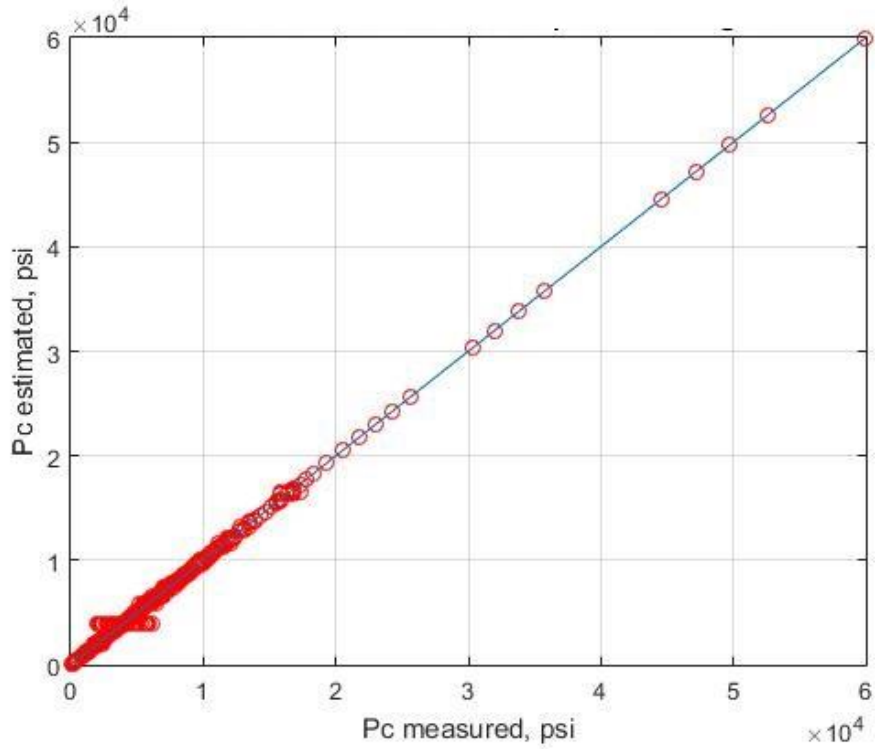


Figure 32: Predicted vs. measured values using Decision tree algorithm (Training).

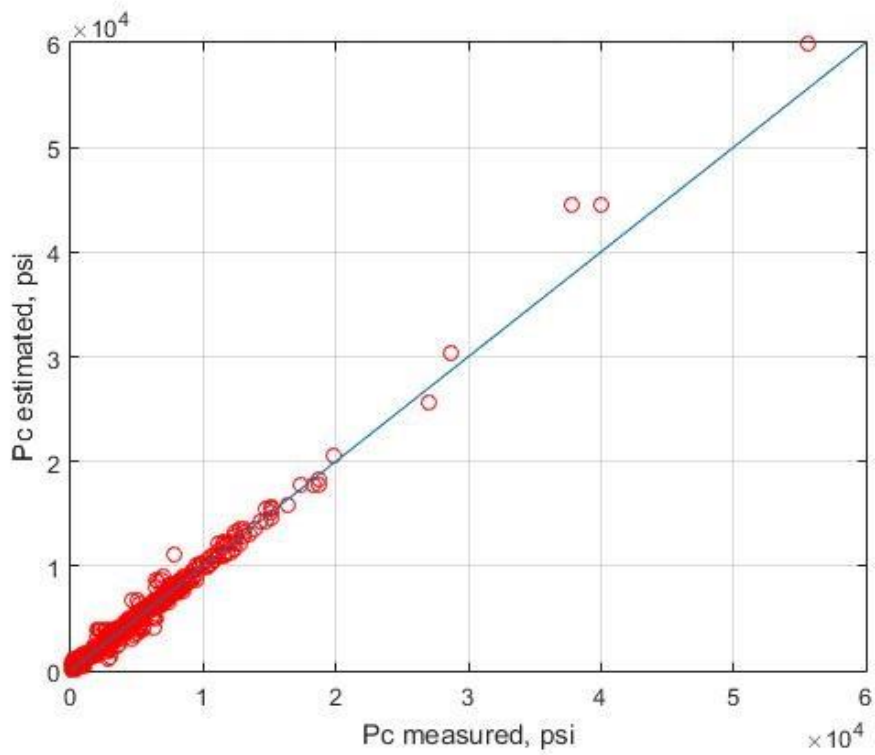


Figure 33: Predicted vs. measured values using Decision tree algorithm (Testing).

Cross plots of the results for training and testing for the rest of the techniques for uni-modal, bi-modal and combined modals cases are provided in **Appendix-B**.

5.10 Nearest Neighbor Curve Prediction (NNCP)

Using the above methods to predict the capillary pressure problem is one way to solve this problem which showed good results for some techniques. However, it was noticed that the results were not satisfactory when individual curves were plotted. Another way to solve this problem is by using the Nearest Neighbor Curve Prediction (NNCP) method. The approach has yielded promising results and is under patenting process. As mentioned earlier, the objective of this study is to predict capillary pressure curves of untested core samples. The input data is a set obtained from conventional core analysis and consists of porosity, permeability, and grain density data.

202 core samples with corresponding capillary pressure vs saturation curves were used in this study. Each porosity, permeability, and grain density set corresponds to a 50-point capillary pressure vs saturation curve.

A more logical approach to tackle this problem is to make the program learn the target curves with their corresponding input sets and then predict the curve for new input data within the range of the training parameters.

Due to different measurement conditions during MICP tests, generated capillary pressure vs saturation curves do not have the same number of points; i.e. test sample # 1 has 50 points of capillary pressure vs. saturation but test sample # 2 has 72 points of capillary pressure vs. saturation. This issue creates a difficulty in comparing statistically between results generated from

the lab and results generated from the NNCP technique. Therefore, an interpolation routine was used to estimate the error between the predicted curve and the actual curve.

In the proposed model (Figure 34), randomly selected 70% of the samples is considered for training and the remaining is used for testing. It may be noted that in case of NNCP, the training data is basically a reference data with no specific training involved. Each training sample corresponds to a Capillary Pressure (P_c) curve against Mercury Saturation (S). It has been observed that saturation points, S , are different for each sample. Therefore, to ensure portraying the P_c curve in a fixed S scale, that saturation points are standardized and the corresponding P_c is computed either by interpolation or extrapolation.

In the next phase, the nearest sample is selected from the training dataset which has minimum distance with respect to the test sample (Figure 34). The standardized P_c curve corresponding to the nearest sample is selected and drawn against the actual standardized P_c curve of the target sample. The errors and other other checks are carried out to test the performance of this method.

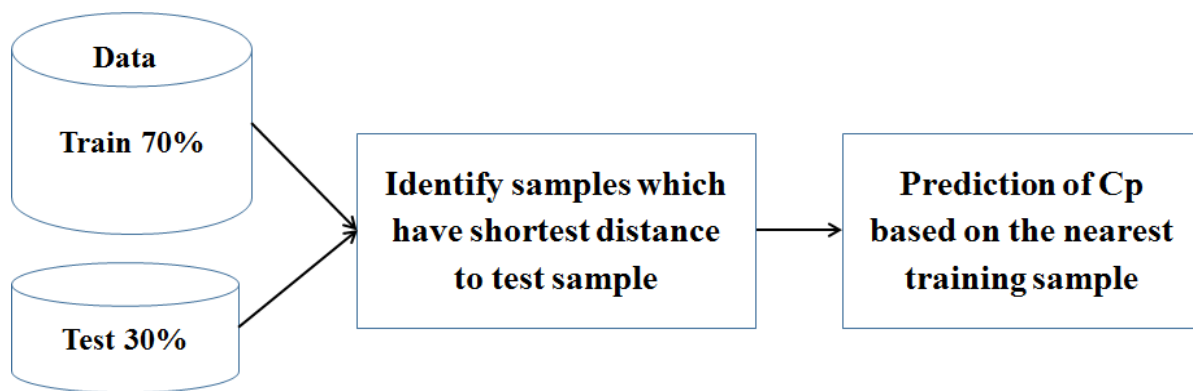


Figure 34. Capillary pressure curve prediction based on the nearest datapoint

5.11 Data Classification

In order to use this method correctly and to produce the best results, classification of the data has to be done based on a certain criterion.

Modality: Rock modality identifies the number of porosity systems a core sample possesses. Amongst the available data, 65 core samples showed uni-modal behavior and 137 core samples showed bi-modal behavior.

Flow Zone Units: Using this classification method, each sample is assigned to a class representing a flow zone unit. Amongst the available data, uni-modal group had three classes and bi-modal group had 5 classes. Figures (35) and (36) show the data points with respect to flow zones for both uni-modal and bi-modal groups. As these figures show, uni-modal data can be classified into three classes of flow units and bi-modal data into five classes of flow units.

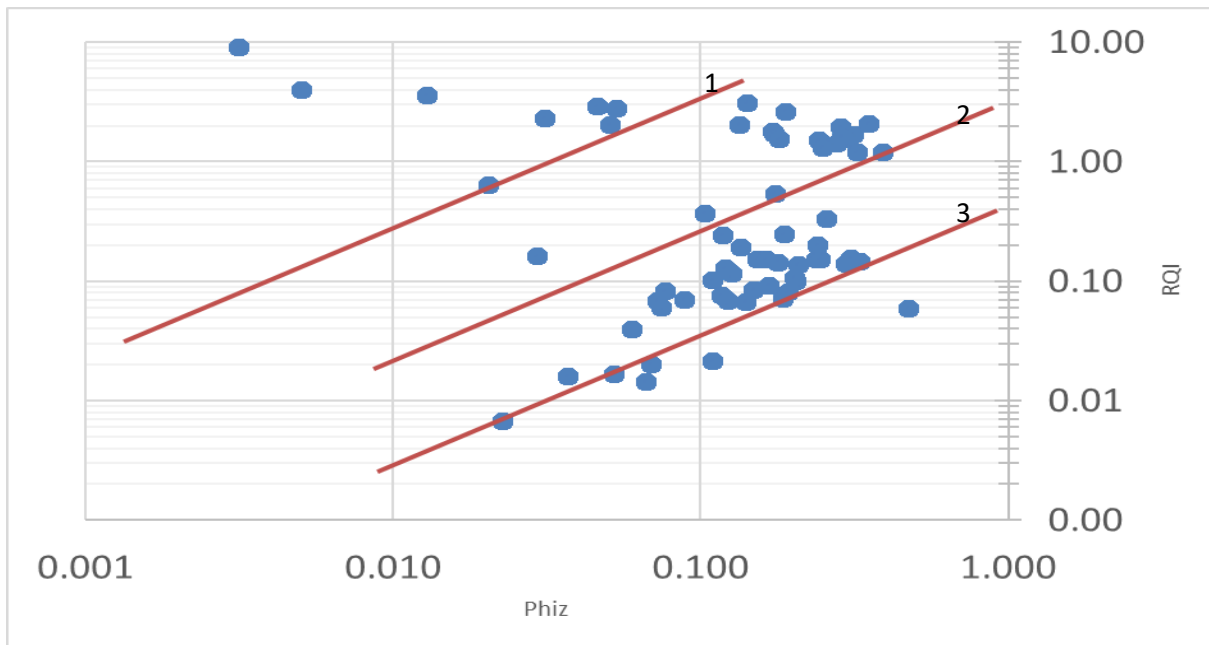


Figure 35: Flow Zone Units for Uni-modal group

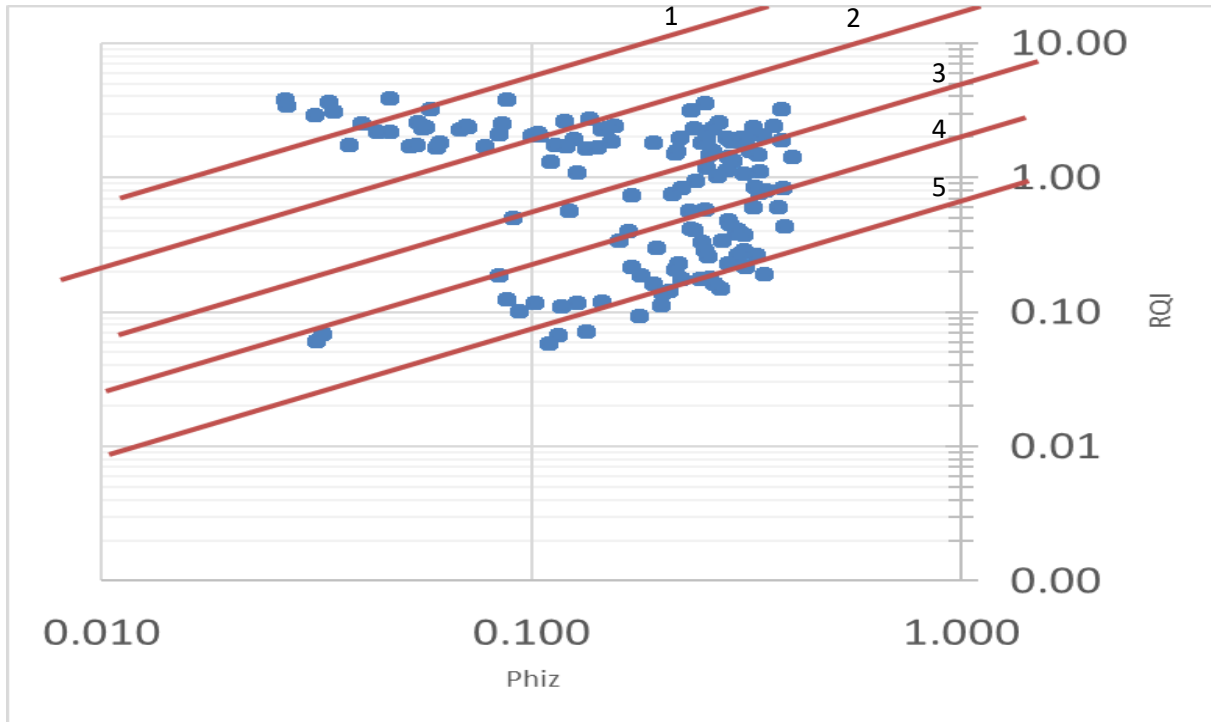


Figure 36: Flow Zone Units for Bi-modal group

Table 8 shows the number of core samples under each class for the two modal groups.

Table 8: Number of core samples in each flow zone

Modal	Uni-modal	Bi-modal
Flow Zone 1	6	15
Flow Zone 2	19	27
Flow Zone 3	33	35
Flow Zone 4	-	24
Flow Zone 5	-	35
% of data used in training	70	70
% of data used in testing	30	30

5.12 J-function Approach

J-function is a mathematical averaging method representing samples having different porosities and permeabilities within a given formatoin. In this study, J-function is used to create an average capillary pressure equation for each flow zone for each modal behavior. For a given range of FZI values, each core sample refers to a J-function curve. Tables (9) and (10) show the ranges of FZI values for each J-function group for the uni-modal data and the bi-modal data, respectively.

Table 9: FZI range of each J-function group for uni-modal data

J-function Group	FZI Range
1	(691 – 2337)
2	(64 – 483)
3	(9 – 45)

Table 10: FZI range of each J-function group for bi-modal data

J-function Group	FZI Range
1	(42 – 142)
2	(12 – 34)
3	(4 – 10)
4	(1.4 – 3)
5	(0.5 – 1.3)

Figures (37-39) show the J-function values for each class for the uni-modal dataset. Figure (40) shows the J-function curves of each group vs. saturation for the uni-modal data for each FZI range.

It may be noted that these curves are obtained by averaging the relevant values in each class. These curves show a uni-modal behavior as their original curves did.

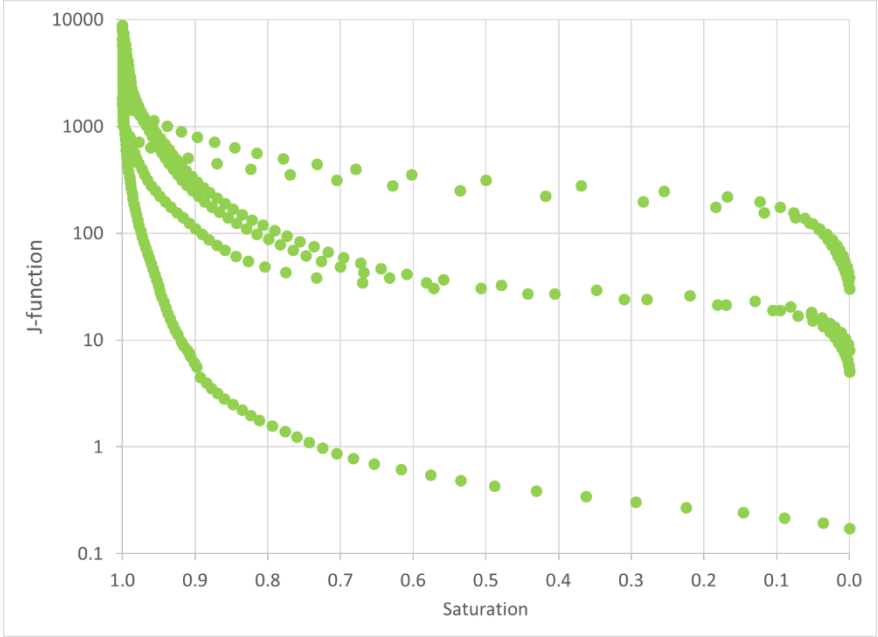


Figure 37: J-function values for uni-modal class # 1 samples

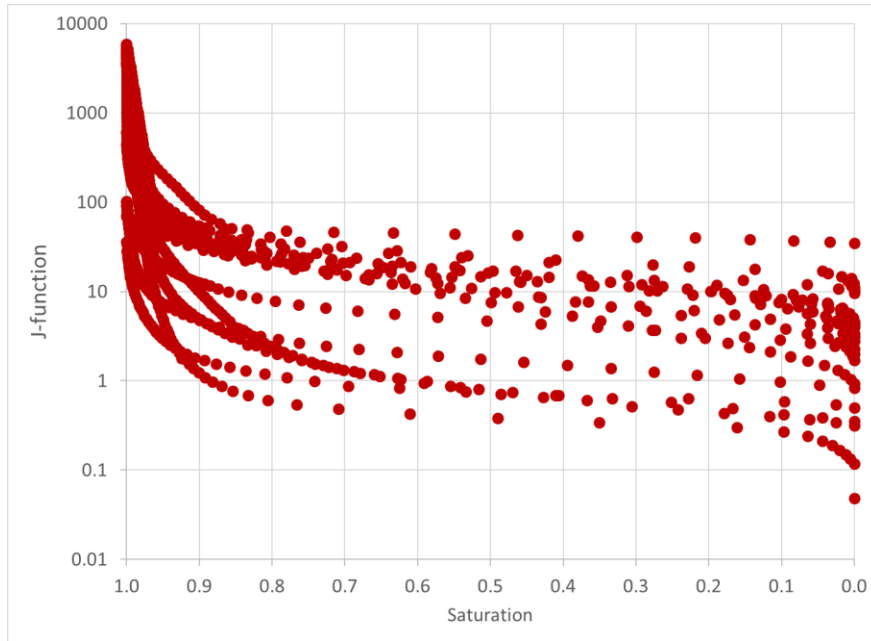


Figure 38: J-function values for uni-modal class # 2 samples

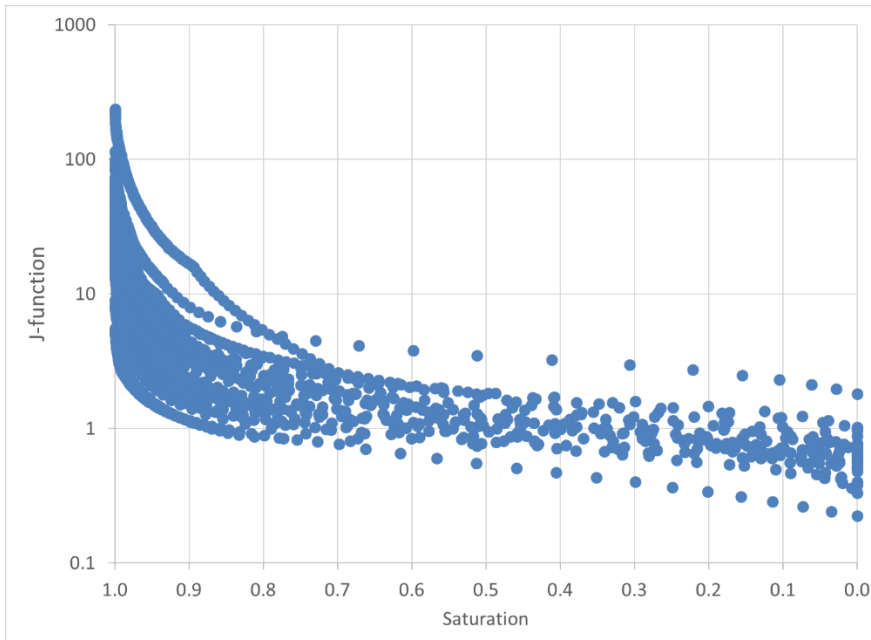


Figure 39: J-function values for uni-modal class # 3 samples

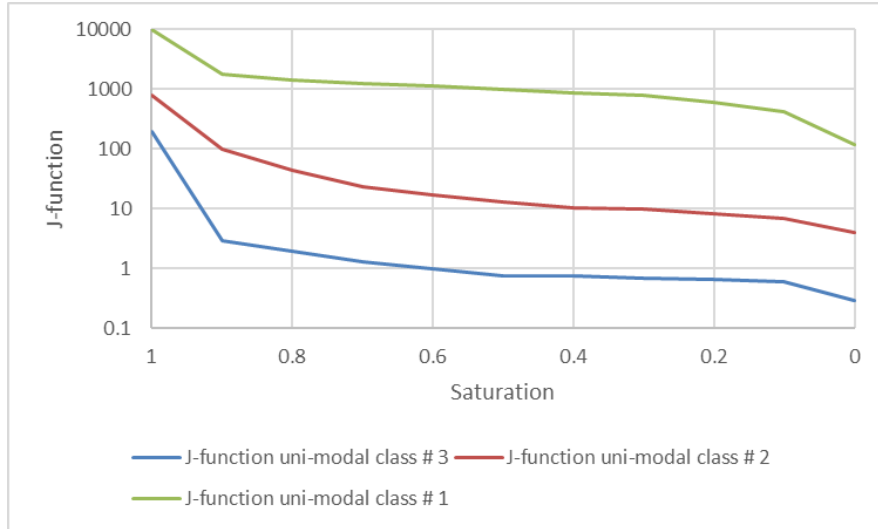


Figure 40: J-function curves based on ranges of FZI for uni-modal data

Figures (41-45) show the J-function values for the bi-modal dataset for classes 1 through 5, respectively. Figure (46) shows J-function curves of each group vs. saturation for the bi-modal data for each FZI range. It can be seen from the figure that these curves do not show bi-modal behavior as their original curves did. Therefore, applying these curves to predict capillary pressure of new samples will not generate bi-modal curves. Thus, it will not be used to predict the capillary pressure using this method as it will generate non-bi-modal results. It may be noted here that the J-function curves were generated by averaging curves that fall under the same class. These curves have different porosity systems. These systems do not have the same volume for all the core samples in that class. At some point in the averaging process, small and large systems are mixed up together. Hence, averaging at this stage generates non-uniform J-curves. Consequently, produced J-function is not going to be a bi-modal curve that represents an average for bi-modal capillary pressure curves.

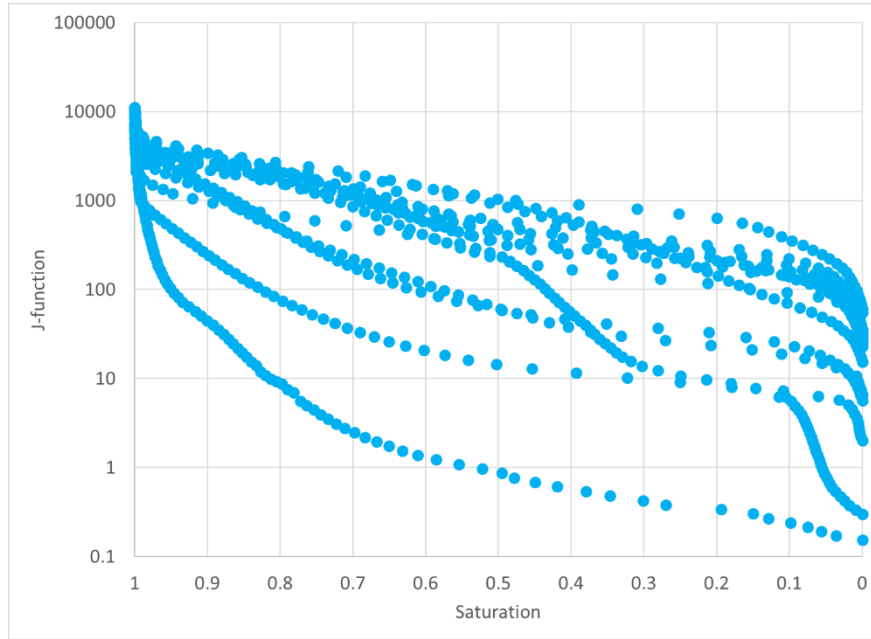


Figure 41: J-function values for bi-modal class # 1 samples

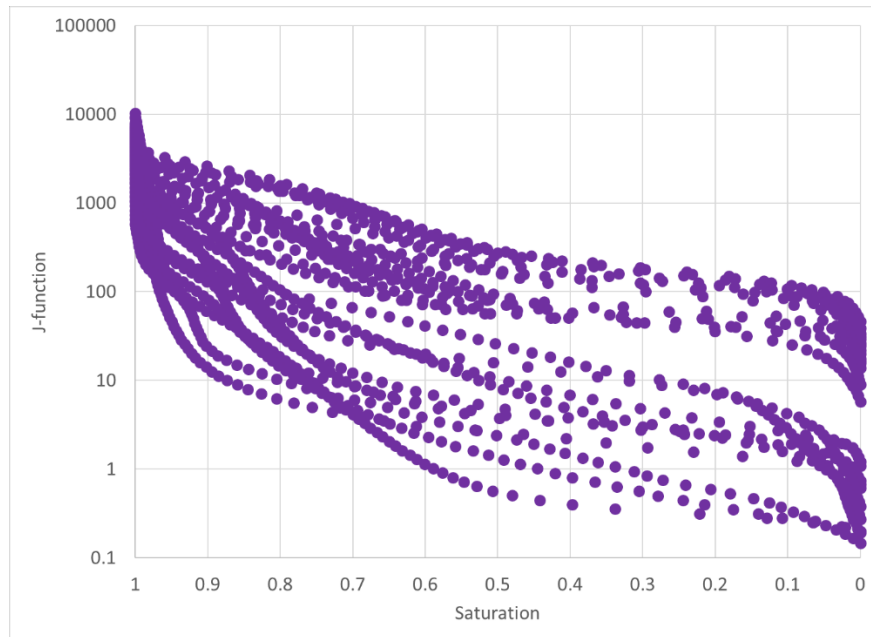


Figure 42: J-function values for bi-modal class # 2 samples

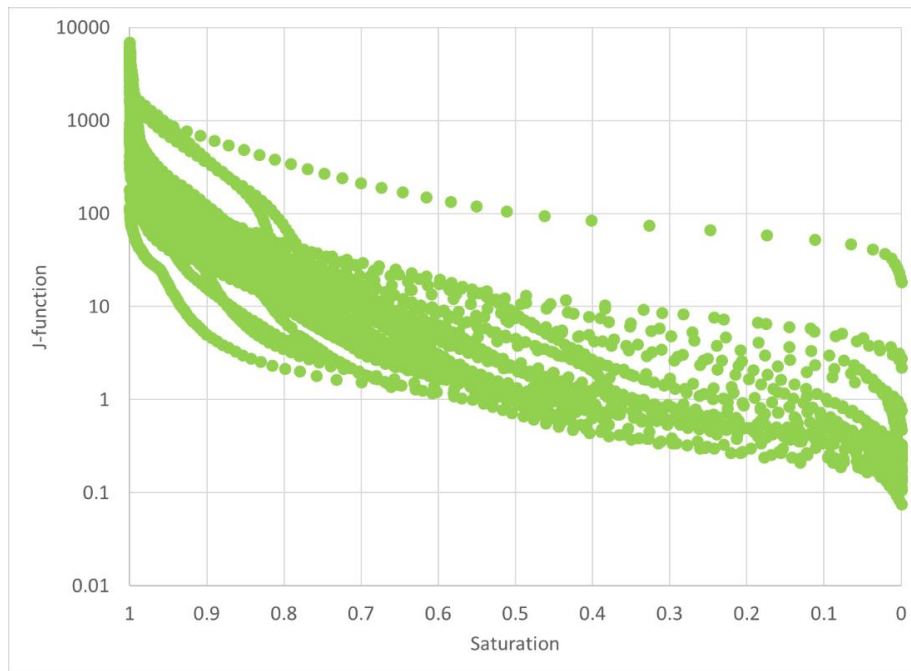


Figure 43: J-function values for bi-modal class # 3 samples

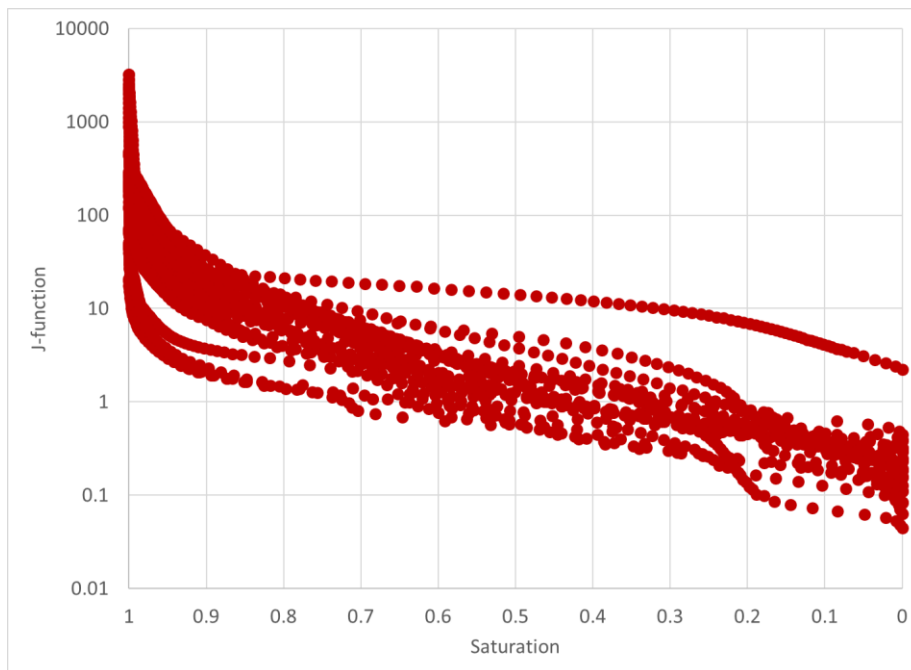


Figure 44: J-function values for bi-modal class # 4 samples

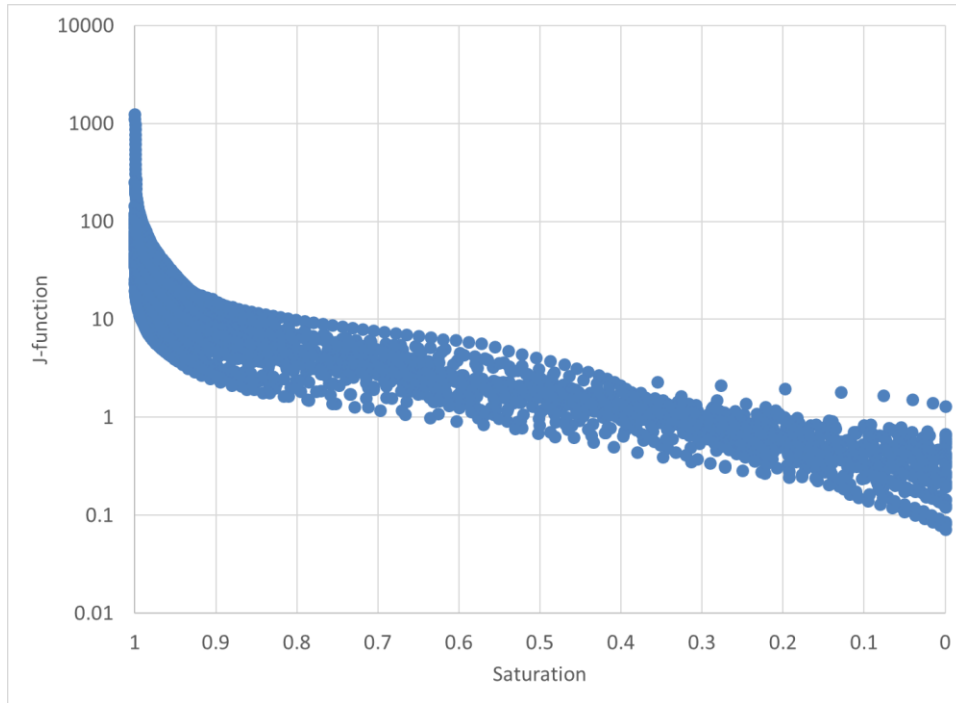


Figure 45: J-function values for bi-modal class # 5 samples

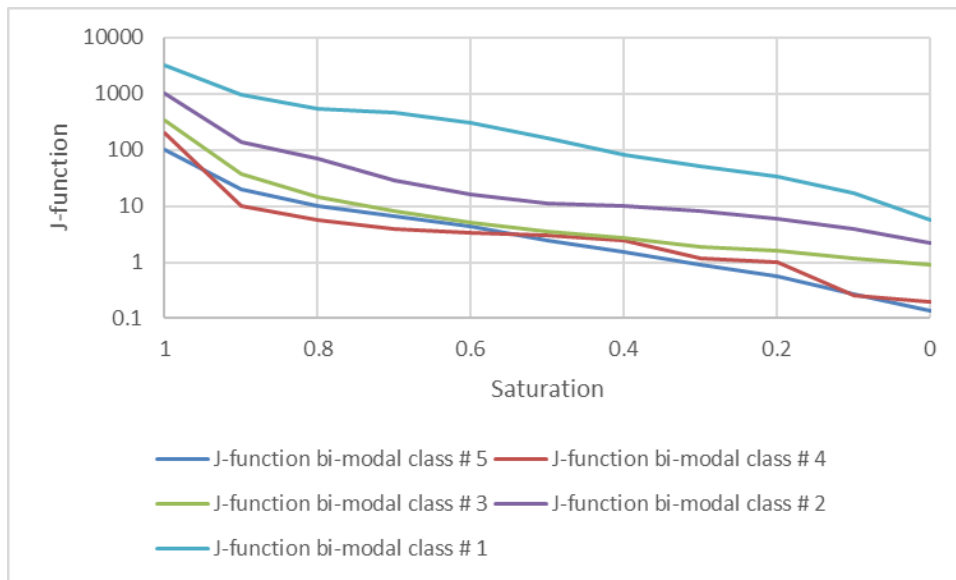


Figure 46: J-function curves based on ranges of FZI for bi-modal data

5.13 Discussion of Results from NNCP and J-function approach

Uni-modal class # 1: According to the flow zone unit classification technique, only six samples fall under uni-modal class 1 group. 4 samples were used for training and 2 for testing. Figures (47-48) show the comparison between the NNCP and J-function predictions with the laboratory data for the uni-modal class # 1 samples. The results from the NNCP model are the closest curve presented in blue and the average of the closest three curves presented in green. The J-function result is presented in purple and the laboratory curve is presented in red. As shown in figure (47) and table (11), the average of the colosest three curves and the J-function methods produced the worst results with error values of 3.04% and 84.59%, respectively, for test sample # 1. However, the NNCP produced the colsest curve to the target data with an error of 1.77%.

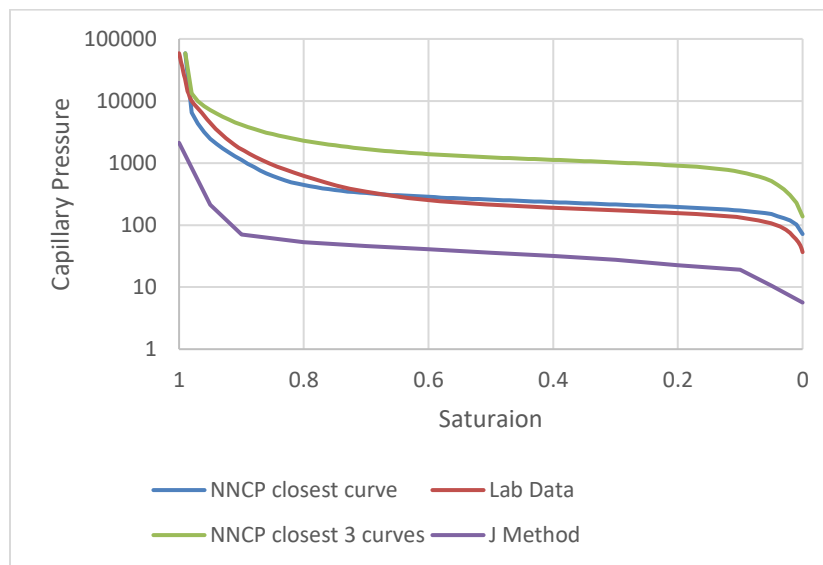


Figure 47: Comparison of NNCP, the average of the closest three curves and J-function to predict the capillary pressure with the laboratory data for testing sample # 1 in class 1

For test sample # 2, all three methods produced bad results with J-function being close to the lab curve with an error of 120%. The NNCP prediction failed for this sample due to the low number

of training data. The NNCP closest curve showed an error of 184% while the average of the three closest curves showed an error of 235%, Figure (48) and table (11).

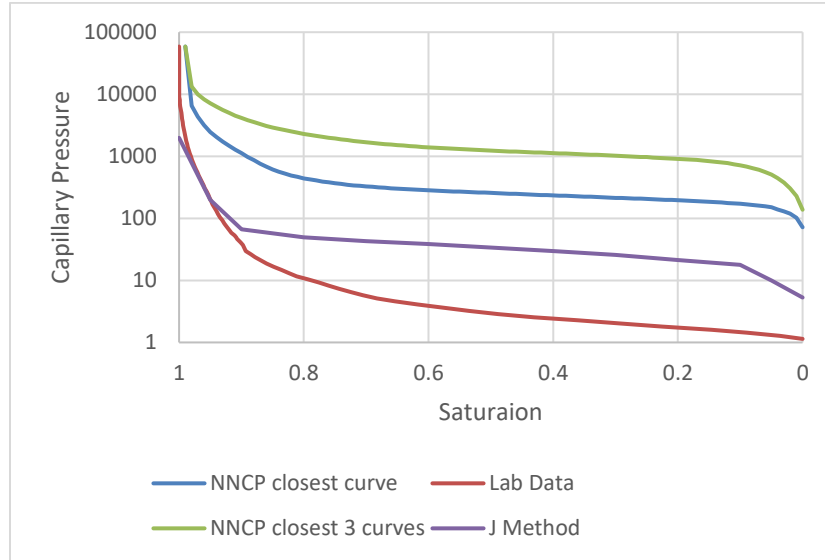


Figure 48: Comparison of NNCP, the average of the closest three curves, and J-function to predict the capillary pressure with the laboratory data for testing sample # 2 in class 1

Table 11: Average error of NNCP and J-function methods versus laboratory data for class 1

Sample #	NNCP average error, %	Average error of average of closest 3 curves, %	J-function average error, %
1	1.77	3.04	84.59
2	184	235	120

Uni-modal class # 2: Similar to uni-modal class # 1, the flow zone unit classification technique shows that 19 samples fall under uni-modal class 2 group. 13 samples were used for training and 6 samples were used for testing. Figures (49-54) show the results of the uni-modal for class # 2 comparing the NNCP and J-function predictions to the laboratory data. In this group, the J-function and the NNCP methods have similar results. Some of them were good with an error range of (1.97 – 5.2) and some of them were poor with an error range of (16.85 – 89.79).

Test sample # 1 shows that the J-function was the furthest curve from the lab results with an error of 76.27% while the NNCP showed excellent results with a low error of 1.93% and 1.65% for the closest curve and the three closest curves, respectively. Figure (49) and table (12).

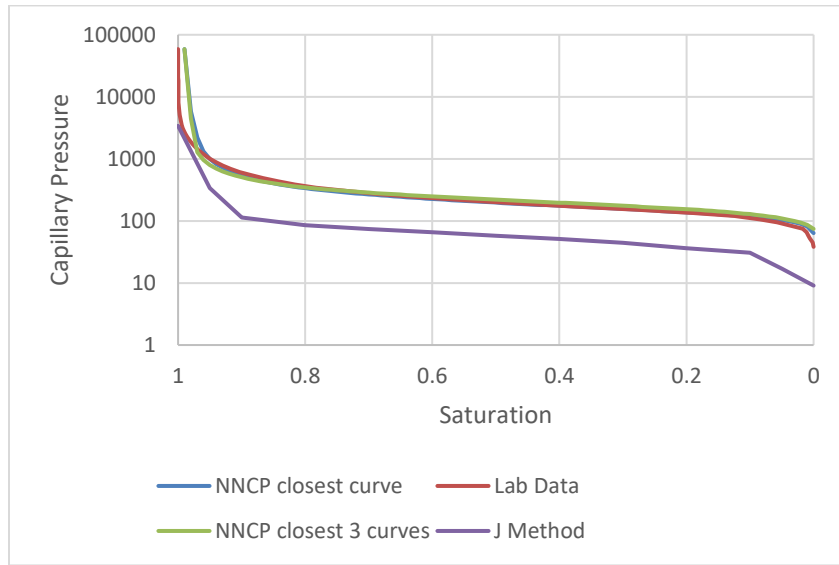


Figure 49: Comparison of NNCP, the average of the closest three curves, and J-function to predict the capillary pressure with the laboratory data for testing sample # 1 in class 2

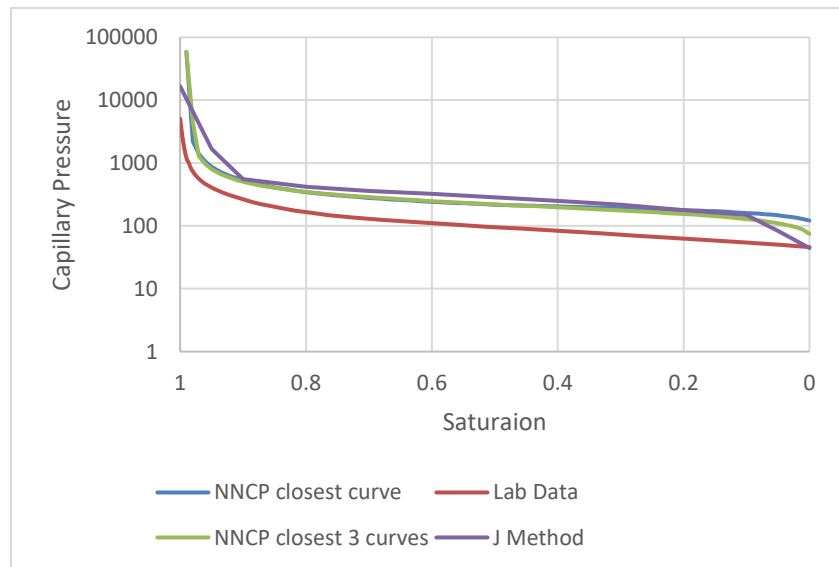


Figure 50: Comparison of NNCP, the average of the closest three curves, and J-function to predict the capillary pressure with the laboratory data for testing sample # 2 in class 2

Test sample # 2 shows all methods produced close curves with low error of 5.2%, 4.99% and 3.35% for the NNCP closest curve, the closest three curves, and the J-function, respectively. Figure (50) and table (12).

Test sample # 3 also shows that all methods produced close curves with fair error of 16.85%, 16.5% and 16.5% for the NNCP closest curve, the closest three curves, and the J-function, respectively. Figure (51) and table (12).

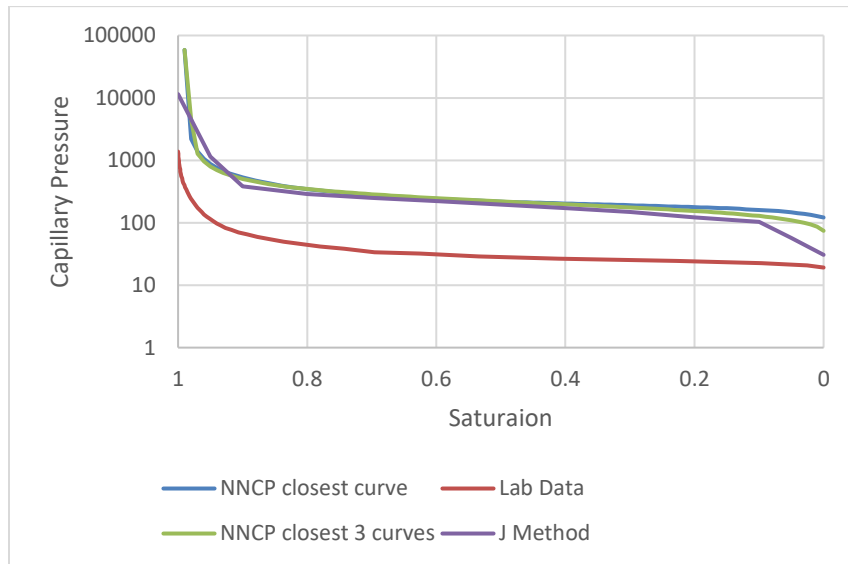


Figure 51: Comparison of NNCP, the average of the closest three curves, and J-function to predict the capillary pressure with the laboratory data for testing sample # 3 in class 2

Test sample # 4 shows that the J-function method produced closer curve to the lab curve than the NNCP method with an error of 57.4%. While the error from the NNCP method was 79.04% and 77.31% for the closest curve and the closest three curves, respectively. Figure (52) and table (12).

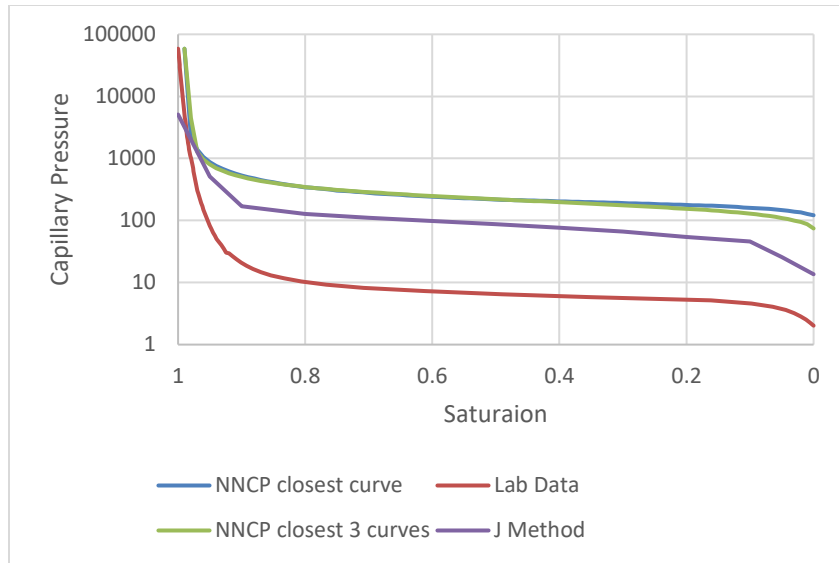


Figure 52: Comparison of NNCP, the average of the closest three curves, and J-function to predict the capillary pressure with the laboratory data for testing sample # 4 in class 2

Test sample # 5 also shows that the J-function method produced closer curve to the lab curve than the NNCP method with an error of 35.6%. while the error from the NNCP method was 48.83% and 47.66% for the closest curve and the closest three curves, respectively. Figure (53) and table (12).

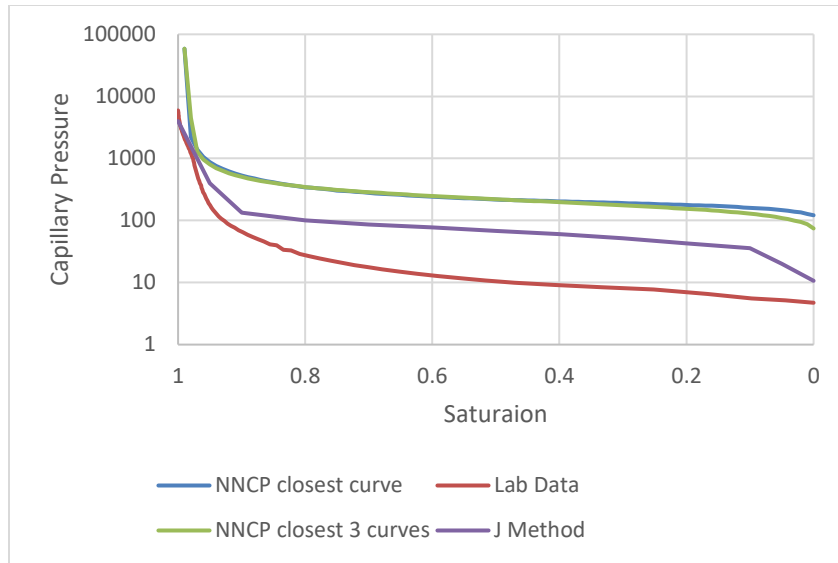


Figure 53: Comparison of NNCP, the average of the closest three curves, and J-function to predict the capillary pressure with the laboratory data for testing sample # 5 in class 2

Test sample # 6 also shows that the J-function method produced closer curve to the lab curve than the NNCP method with an error of 54.45%. While the error from the NNCP method was 89.79% and 87.6% for the closest curve and the closest three curves, respectively. Figure (54) and table (12).

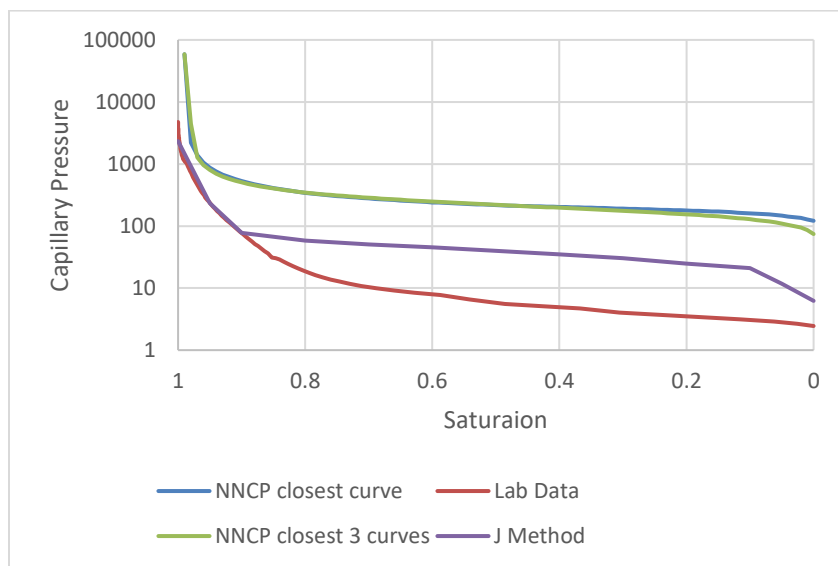


Figure 54: Comparison of NNCP, the average of the closest three curves, and J-function to predict the capillary pressure with the laboratory data for testing sample # 6 in class 2

Table (12) shows the average error of the NNCP and J-function methods compared to laboratory data for class 2 test samples.

Table 12: Average error of NNCP and J-function methods versus laboratory data for class 2

Sample #	NNCP average error, %	Average error of average of closest 3 curves, %	J-function average error, %
1	1.93	1.65	76.27
2	5.2	4.99	3.35
3	16.85	16.5	16.5
4	79.04	77.31	57.4
5	48.83	47.66	35.6
6	89.79	87.6	54.45

Uni-modal class # 3: similar to uni-modal calss # 1 & 2, the flow zone unit classification technique shows 33 samples fall under uni-modal class 3 group. 23 samples were used for training and 10 samples were used for testing. Figures (55-64) show the results of the uni-modal for class 3 comparing the NNCP and J-function predictions to the laboratory data. In this class, all of the methods showed good match to the lab curve, however; the NNCP had the least error (1.45 – 7.6).

Test sample # 1 shows that the J-function was the furthest curve from the lab results with an error of 51.07% while the NNCP showed excellent results with a low error of 1.95% and 2.03% for the closest curve and the three closest curves, respectively. Figure (55) and table (13).

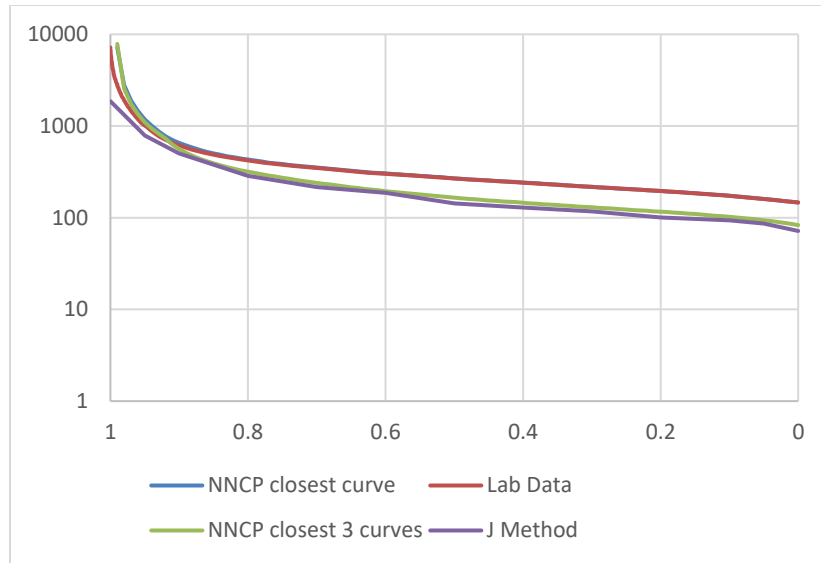


Figure 55: Comparison of NNCP, the average of the closest three curves, and J-function to predict the capillary pressure with the laboratory data for testing sample # 1 in class 3

Similar to test sample # 1, test sample # 2 shows that the J-function was the furthest curve from the lab results with an error of 22.98% while the NNCP showed excellent results with a low error of 2.07% and 2.27% for the closest curve and the three closest curves, respectively. Figure (56) and table (13).

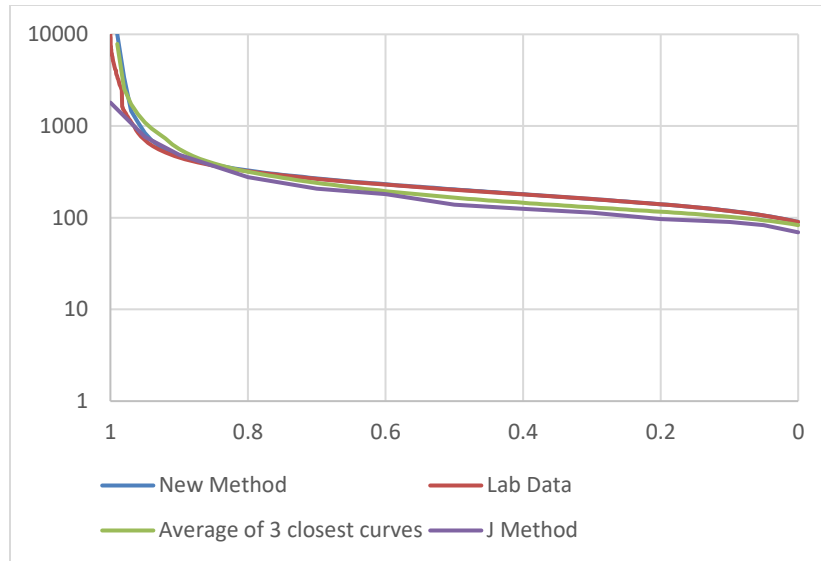


Figure 56: Comparison of NNCP, the average of the closest three curves, and J-function to predict the capillary pressure with the laboratory data for testing sample # 2 in class 3

Also test sample # 3 shows that the J-function was the furthest curve from the lab results with an error of 50.58% while the NNCP showed excellent results with a low error of 2.01% and 2.14% for the closest curve and the three closest curves, respectively. Figure (57) and table (13).

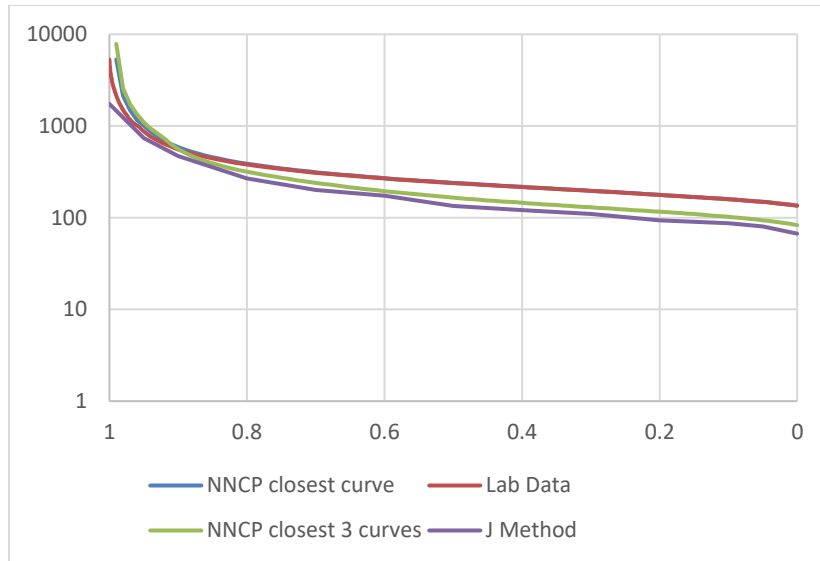


Figure 57: Comparison of NNCP, the average of the closest three curves, and J-function to predict the capillary pressure with the laboratory data for testing sample # 3 in class 3

Test sample # 4 shows that the J-function was the furthest curve from the lab results with an error of 20.73% while the NNCP showed excellent results with a low error of 1.45% and 1.37% for the closest curve and the three closest curves, respectively. Figure (58) and table (13).

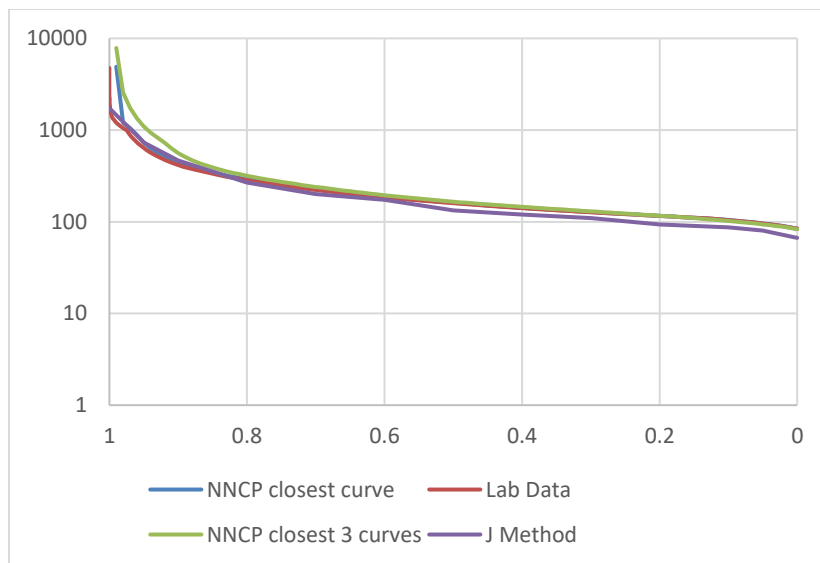


Figure 58: Comparison of NNCP, the average of the closest three curves, and J-function to predict the capillary pressure with the laboratory data for testing sample # 4 in class 3

Test sample # 5 shows that the J-function was the furthest curve from the lab results with an error of 42.96% while the NNCP showed excellent results with a low error of 2.07% and 2.21% for the closest curve and the three closest curves, respectively. Figure (59) and table (13).

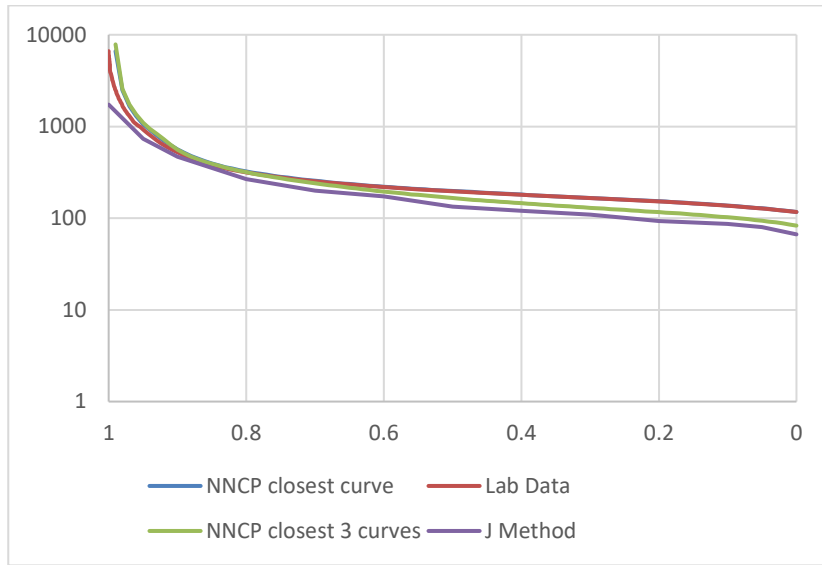


Figure 59: Comparison of NNCP, the average of the closest three curves, and J-function to predict the capillary pressure with the laboratory data for testing sample # 5 in class 3

Test sample # 6 shows that the J-function was the furthest curve from the lab results with an error of 43.04% while the NNCP showed excellent results with a low error of 2.08% and 2.21% for the closest curve and the three closest curves, respectively. Figure (60) and table (13).

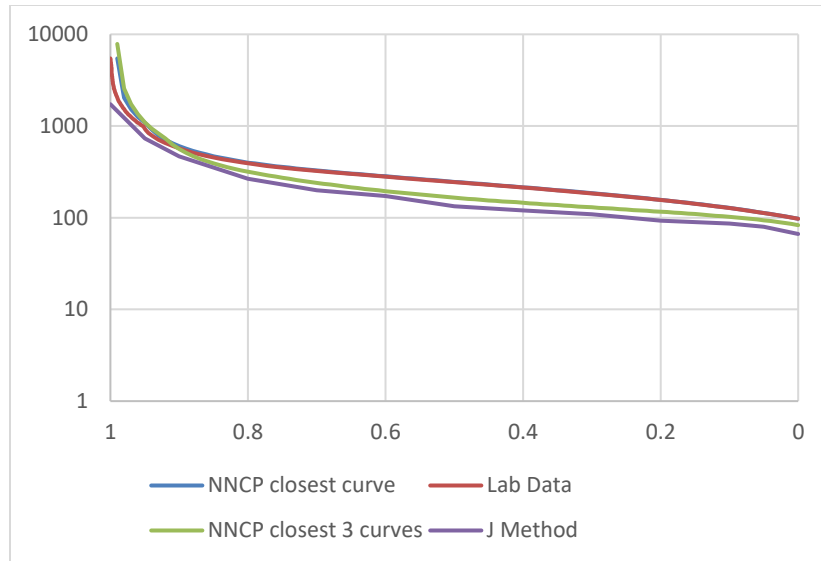


Figure 60: Comparison of NNCP, the average of the closest three curves, and J-function to predict the capillary pressure with the laboratory data for testing sample # 6 in class 3

Test sample # 7 shows that the J-function was the furthest curve from the lab results with an error of 48.09% while the NNCP showed excellent results with a low error of 2.06% and 2.13% for the closest curve and the three closest curves, respectively. Figure (61) and table (13).

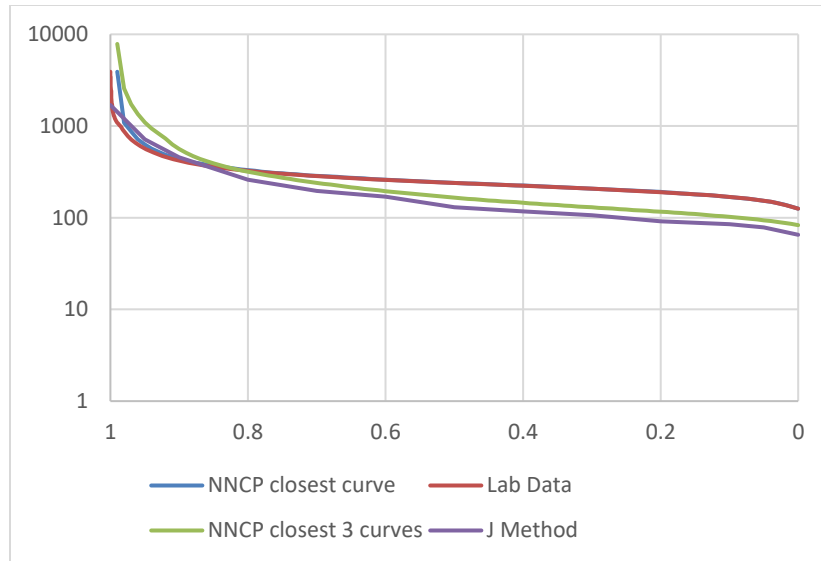


Figure 61: Comparison of NNCP, the average of the closest three curves, and J-function to predict the capillary pressure with the laboratory data for testing sample # 7 in class 3

Test sample # 8 shows that the J-function was the furthest curve from the lab results with an error of 44.56% while the NNCP showed excellent results with a low error of 4.97% and 4.77% for the closest curve and the three closest curves, respectively. Figure (62) and table (13).

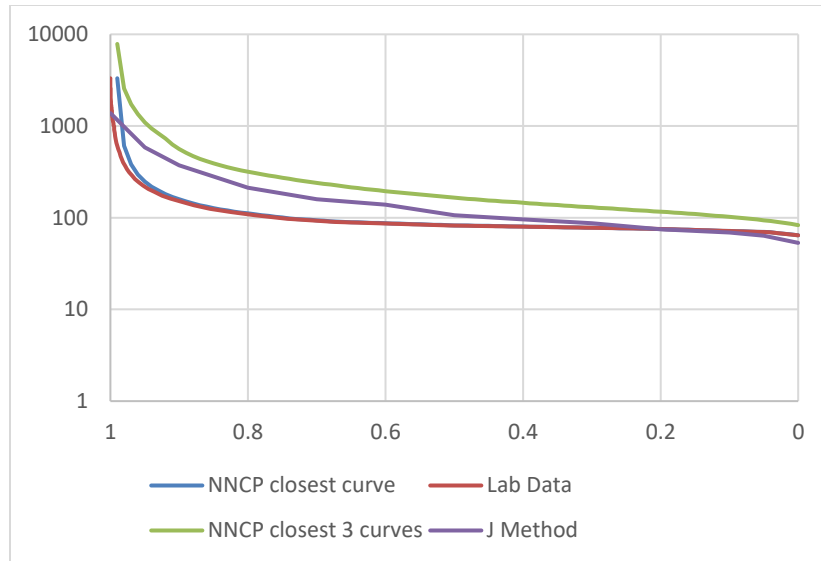


Figure 62: Comparison of NNCP, the average of the closest three curves, and J-function to predict the capillary pressure with the laboratory data for testing sample # 8 in class 3

Test sample # 9 shows that the J-function was the furthest curve from the lab results with an error of 34.03% while the NNCP showed excellent results with a low error of 1.58% and 1.69% for the closest curve and the three closest curves, respectively. Figure (63) and table (13).

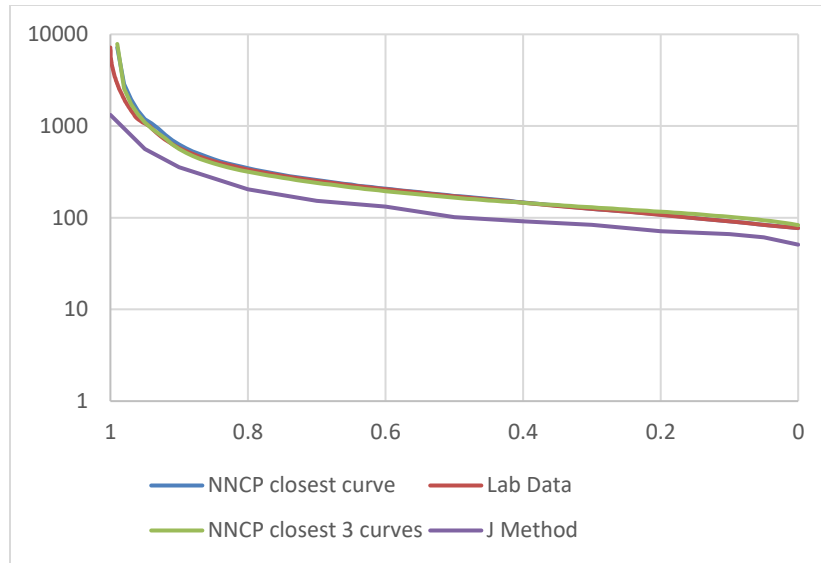


Figure 63: Comparison of NNCP, the average of the closest three curves, and J-function to predict the capillary pressure with the laboratory data for testing sample # 9 in class 3

Test sample # 10 shows that the J-function was the furthest curve from the lab results with an error of 49.80% while the NNCP showed excellent results with a low error of 7.6% and 7.44% for the closest curve and the three closest curves, respectively. Figure (64) and table (13). It is evident that the more samples fall under this flow unit, the better the results from NNCP.

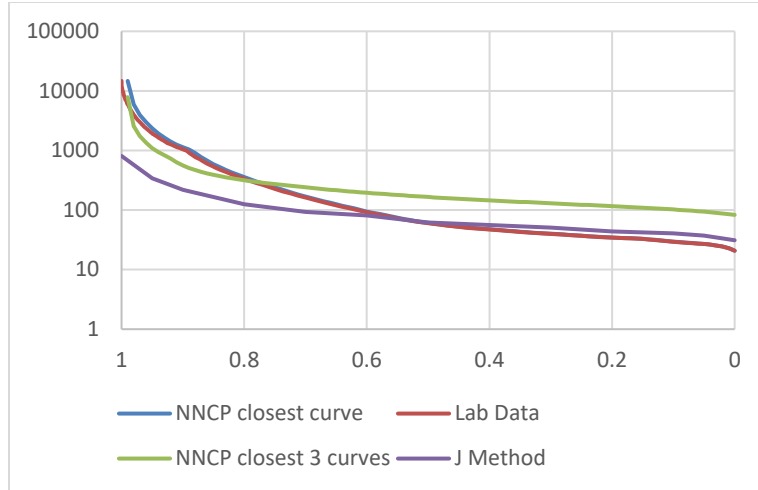


Figure 64: Comparison of NNCP, the average of the closest three curves, and J-function to predict the capillary pressure with the laboratory data for testing sample # 10 in class 3

Table (13) shows the average error of the NNCP and J-function methods compared to laboratory data for class 3 test samples.

Table 13: Average error of NNCP and J-function methods versus laboratory data for class 3

Sample #	NNCP average error, %	Average error of average of closest 3 curves, %	J-function average error, %
1	1.95	2.03	51.07
2	2.07	2.27	22.98
3	2.01	2.14	50.58
4	1.45	1.37	20.73
5	2.07	2.21	42.96
6	2.08	2.21	43.04
7	2.06	2.13	48.09
8	4.97	4.77	44.56
9	1.58	1.69	34.03
10	7.6	7.44	49.80

Bi-modal class # 1: the flow zone unit classification technique shows 15 samples fall under bi-modal class 1 group. 10 samples were used for training and 5 samples were used for testing. Since we have already discussed the difficulty of applying J-function on bi-modal data, it is not going to

be part of the comparison between the different methods below, however; for the sake of trying it and to show its limitation, it is going to be discussed in bi-modal class # 5. Figures (65-69) show the results of the bi-modal for class 1 comparing the NNCP predictions to the laboratory data.

Test sample # 1 shows that the NNCP for the closest curve and the NNCP closest three curves produced close curves to the lab curve with low error of 2.01% and 2.19%, respectively. Figure (65) and table (14).

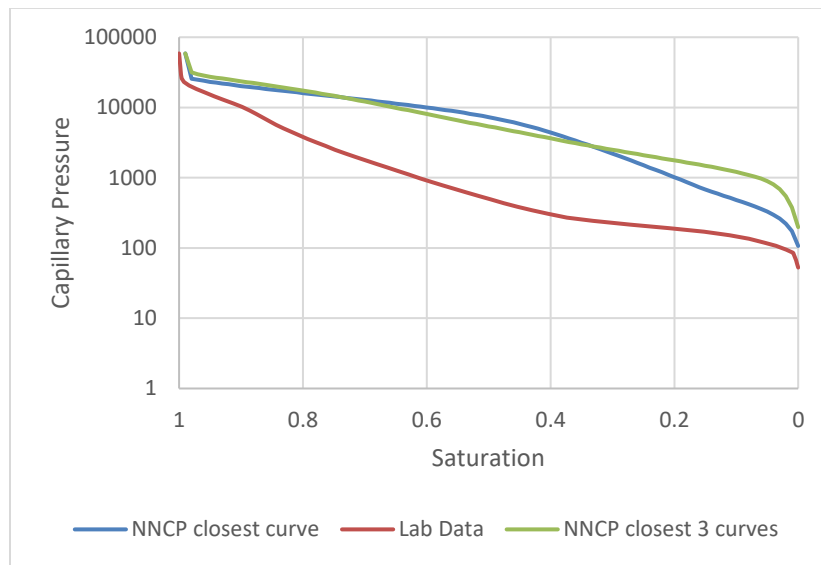


Figure 65: Comparison of NNCP, the average of the closest three curves to predict the capillary pressure compared to laboratory data for testing sample # 1 in class 1

Similarly, test sample # 2 shows that the NNCP for the closest curve and the NNCP closest three curves produced close curves to the lab curve with low error of 4.8% and 4.78%, respectively. Figure (66) and table (14).

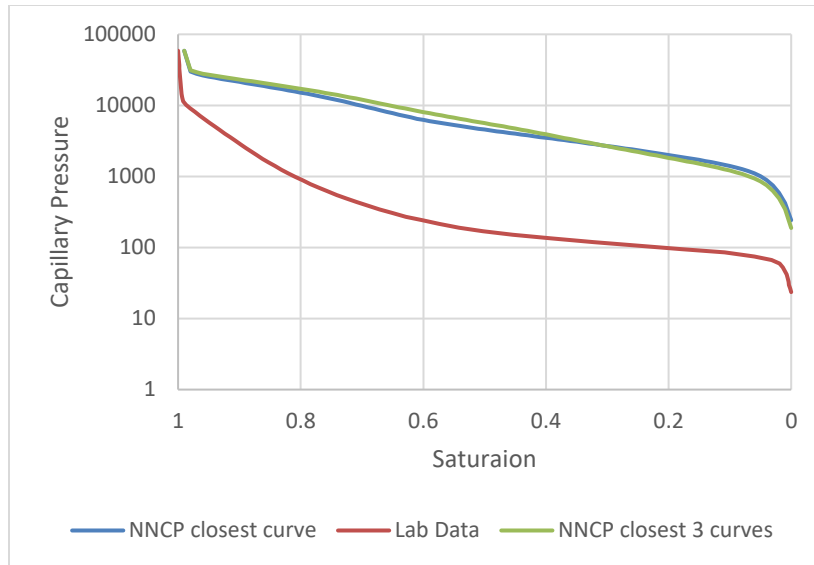


Figure 66: Comparison of NNCP, the average of the closest three curves to predict the capillary pressure compared to laboratory data for testing sample # 2 in class 1

Test sample # 3 shows excellent match between the NNCP closest curve and the closest three curves with respect to lab curves with a very low error of 0.18% and 0.2%, respectively. Figure (67) and table (14).

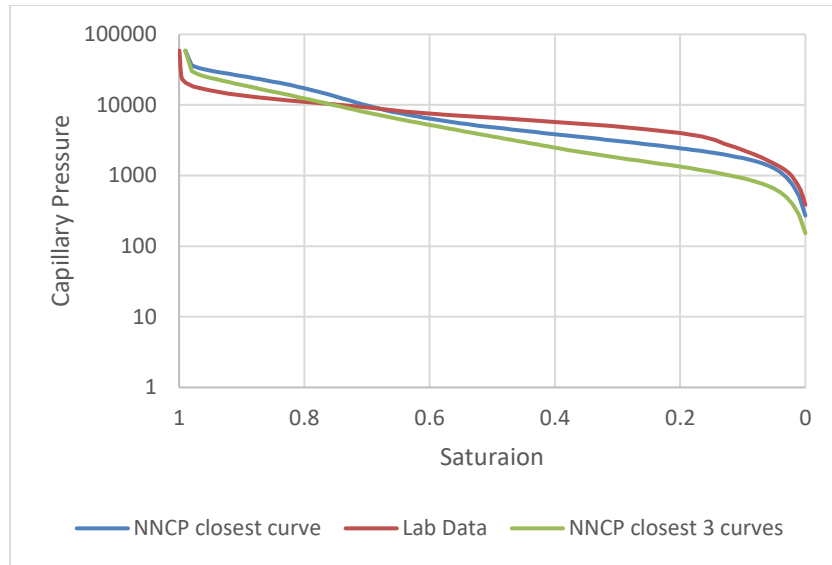


Figure 67: Comparison of NNCP, the average of the closest three curves to predict the capillary pressure compared to laboratory data for testing sample # 3 in class 1

Test sample # 4 shows poor match between the NNCP closest curve and the closest three curves with respect to lab curve with a very high error of 205.31% and 228.82%, respectively. Figure (68) and table (14).

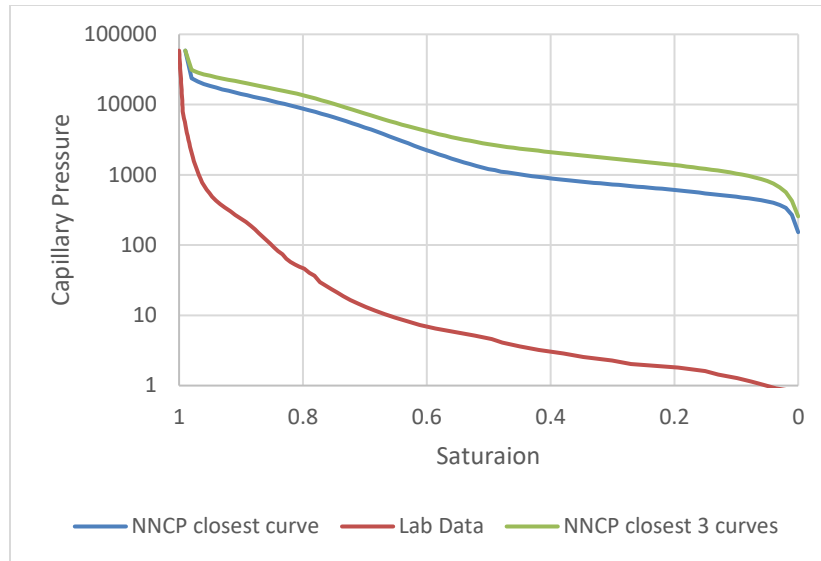


Figure 68: Comparison of NNCP, the average of the closest three curves to predict the capillary pressure compared to laboratory data for testing sample # 4 in class 1

Test sample # 5 shows good match between the NNCP closest curve and the closest three curves with respect to lab curve with a very high error of 23.11% and 20.95%, respectively. Figure (69) and table (14).

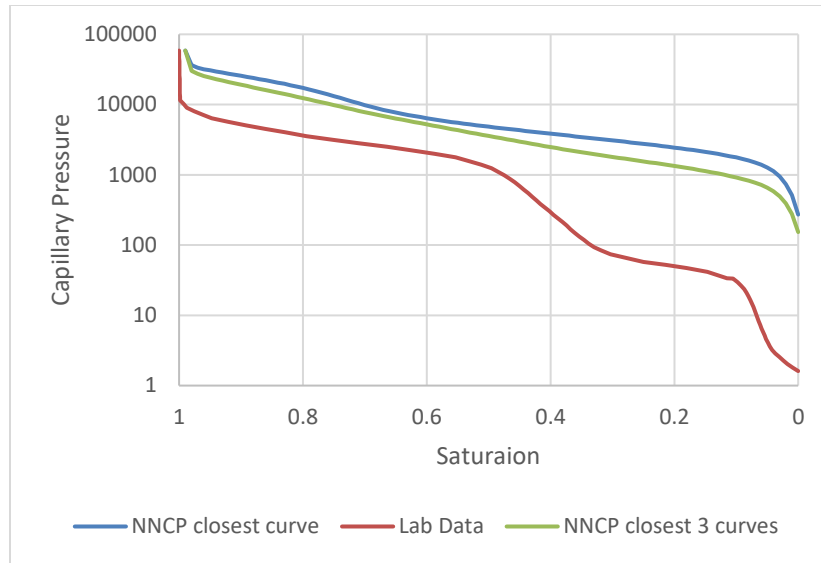


Figure 69: Comparison of NNCP, the average of the closest three curves to predict the capillary pressure compared to laboratory data for testing sample # 5 in class 1

Table 14 shows the average error of the NNCP method compared to laboratory data for class 1 test samples.

Table 14: Average error of NNCP method versus laboratory data for class 1

Sample #	NNCP average error, %	Average error of average of closest 3 curves, %
1	2.01	2.19
2	4.8	4.78
3	0.18	0.2
4	205.31	228.82
5	23.11	20.95

Bi-modal class # 2: similar to previous classes, according the flow zone unit classification technique, 27 samples fall under bi-modal class 2 group. 18 samples were used for training and 9 samples were used for testing. Figures (70-78) show the results of the bi-modal for class 2 comparing the NNCP predictions to the laboratory data.

Test sample # 1 shows that NNCP closest curve method produced closer results to the lab curve than the closest three curves with an error of 85.2% and 142.06%, respectively. Figure (70) and table (15).

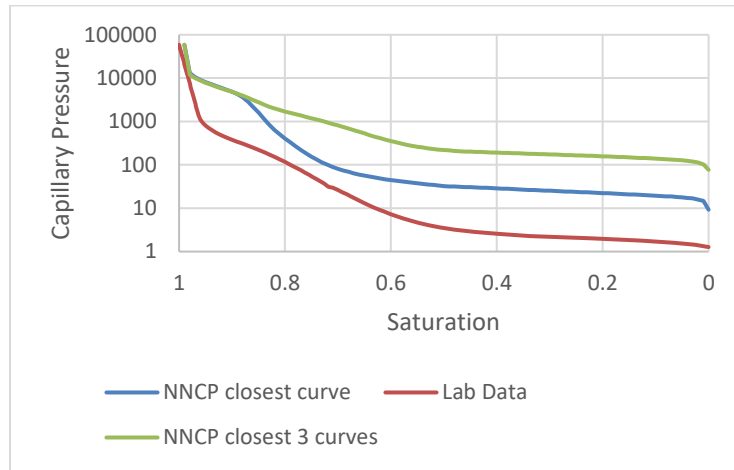


Figure 70: Comparison of NNCP, the average of the closest three curves to predict the capillary pressure compared to laboratory data for testing sample # 1 in class 2

Test sample # 2 shows that NNCP closest curve method produced closer results to the lab curve than the closest three curves with an error of 16.33% and 15.97%, respectively. Figure (71) and table (15).

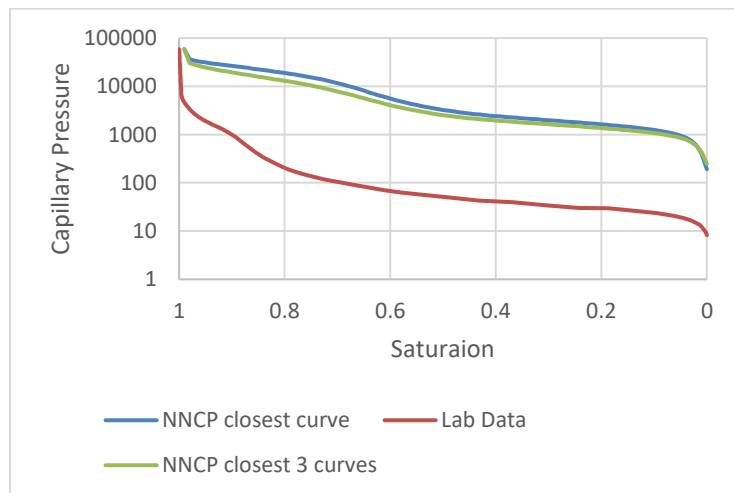


Figure 71: Comparison of NNCP, the average of the closest three curves to predict the capillary pressure compared to laboratory data for testing sample # 2 in class 2

Test sample # 3 shows that NNCP closest curve method produced closer results to the lab curve than the closest three curves with an error of 1.16% and 1.37%, respectively. Figure (72) and table (15).

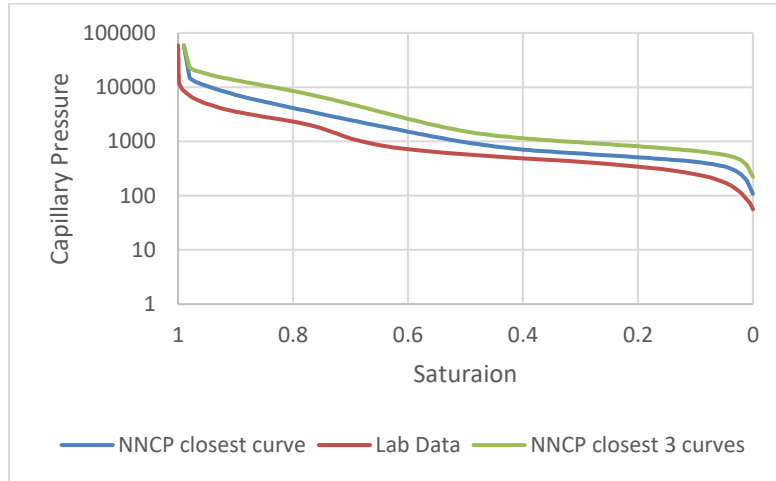


Figure 72: Comparison of NNCP, the average of the closest three curves to predict the capillary pressure compared to laboratory data for testing sample # 3 in class 2

Test sample # 4 shows that NNCP closest curve method produced closer results to the lab curve than the closest three curves with an error of 29.61% and 59.95%, respectively. Figure (73) and table (15).

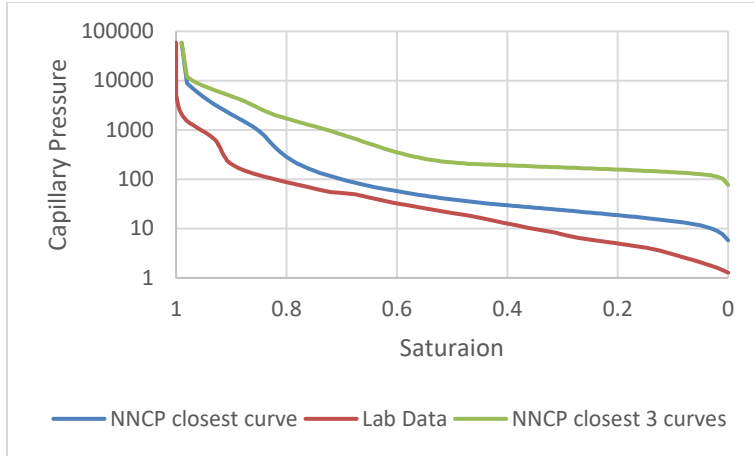


Figure 73: Comparison of NNCP, the average of the closest three curves to predict the capillary pressure compared to laboratory data for testing sample # 4 in class 2

Test sample # 5 shows that NNCP closest curve method produced closer results to the lab curve than the closest three curves with an error of 9.1% and 9.61%, respectively. Figure (74) and table (15).

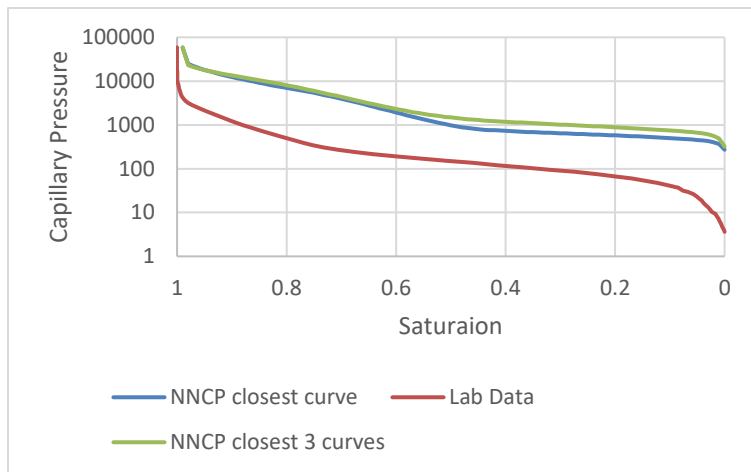


Figure 74: Comparison of NNCP, the average of the closest three curves to predict the capillary pressure compared to laboratory data for testing sample # 5 in class 2

Test sample # 6 shows that NNCP closest curve method produced closer results to the lab curve than the closest three curves with an error of 11.44% and 11.49%, respectively. Figure (75) and table (15).

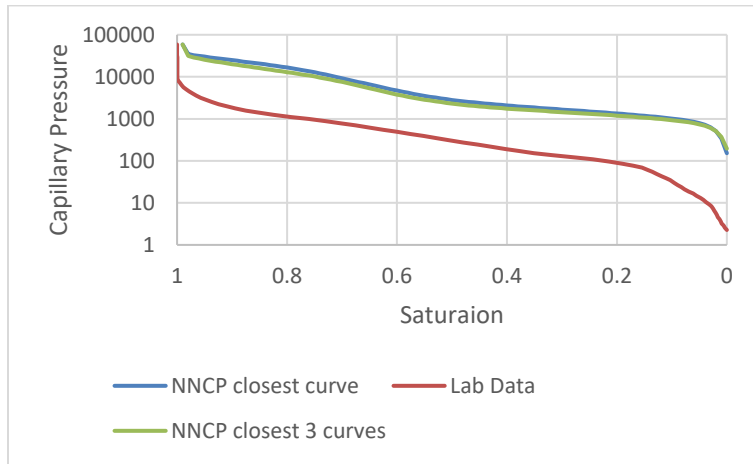


Figure 75: Comparison of NNCP, the average of the closest three curves to predict the capillary pressure compared to laboratory data for testing sample # 6 in class 2

Test sample # 7 shows that NNCP closest curve method produced closer results to the lab curve than the closest three curves with an error of 8.54% and 9.1%, respectively. Figure (76) and table (15).

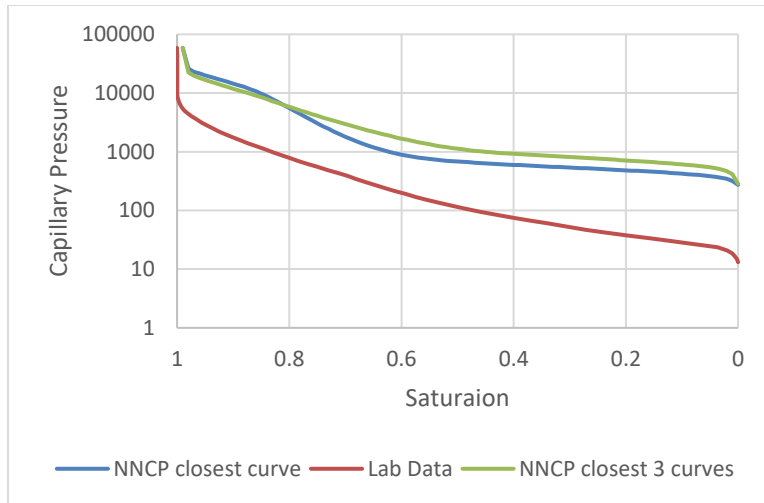


Figure 76: Comparison of NNCP, the average of the closest three curves to predict the capillary pressure compared to laboratory data for testing sample # 7 in class 2

Test sample # 8 shows that NNCP closest curve method produced closer results to the lab curve than the closest three curves with an error of 68.2% and 115.83%, respectively. Figure (77) and table (15).

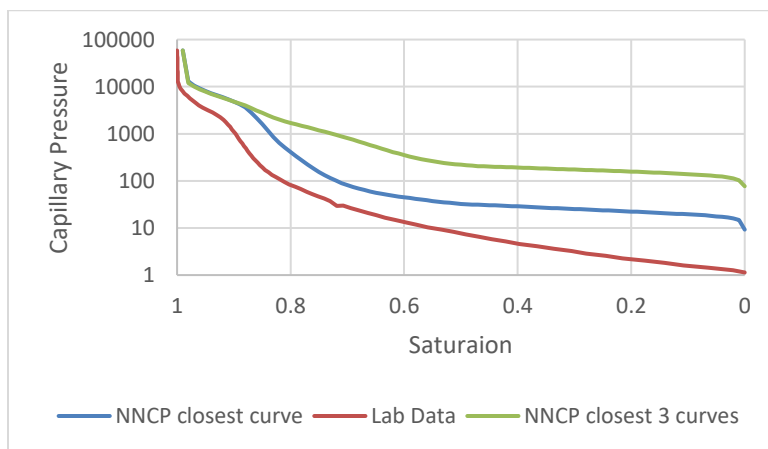


Figure 77: Comparison of NNCP, the average of the closest three curves to predict the capillary pressure compared to laboratory data for testing sample # 8 in class 2

Test sample # 9 shows that NNCP closest curve method produced closer results to the lab curve than the closest three curves with an error of 9.19% and 18.56%, respectively. Figure (78) and table (15).

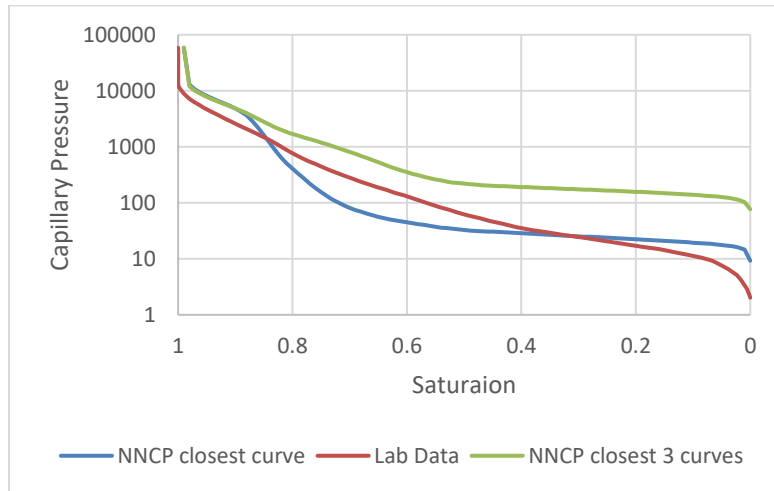


Figure 78: Comparison of NNCP, the average of the closest three curves to predict the capillary pressure compared to laboratory data for testing sample # 9 in class 2

Table 15 shows the average error of the NNCP method compared to laboratory data for class 2 test samples.

Table 15: Average error of NNCP method versus laboratory data for class 2

Sample #	NNCP average error, %	Average error of average of closest 3 curves, %
1	85.2	142.06
2	16.33	15.97
3	1.16	1.37
4	29.61	59.95
5	9.1	9.61
6	11.44	11.49
7	8.54	9.1
8	68.2	115.83
9	9.19	18.56

Bi-modal class # 3: according to the flow zone unit classification technique, 35 samples fall under bi-modal class 3 group. 24 samples were used for training and 11 samples were used for testing. Figures (79-89) show the results of the bi-modal for class 3 comparing the NNCP predictions to the laboratory data.

Test sample # 1 shows that NNCP closest curve method produced closer results to the lab curve than the closest three curves with an error of 24.56% and 25.36%, respectively. Figure (79) and table (16).

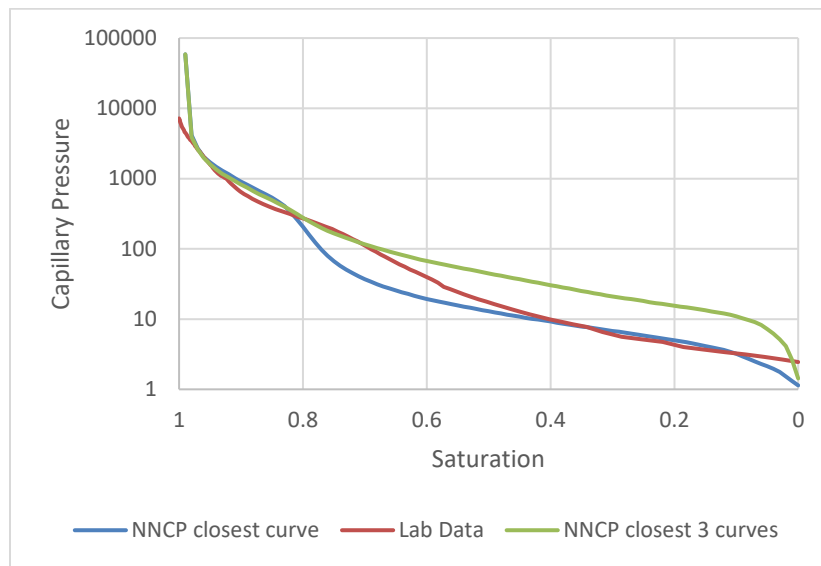


Figure 79: Comparison of NNCP, the average of the closest three curves to predict the capillary pressure compared to laboratory data for testing sample # 1 in class 3

Test sample # 2 shows that NNCP closest curve method produced closer results to the lab curve than the closest three curves with an error of 16.58% and 21.91%, respectively. Figure (80) and table (16).

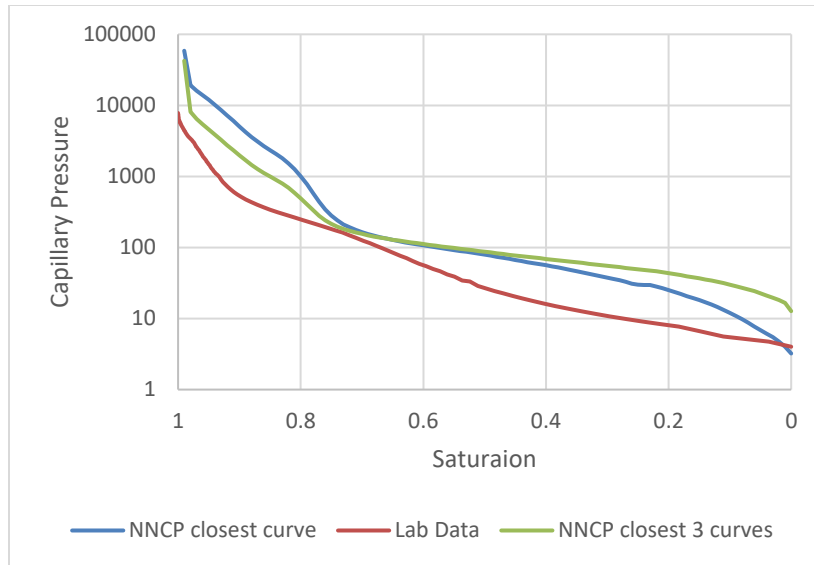


Figure 80: Comparison of NNCP, the average of the closest three curves to predict the capillary pressure compared to laboratory data for testing sample # 2 in class 3

Test sample # 3 shows that NNCP closest curve method produced closer results to the lab curve than the closest three curves with an error of 17.47% and 12.74%, respectively. Figure (81) and table (16jhk).

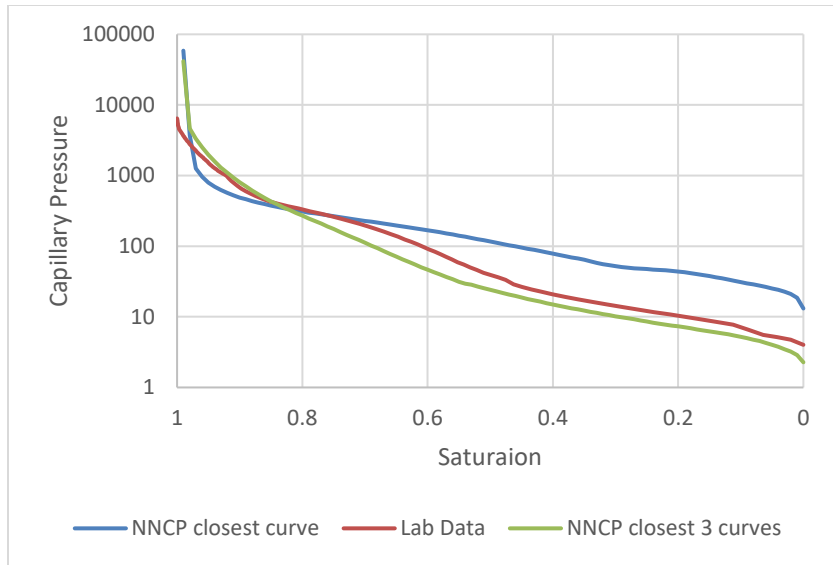


Figure 81: Comparison of NNCP, the average of the closest three curves to predict the capillary pressure compared to laboratory data for testing sample # 3 in class 3

Test sample # 4 shows that NNCP closest curve method produced closer results to the lab curve than the closest three curves with an error of 12.75% and 15.6%, respectively. Figure (82) and table (16).

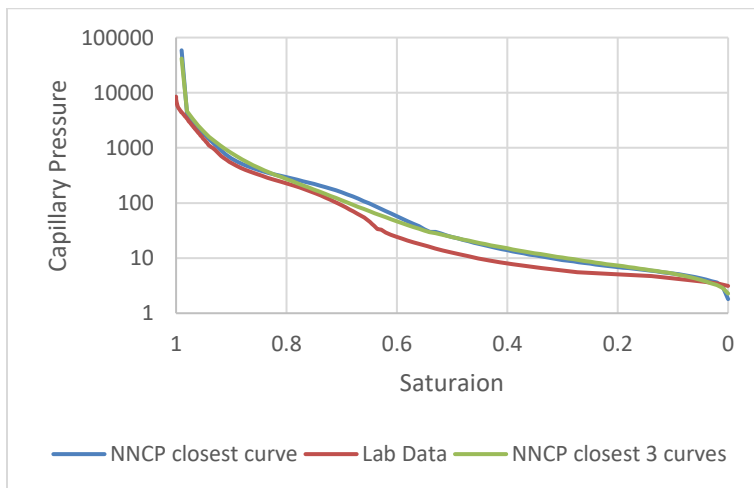


Figure 82: Comparison of NNCP, the average of the closest three curves to predict the capillary pressure compared to laboratory data for testing sample # 4 in class 3

Test sample # 5 shows that NNCP closest curve method produced closer results to the lab curve than the closest three curves with an error of 12.11% and 14.59%, respectively. Figure (83) and table (16).

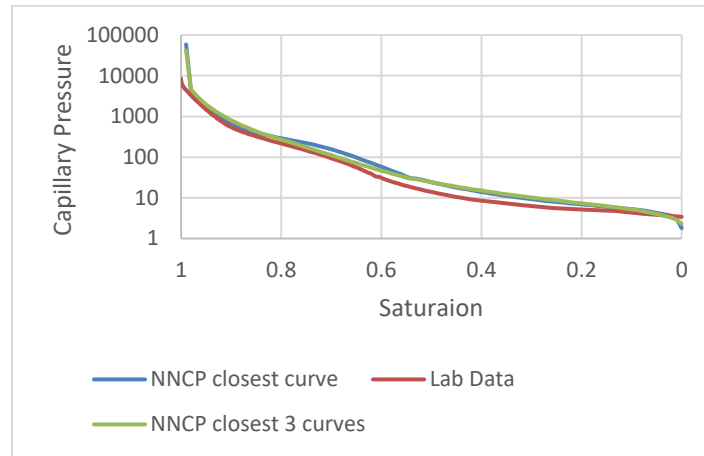


Figure 83: Comparison of NNCP, the average of the closest three curves to predict the capillary pressure compared to laboratory data for testing sample # 5 in class 3

Test sample # 6 shows that NNCP closest curve method produced closer results to the lab curve than the closest three curves with an error of 17.37% and 18.2%, respectively. Figure (84) and table (16).

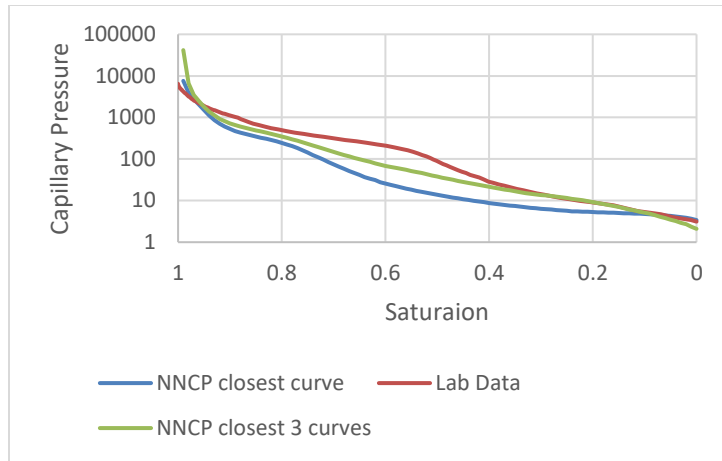


Figure 84: Comparison of NNCP, the average of the closest three curves to predict the capillary pressure compared to laboratory data for testing sample # 6 in class 3

Test sample # 7 shows that NNCP closest curve method produced closer results to the lab curve than the closest three curves with an error of 51.14% and 25.82%, respectively. Figure (85) and table (16).

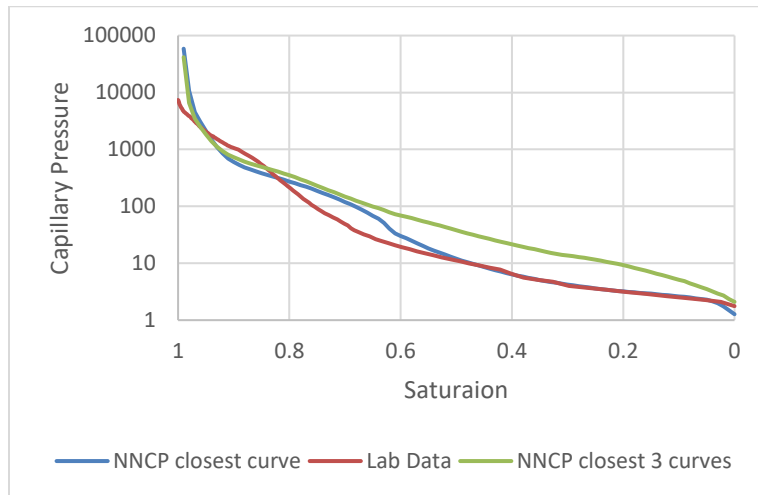


Figure 85: Comparison of NNCP, the average of the closest three curves to predict the capillary pressure compared to laboratory data for testing sample # 7 in class 3

Test sample # 8 shows that NNCP closest curve method produced closer results to the lab curve than the closest three curves with an error of 50.91% and 53.91%, respectively. Figure (86) and table (16).

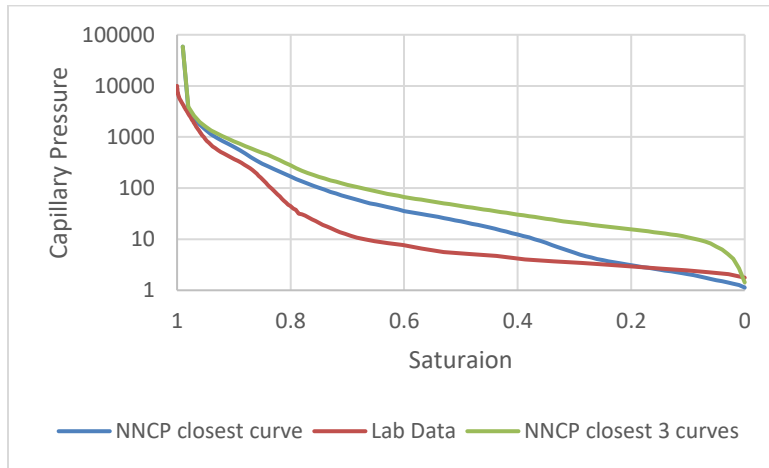


Figure 86: Comparison of NNCP, the average of the closest three curves to predict the capillary pressure compared to laboratory data for testing sample # 8 in class 3

Test sample # 9 shows that NNCP closest curve method produced closer results to the lab curve than the closest three curves with an error of 21.73% and 25.97%, respectively. Figure (87) and table (16).

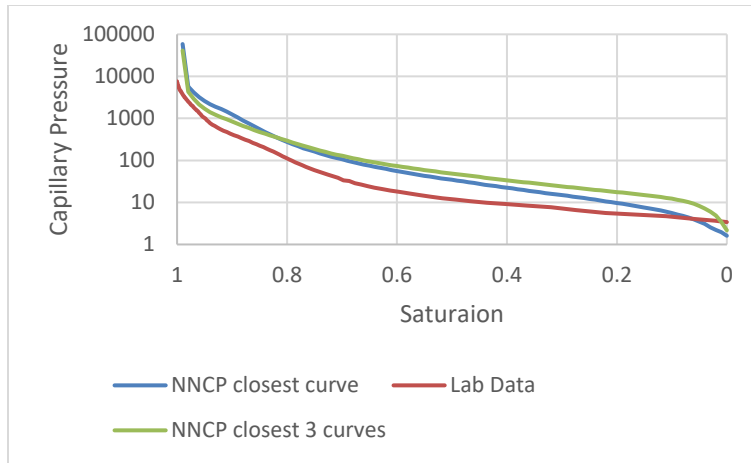


Figure 87: Comparison of NNCP, the average of the closest three curves to predict the capillary pressure compared to laboratory data for testing sample # 9 in class 3

Test sample # 10 shows that NNCP closest curve method produced closer results to the lab curve than the closest three curves with an error of 14.94% and 31.52%, respectively. Figure (88) and table (16).

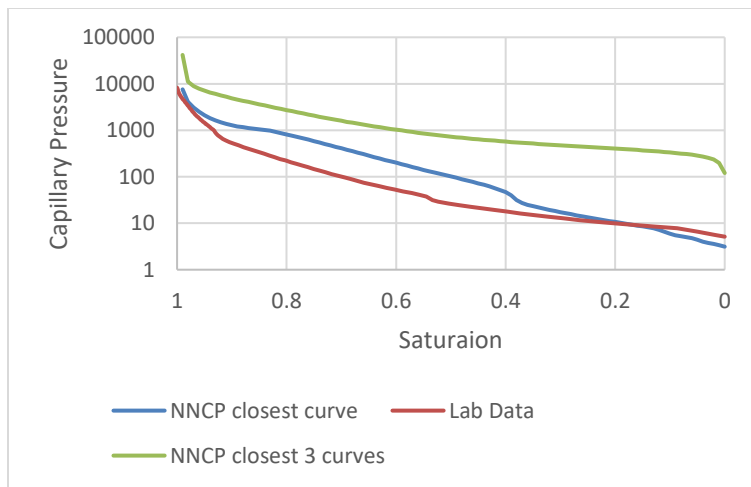


Figure 88: Comparison of NNCP, the average of the closest three curves to predict the capillary pressure compared to laboratory data for testing sample # 10 in class 3

Test sample # 11 shows that NNCP closest curve method produced closer results to the lab curve than the closest three curves with an error of 13.78% and 23.9%, respectively. Figure (89) and table (16).

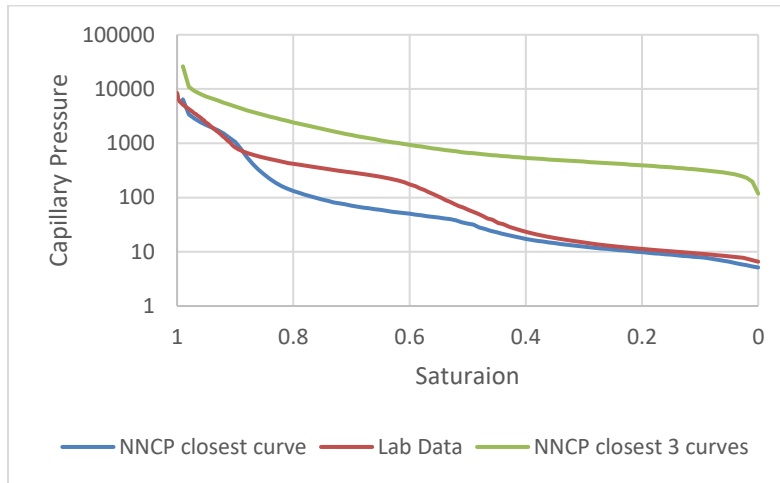


Figure 89: Comparison of NNCP, the average of the closest three curves to predict the capillary pressure compared to laboratory data for testing sample # 11 in class 3

Table 16 shows the average error of the NNCP method compared to laboratory data for class 3 test samples.

Table 16: Average error of NNCP method versus laboratory data for class 3

Sample #	NNCP average error, %	Average error of average of closest 3 curves, %
1	24.56	25.36
2	16.58	21.91
3	17.47	12.74
4	12.75	15.6
5	12.11	14.59
6	17.37	18.2
7	51.14	25.82
8	50.91	53.91
9	21.73	25.97
10	14.94	31.52
11	13.78	23.9

Bi-modal class # 4: flow zone unit classification technique shows 24 samples fall under bi-modal class 4 group. 16 samples were used for training and 8 samples were used for testing. Figures (90-97) show the results of the bi-modal for class 4 comparing the NNCP predictions to the laboratory data. Test sample # 1 shows that NNCP closest curve method produced closer results to the lab curve than the closest three curves with an error of 9.55% and 10.35%, respectively. Figure (90) and table (17).

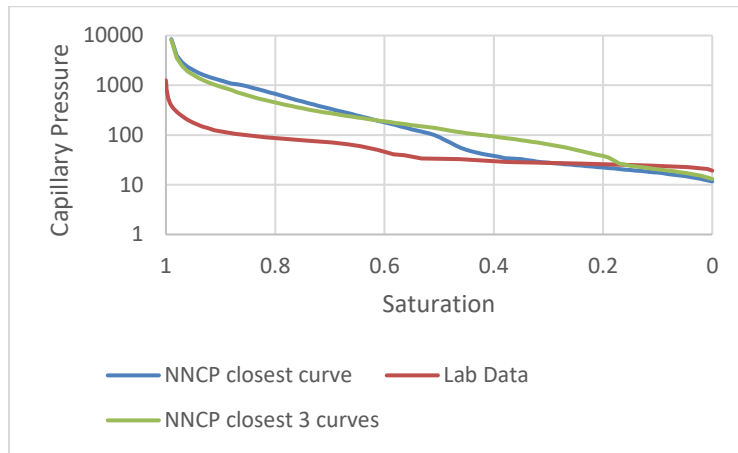


Figure 90: Comparison of NNCP, the average of the closest three curves to predict the capillary pressure compared to laboratory data for testing sample # 1 in class 4

Test sample # 2 shows that NNCP closest curve method produced closer results to the lab curve than the closest three curves with an error of 17.38% and 15.43%, respectively. Figure (91) and table (17).

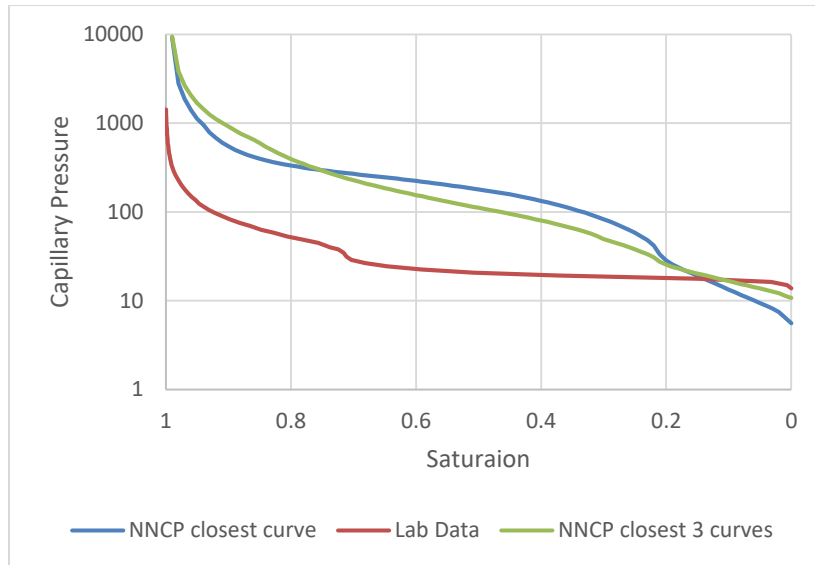


Figure 91: Comparison of NNCP, the average of the closest three curves to predict the capillary pressure compared to laboratory data for testing sample # 2 in class 4

Test sample # 3 shows that NNCP closest curve method produced closer results to the lab curve than the closest three curves with an error of 8.3% and 9.03%, respectively. Figure (92) and table (17).

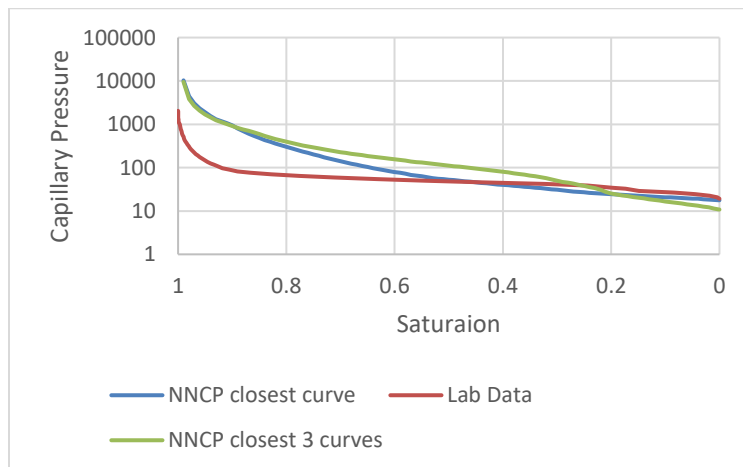


Figure 92: Comparison of NNCP, the average of the closest three curves to predict the capillary pressure compared to laboratory data for testing sample # 3 in class 4

Test sample # 4 shows that NNCP closest curve method produced closer results to the lab curve than the closest three curves with an error of 14.79% and 11.67%, respectively. Figure (93) and table (17).

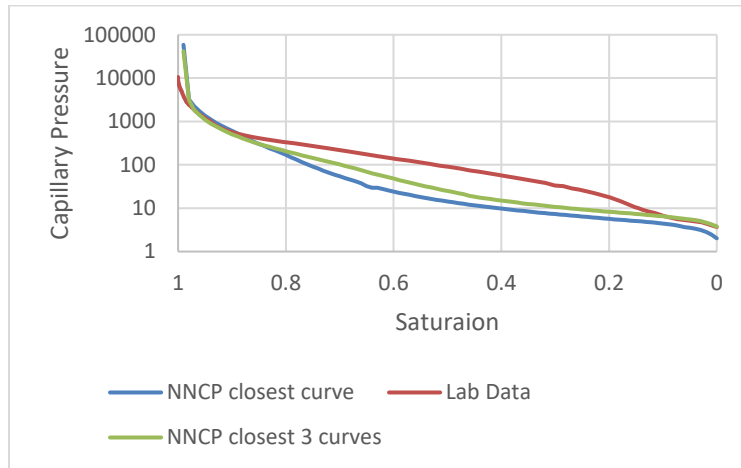


Figure 93: Comparison of NNCP, the average of the closest three curves to predict the capillary pressure compared to laboratory data for testing sample # 4 in class 4

Test sample # 5 shows that NNCP closest curve method produced closer results to the lab curve than the closest three curves with an error of 10.49% and 6.08%, respectively. Figure (94) and table (17).

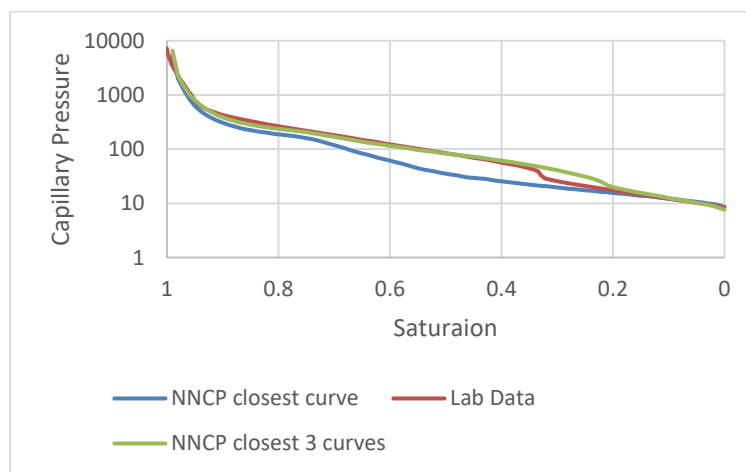


Figure 94: Comparison of NNCP, the average of the closest three curves to predict the capillary pressure compared to laboratory data for testing sample # 5 in class 4

Test sample # 6 shows that NNCP closest curve method produced closer results to the lab curve than the closest three curves with an error of 22.87% and 22.8%, respectively. Figure (95) and table (17).

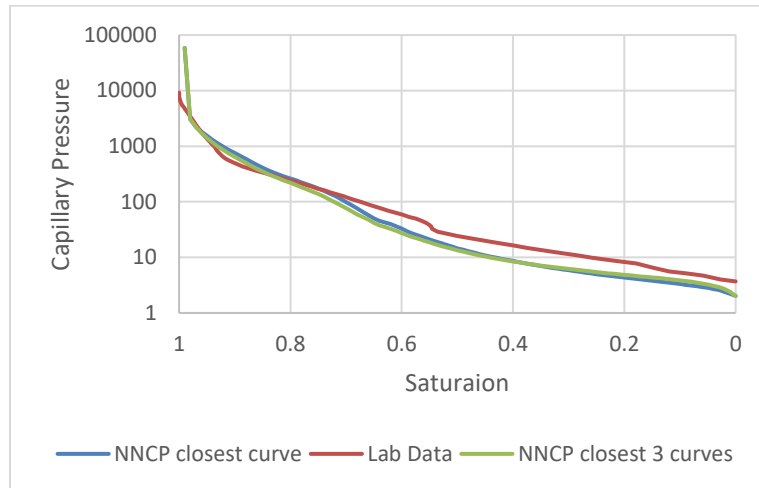


Figure 95: Comparison of NNCP, the average of the closest three curves to predict the capillary pressure compared to laboratory data for testing sample # 6 in class 4

Test sample # 7 shows that NNCP closest curve method produced closer results to the lab curve than the closest three curves with an error of 5.99% and 6.08%, respectively. Figure (96) and table (17).

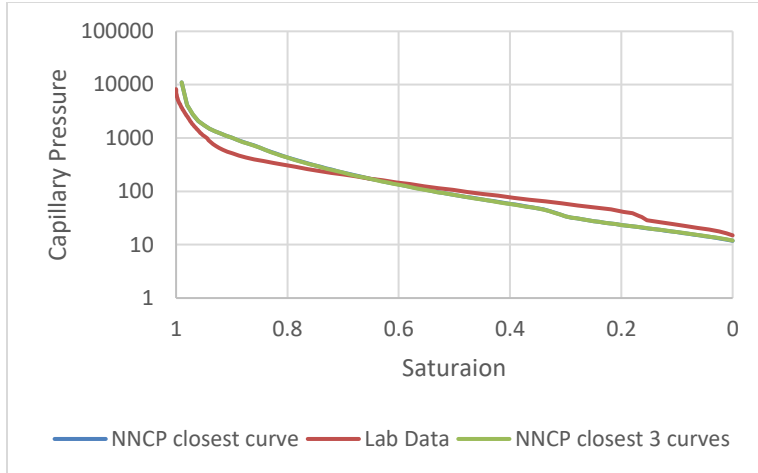


Figure 96: Comparison of NNCP, the average of the closest three curves to predict the capillary pressure compared to laboratory data for testing sample # 7 in class 4

Test sample # 8 shows that NNCP closest curve method produced closer results to the lab curve than the closest three curves with an error of 6.08% and 4.74%, respectively. Figure (97) and table (17).

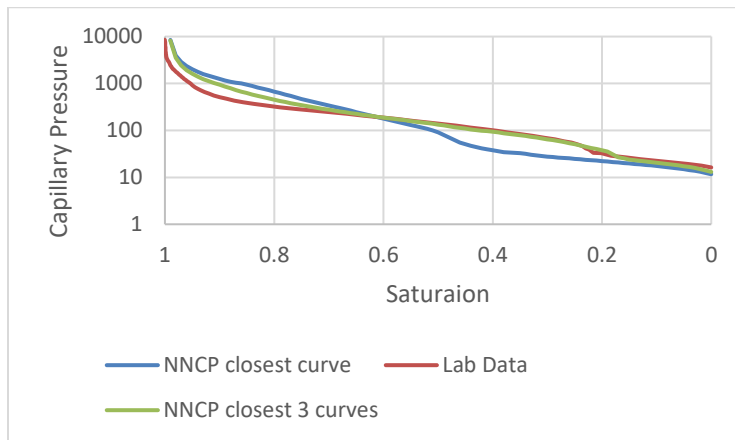


Figure 97: Comparison of NNCP, the average of the closest three curves to predict the capillary pressure compared to laboratory data for testing sample # 8 in class 4

Table 17 shows the average error of the NNCP method compared to laboratory data for class 4 test samples.

Table 17: Average error of NNCP method versus laboratory data for class 4

Sample #	NNCP average error, %	Average error of average of closest 3 curves, %
1	9.55	10.35
2	17.38	15.43
3	8.3	9.03
4	14.79	11.67
5	10.49	6.08
6	22.87	22.8
7	5.99	6.08
8	6.08	4.74

Bi-modal class # 5: according to flow zone unit classification technique, 35 samples fall under bi-modal class 5 group. 24 samples were used for training and 11 samples were used for testing. Figures (98-108) show the results of the bi-modal for class 5 comparing the NNCP predictions to the laboratory data. In this class, we incorporated the results from J-function averaging technique to show that it does not produce desired output due to its limitation in averaging bi-modal curves. Test sample # 1 shows that NNCP closest curve method and the closest three curves produced close results to the lab curve with an error of 1.95% and 2%, respectively. However, the J-function showed an error of 248.16%. Figure (98) and table (18).

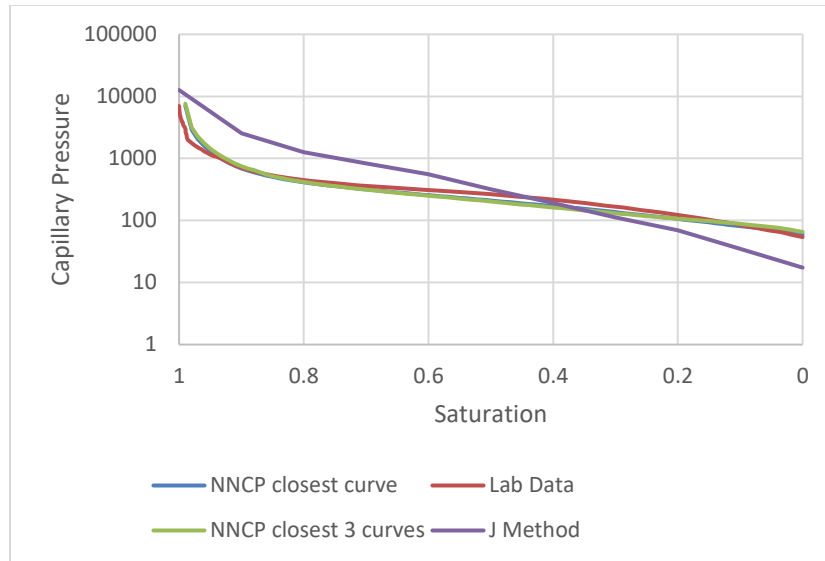


Figure 98: Comparison of NNCP, the average of the closest three curves to predict the capillary pressure compared to laboratory data for testing sample # 1 in class 5

Test sample # 2 shows that NNCP closest curve method and the closest three curves produced close results to the lab curve with an error of 2.84% and 3.32%, respectively. However, the J-function showed an error of 129.64%. Figure (99) and table (18).

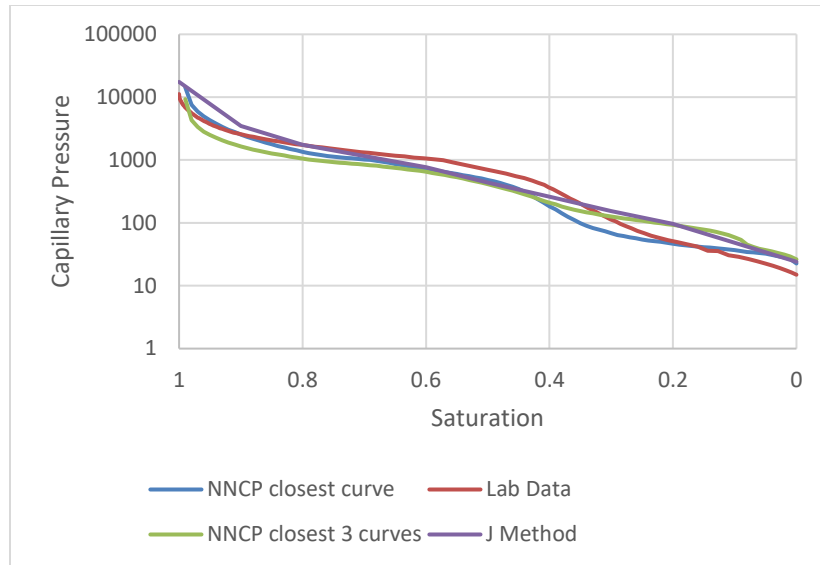


Figure 99: Comparison of NNCP, the average of the closest three curves to predict the capillary pressure compared to laboratory data for testing sample # 2 in class 5

Test sample # 3 shows that NNCP closest curve method and the closest three curves produced close results to the lab curve with an error of 1.63% and 1.59%, respectively. However, the J-function showed an error of 258.62%. Figure (100) and table (18).

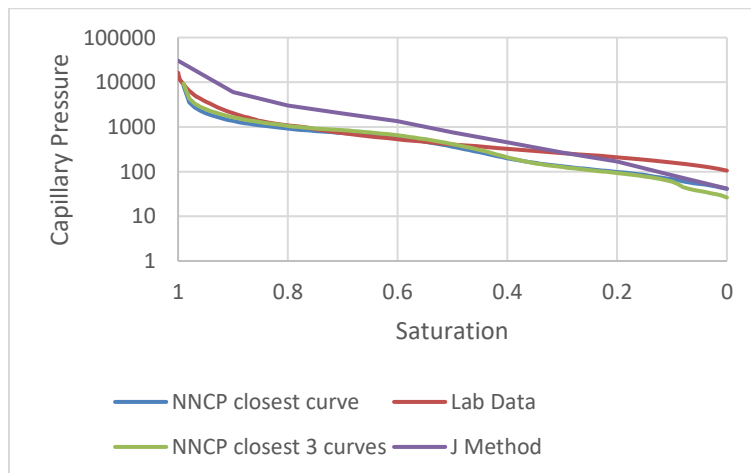


Figure 100: Comparison of NNCP, the average of the closest three curves to predict the capillary pressure compared to laboratory data for testing sample # 3 in class 5

Test sample # 4 shows that NNCP closest curve method and the closest three curves produced close results to the lab curve with an error of 1.81% and 1.77%, respectively. However, the J-function showed an error of 505.37%. Figure (101) and table (18).

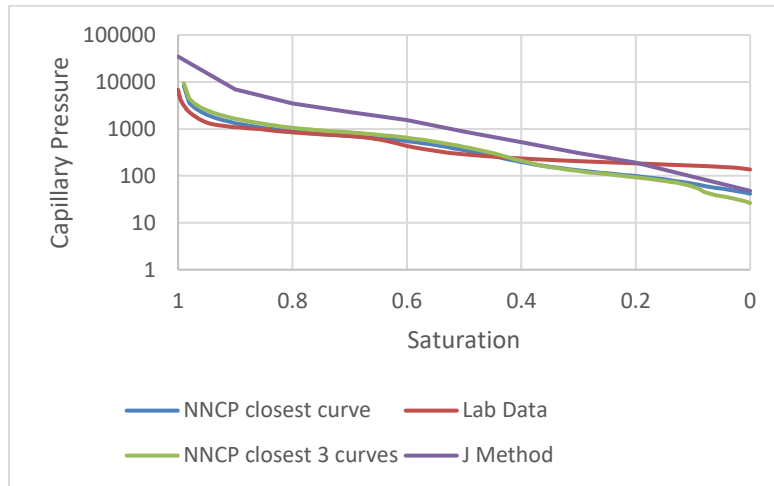


Figure 101: Comparison of NNCP, the average of the closest three curves to predict the capillary pressure compared to laboratory data for testing sample # 4 in class 5

Test sample # 5 shows that NNCP closest curve method and the closest three curves produced close results to the lab curve with an error of 4.24% and 3.71%, respectively. However, the J-function showed an error of 627.69%. Figure (102) and table (18).

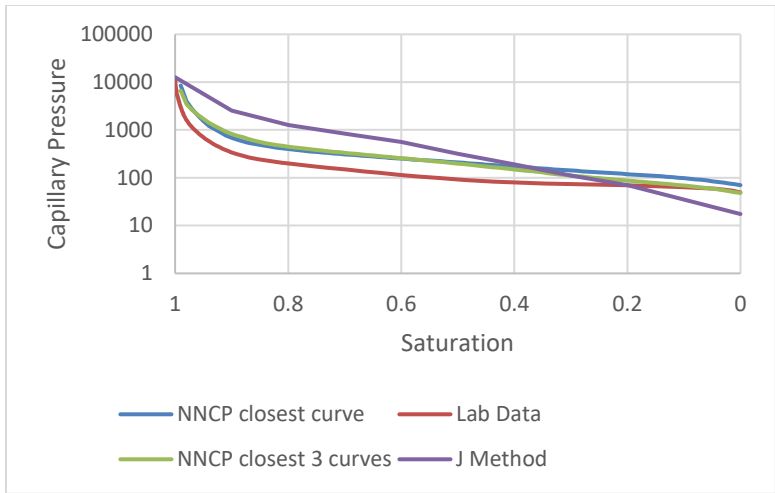


Figure 102: Comparison of NNCP, the average of the closest three curves to predict the capillary pressure compared to laboratory data for testing sample # 5 in class 5

Test sample # 6 shows that NNCP closest curve method and the closest three curves produced close results to the lab curve with an error of 0.81% and 0.84%, respectively. However, the J-function showed an error of 158.12%. Figure (103) and table (18).

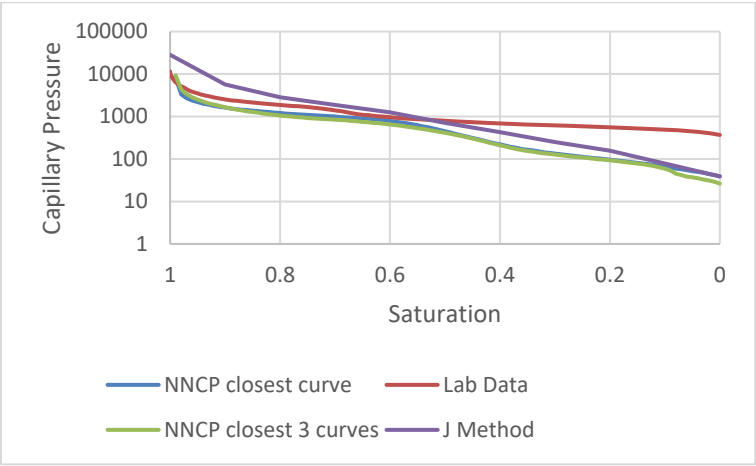


Figure 103: Comparison of NNCP, the average of the closest three curves to predict the capillary pressure compared to laboratory data for testing sample # 6 in class 5

Test sample # 7 shows that NNCP closest curve method and the closest three curves produced close results to the lab curve with an error of 5.31% and 4.84%, respectively. However, the J-function showed an error of 191.14%. Figure (104) and table (18).

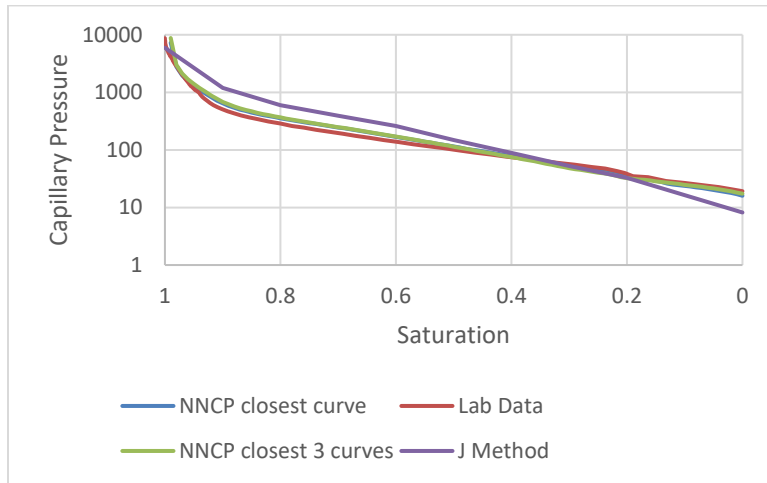


Figure 104: Comparison of NNCP, the average of the closest three curves to predict the capillary pressure compared to laboratory data for testing sample # 7 in class 5

Test sample # 8 shows that NNCP closest curve method and the closest three curves produced close results to the lab curve with an error of 3.08% and 2.29%, respectively. However, the J-function showed an error of 213.69%. Figure (105) and table (18).

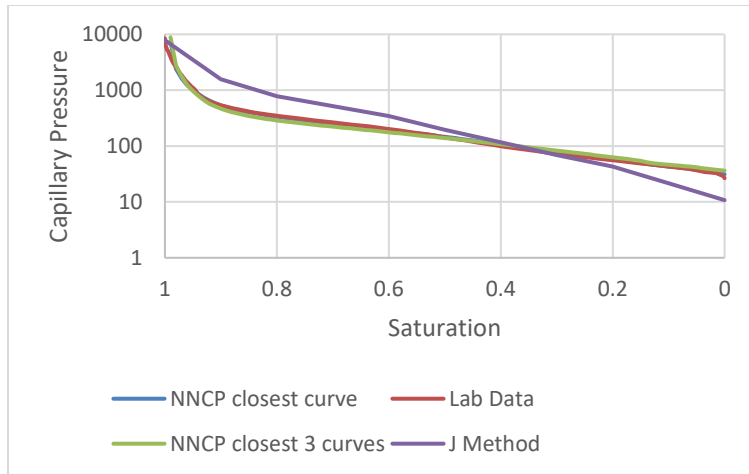


Figure 105: Comparison of NNCP, the average of the closest three curves to predict the capillary pressure compared to laboratory data for testing sample # 8 in class 5

Test sample # 9 shows that NNCP closest curve method and the closest three curves produced close results to the lab curve with an error of 2.66% and 1.96%, respectively. However, the J-function showed an error of 267.9%. Figure (106) and table (18).

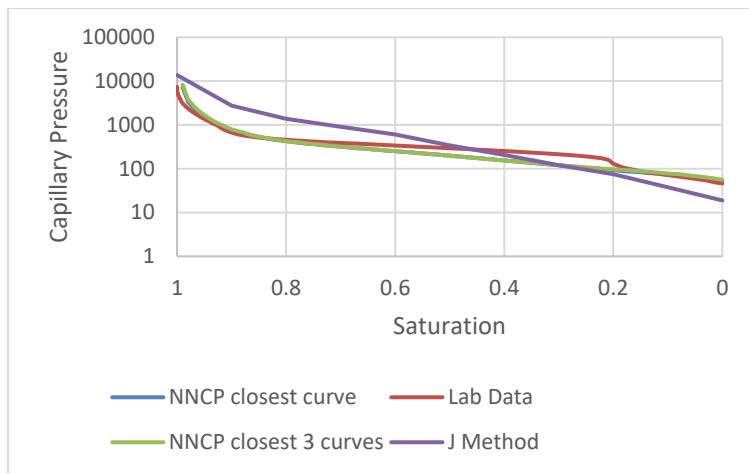


Figure 106: Comparison of NNCP, the average of the closest three curves to predict the capillary pressure compared to laboratory data for testing sample # 9 in class 5

Test sample # 10 shows that NNCP closest curve method and the closest three curves produced close results to the lab curve with an error of 3.3% and 2.83%, respectively. However, the J-function showed an error of 209.57%. Figure (107) and table (18).

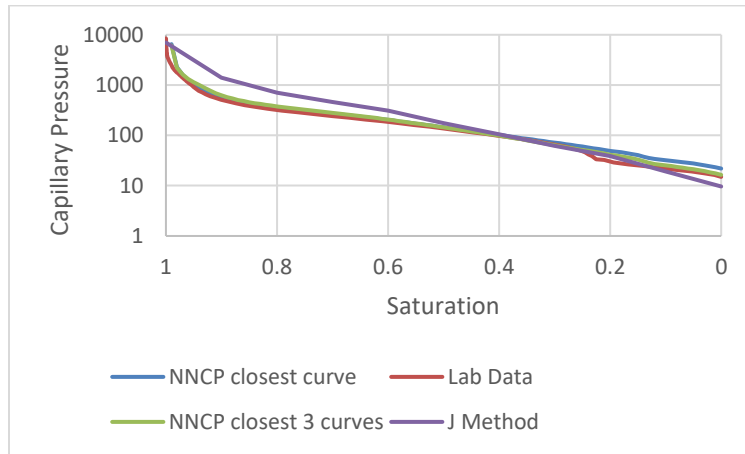


Figure 107: Comparison of NNCP, the average of the closest three curves to predict the capillary pressure compared to laboratory data for testing sample # 10 in class 5

Test sample # 11 shows that NNCP closest curve method and the closest three curves produced close results to the lab curve with an error of 4.6% and 4.49%, respectively. However, the J-function showed an error of 95.18%. Figure (108) and table (18).

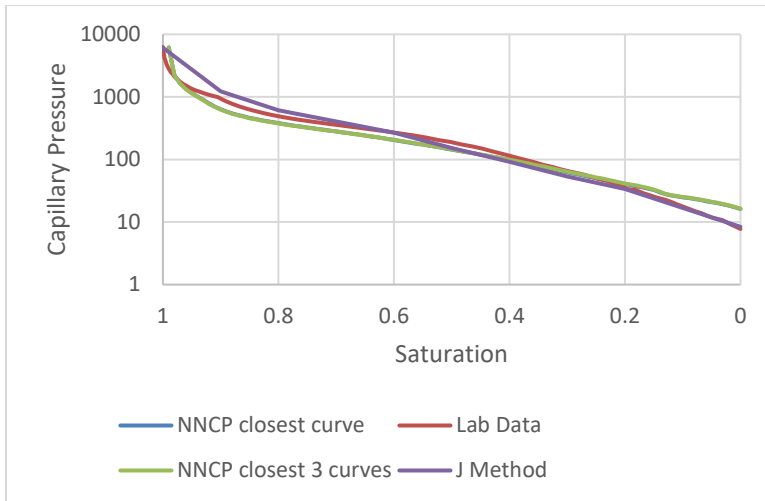


Figure 108: Comparison of NNCP, the average of the closest three curves to predict the capillary pressure compared to laboratory data for testing sample # 11 in class 5

Table 18 shows the average error of the NNCP method compared to laboratory data for class 5 test samples.

Table 18: Average error of NNCP method versus laboratory data for class 5

Sample #	NNCP average error, %	Average error of average of closest 3 curves, %	J-function average error, %
1	1.95	2	248.16
2	2.84	3.32	129.64
3	1.63	1.59	258.62
4	1.81	1.77	505.37
5	4.24	3.71	627.69
6	0.81	0.84	158.12
7	5.31	4.84	191.14
8	3.08	2.29	213.69
9	2.66	1.96	267.90
10	3.3	2.83	209.57
11	4.6	4.49	95.18

CHAPTER 6

Conclusions and Recommendations

6.1 Conclusions

Conclusion of this study could be summarized in the points below:

- This study shows an attempt of using artificial intelligence technology to predict the capillary pressure. Very few studies are reported in the literature on this topic.
- This study investigated the use of different artificial intelligence techniques to predict drainage capillary pressure of oil carbonate reservoir core samples. The techniques applied, especially **ANN - trainlm algorithm** and **decision tree** showed good potential in training and testing with fair accuracy when applied on uni-modal and bi-modal datasets separately rather than combined modals dataset.
- The study also presented a new technique (NNCP) to solve capillary pressure prediction problem by analyzing the training data in terms of similarity. The tesing data is then fitted on the nearest training data point. The new technique showed excellent results in solving this problem epecially after applying the two-step classification approach. The NNCP technique was found to give better results than those given by the standard J-function method.

6.2 Recommendations

- A further work to this study could be done by applying different rock classification methods using the NNCP technique.
- More work needs to be done to come up with a way to statistically compare the new technique to the lab data especially when the number of the x-axis points are not similar.

- There is still room for improvement if curve points are to be predicted when other artificial intelligence and rock classification techniques are implemented.
- Although the number of samples used in this study is good, the more available data, the better the results.
- Explore the strength of different AI techniques especially when more data is available.

References

- B. Guler, T. Ertekin and A.S Grader, “An Artificial Neural Network Based Relative Permeability Predictor”; *JCPT, No. 4, Volume 42, April 2003*.
- Ajith Abraham, “Artificial Neural Networks”; *Handbook of Measuring System Design, edited by Peter H. Sydenham and Richard Thorn, pages 901-908, 2005 John Wily & Sons, Ltd. ISBN: 0-470-02143-8*.
- Ali Abedini and Farshad Torabi, “Implementing Artificial Neural Network for Predicting Capillary Pressure in Reservoir Rocks”; *Special Topics & Review in Porous Media – An International Journal, 4 (4) 315-325, 2013*.
- Amar J Alshehri, “Capillary Pressure”, *Laboratory 7, March 01, 2011*.
- Beale M. H., Hagan M T., and Demuth, H. B. September 2010. Neural Network Toolbox 7 User's Guide. Natick, MA: The MathWorks, Inc.
- Carlos Gershenson, “Artificial Neural Networks for Beginners”; *Neural and Evolutionary Computing, 20 August 2003*.
- Dr. Paul Glover, Chapter 8: “Capillary Pressure”; *Formation Evaluation MSc Course Notes, Pages 84-94*.

Edward A. Clerke, Harry W. Mueller III, Eugene Craig Phillips, Ramsin Y. Eyvazzadeh, David H. Jones, Raghu Ramamoorthy and Ashok Sirvastava, “Application of Thomeer Hyperbolas to decode the pore systems, facies and reservoir properties of the Upper Jurassic Arab D Limestone, Ghawar field, Saudi Arabia: A "Rosetta Stone" approach”; *Gulf PetroLink, Bahrain, GeoArabia, vol 13, no. 4, 2008, pages 113-160.*

Eric Sondena, “An Empirical Method for Evaluation of Capillary Pressure Data”; *Elf Petroleum Norge A/S, Pages 129-146, 1992.*

Fuzzy Logic Toolbox 2 User's Guide Natic, MA: The MathWorks, Inc.

Harry W. Brown, “Capillary Pressure Investigations”; *Petroleum Transactions, AME, Vol. 192, pages 67-74, 1951.*

Hasan A. Nooruddin, Fatai Anifowose and Abdulazeez Abdulraheem, “Applying Artificial Intelligence Techniques to Develop Permeability Predictive Models using Mercury Injection Capillary–Pressure Data”; *SPE 168109, 2013.*

Hasan A. Nooruddin, Fatai Anifowose and Abdulazeez Abdulraheem, “Using soft computing techniques to predict corrected air permeability using Thomeer parameters, air porosity and grain density”; *Computers & Geosciences, issue 64, pages 72-80, 2014.*

J. H. M. Thomeer, "Introduction of a Pore Geometrical Factor Defined by the Capillary Pressure Curve"; *Technical Note 2057, pages 73-77, March 1960.*

James H. Schneider, "Empirical Capillary Pressure Relative Permeability Correlation"; *Jhschneider Consulting, 2003.*

Joost N. Kok et. al., "Artificial Intelligence: Definition, trends, techniques and cases"; *Encyclopedia of Life Support Systems (EOLSS).*

K. E. Newsham, J. A. Rushing, P. M. Lasswell and T. A. Blasingame, "A Comparative Study of Laboratory Techniques for Measuring Capillary Pressure in Tight Gas Sands"; *SPE 89866, 2004.*

M. C. Leverett, "Capillary Behavior in Porous Solids"; *Petroleum Technology, pages 152-169, August 1940.*

Malik K. Alarfaj, Abdulazeez Abdulraheem, Yasser R. Busaleh, "Estimating Dewpoint Pressure Using Artificial Intelligence"; *SPE 160919, 2012.*

Michael S. Lewicki, "Artificial Intelligence: Learning and Decision Trees"; *April 10, 2007.*

O. Jaimes, Ecopetrol-ICP, "Centrifuge Capillary Pressure: Method of the Center of Forces"; *SPE 22687, 1991.*

Pedro G. Toledo, et. al, “Pore-Space Statistics and Capillary Pressure Curves from Volume-Controlled Porosimetry”; *SPE Formation Evaluation*, 1994.

Phillips, E. C., “Full Pore System Petrophysical Characterization Technology for Complex Carbonate Reservoirs - Results from Saudi Arabia”; *Quantum Reservoir Impact, Houston, Texas*, 2011.

R. H. Brooks and A. T. Corey, “Hydraulic Properties of Porous Media”; *Hydrology Papers, Colorado State University, March 1964*.

Riyaz Kharrat, Ramin Mahdavi, Mohammed Hashem Bagherpour, Shahab, Hejri, “Rock Type and Permeability Prediction, of a Heterogeneous Carbonate Reservoir Using Artificial Neural Networks Based on Flow Zone Index Approach”; *SPE 120166*, 2009.

Roberto Sepulveda, Patricia Melin, Antonio Rodriguez, Alejandra Mancilla, Oscar Montiel, “Analyzing the effects of Footprint of Uncertainty in Type-2 Fuzzy Logic Controllers”; *Engineering Letter*, 13:2, EL_13_2_12, *Advance online Publication: 4 August 2006*.

Saud Fattah, et.al., “Artificial Intelligence Technology Predicts Relative Permeability of Giant Carbonate Reservoirs”; *SPE paper 109018*, 2009.

Sidqi A. Abu-Khamsin, “Basic Properties of Reservoir Rocks”; 2004.

Tarek Ahmed, “Reservoir Engineering Handbook 4th Edition”; *Gulf Professional Publishing*,
eBook ISBN: 9780080966670, pages 218-220, 12th January 2010.

Trevor Hastie, Robert Tibshirani, Jerome Friedman, “The Elements of Statistical Learning Data
Mining, Inference, and Prediction”; *Springer Series in Statistics, Second Edition, August
2008.*

APPENDIX-A
(Sample data)

Sample #	Grain Density	Permeability	Porosity	Saturation	Capillary Pressure
1	2.6503904	676.6309	0.044747409	0	152.5525665
1	2.6503904	676.6309	0.044747409	0.001823765	171.3418427
1	2.6503904	676.6309	0.044747409	0.003602834	192.9680176
1	2.6503904	676.6309	0.044747409	0.005471565	216.3983002
1	2.6503904	676.6309	0.044747409	0.007347654	242.6000519
1	2.6503904	676.6309	0.044747409	0.010488121	272.9809265
1	2.6503904	676.6309	0.044747409	0.014362828	308.6576233
1	2.6503904	676.6309	0.044747409	0.021241719	344.7563171
1	2.6503904	676.6309	0.044747409	0.034951561	388.8425293
1	2.6503904	676.6309	0.044747409	0.060657574	436.0651245
1	2.6503904	676.6309	0.044747409	0.10361403	490.3520508
1	2.6503904	676.6309	0.044747409	0.156026659	550.4271851
1	2.6503904	676.6309	0.044747409	0.212578598	621.4475708
1	2.6503904	676.6309	0.044747409	0.277849994	697.4008789
1	2.6503904	676.6309	0.044747409	0.343274762	782.1536865
1	2.6503904	676.6309	0.044747409	0.399073343	878.6734009
1	2.6503904	676.6309	0.044747409	0.446163441	988.862915
1	2.6503904	676.6309	0.044747409	0.484376593	1110.485718
1	2.6503904	676.6309	0.044747409	0.51257091	1247.059814
1	2.6503904	676.6309	0.044747409	0.53367272	1402.666748
1	2.6503904	676.6309	0.044747409	0.553083499	1575.34082
1	2.6503904	676.6309	0.044747409	0.571419153	1771.114014
1	2.6503904	676.6309	0.044747409	0.588737638	1989.464844
1	2.6503904	676.6309	0.044747409	0.605366687	2235.90332
1	2.6503904	676.6309	0.044747409	0.621747266	2512.853516
1	2.6503904	676.6309	0.044747409	0.637384878	2824.039795
1	2.6503904	676.6309	0.044747409	0.652953733	3173.408203
1	2.6503904	676.6309	0.044747409	0.668482283	3566.118164
1	2.6503904	676.6309	0.044747409	0.684170132	4008.406738
1	2.6503904	676.6309	0.044747409	0.700313559	4501.570313
1	2.6503904	676.6309	0.044747409	0.717139259	5060.717773
1	2.6503904	676.6309	0.044747409	0.734593134	5686.730957
1	2.6503904	676.6309	0.044747409	0.75282317	6391.120117
1	2.6503904	676.6309	0.044747409	0.772283661	7182.38916
1	2.6503904	676.6309	0.044747409	0.792755057	8072.173828
1	2.6503904	676.6309	0.044747409	0.814869901	9072.478516
1	2.6503904	676.6309	0.044747409	0.838232005	10196.22168
1	2.6503904	676.6309	0.044747409	0.862817331	11458.72754
1	2.6503904	676.6309	0.044747409	0.887732134	12876.69727
1	2.6503904	676.6309	0.044747409	0.912966974	14471.52051

1	2.6503904	676.6309	0.044747409	0.93711363	16264.65039
1	2.6503904	676.6309	0.044747409	0.958881693	18278.37695
1	2.6503904	676.6309	0.044747409	0.976674873	20543.21484
1	2.6503904	676.6309	0.044747409	0.988235349	23087.84766
1	2.6503904	676.6309	0.044747409	0.9952145	25947.125
1	2.6503904	676.6309	0.044747409	0.998153283	29160.48438
1	2.6503904	676.6309	0.044747409	0.999001669	32772.77344
1	2.6503904	676.6309	0.044747409	0.999474956	36825.03516
1	2.6503904	676.6309	0.044747409	0.999755876	41376.70703
1	2.6503904	676.6309	0.044747409	0.999890579	46500.78516
1	2.6503904	676.6309	0.044747409	0.99996031	52258.66016
1	2.6503904	676.6309	0.044747409	1	58712.1875
2	2.657290913	738.8592	0.106782226	0	5.781690121
2	2.657290913	738.8592	0.106782226	0.003017064	6.495548248
2	2.657290913	738.8592	0.106782226	0.006996085	7.302698135
2	2.657290913	738.8592	0.106782226	0.014035902	8.207427025
2	2.657290913	738.8592	0.106782226	0.02212513	9.227519989
2	2.657290913	738.8592	0.106782226	0.034455737	10.36242104
2	2.657290913	738.8592	0.106782226	0.051450533	11.64920807
2	2.657290913	738.8592	0.106782226	0.077467668	13.09979153
2	2.657290913	738.8592	0.106782226	0.113906319	14.72163391
2	2.657290913	738.8592	0.106782226	0.154884799	16.59445
2	2.657290913	738.8592	0.106782226	0.201321319	18.64051056
2	2.657290913	738.8592	0.106782226	0.249630854	20.93984795
2	2.657290913	738.8592	0.106782226	0.300192459	23.53160477
2	2.657290913	738.8592	0.106782226	0.353100366	26.43277168
2	2.657290913	738.8592	0.106782226	0.403450529	29.71369553
2	2.657290913	738.8592	0.106782226	0.449196157	32.77413559
2	2.657290913	738.8592	0.106782226	0.490203277	37.28495789
2	2.657290913	738.8592	0.106782226	0.527234743	41.91374969
2	2.657290913	738.8592	0.106782226	0.560226105	47.23648071
2	2.657290913	738.8592	0.106782226	0.588632161	53.1113205
2	2.657290913	738.8592	0.106782226	0.613157928	59.22639084
2	2.657290913	738.8592	0.106782226	0.63848431	66.085495
2	2.657290913	738.8592	0.106782226	0.660186346	74.90632629
2	2.657290913	738.8592	0.106782226	0.681299529	84.54078674
2	2.657290913	738.8592	0.106782226	0.700180547	94.76128387
2	2.657290913	738.8592	0.106782226	0.716628005	106.9395523
2	2.657290913	738.8592	0.106782226	0.732460666	120.2393875
2	2.657290913	738.8592	0.106782226	0.746694537	134.6430359
2	2.657290913	738.8592	0.106782226	0.759393153	151.3357239

2	2.657290913	738.8592	0.106782226	0.771061186	170.3102722
2	2.657290913	738.8592	0.106782226	0.781491945	191.9442139
2	2.657290913	738.8592	0.106782226	0.790671176	215.8517303
2	2.657290913	738.8592	0.106782226	0.798680248	243.0192719
2	2.657290913	738.8592	0.106782226	0.805900091	272.8860168
2	2.657290913	738.8592	0.106782226	0.812268594	306.4613037
2	2.657290913	738.8592	0.106782226	0.817954282	343.5313416
2	2.657290913	738.8592	0.106782226	0.823098902	387.3198547
2	2.657290913	738.8592	0.106782226	0.827926916	435.3630981
2	2.657290913	738.8592	0.106782226	0.832350803	488.7467651
2	2.657290913	738.8592	0.106782226	0.83702467	549.1375732
2	2.657290913	738.8592	0.106782226	0.84135063	618.1936035
2	2.657290913	738.8592	0.106782226	0.845363413	693.4348145
2	2.657290913	738.8592	0.106782226	0.849604487	781.2393799
2	2.657290913	738.8592	0.106782226	0.854504177	876.4094238
2	2.657290913	738.8592	0.106782226	0.860110436	985.258728
2	2.657290913	738.8592	0.106782226	0.866278906	1108.531982
2	2.657290913	738.8592	0.106782226	0.873408538	1245.171875
2	2.657290913	738.8592	0.106782226	0.881205942	1401.491699
2	2.657290913	738.8592	0.106782226	0.889585233	1573.675415
2	2.657290913	738.8592	0.106782226	0.897857591	1768.852905
2	2.657290913	738.8592	0.106782226	0.905968624	1988.601074
2	2.657290913	738.8592	0.106782226	0.914259723	2234.063477
2	2.657290913	738.8592	0.106782226	0.922280336	2510.894775
2	2.657290913	738.8592	0.106782226	0.930309386	2822.197998
2	2.657290913	738.8592	0.106782226	0.937652623	3172.262451
2	2.657290913	738.8592	0.106782226	0.944568264	3564.365234
2	2.657290913	738.8592	0.106782226	0.95122707	4005.474121
2	2.657290913	738.8592	0.106782226	0.957642879	4502.405273
2	2.657290913	738.8592	0.106782226	0.964138481	5057.769043
2	2.657290913	738.8592	0.106782226	0.970311377	5684.839844
2	2.657290913	738.8592	0.106782226	0.976158528	6389.143066
2	2.657290913	738.8592	0.106782226	0.981603307	7181.583984
2	2.657290913	738.8592	0.106782226	0.98655099	8070.617676
2	2.657290913	738.8592	0.106782226	0.990606664	9071.518555
2	2.657290913	738.8592	0.106782226	0.993829647	10193.76855
2	2.657290913	738.8592	0.106782226	0.995982195	11455.58887
2	2.657290913	738.8592	0.106782226	0.997499097	12875.71094
2	2.657290913	738.8592	0.106782226	0.998037193	14468.91309
2	2.657290913	738.8592	0.106782226	0.998381492	16262.38281
2	2.657290913	738.8592	0.106782226	0.998660395	18276.24414

2	2.657290913	738.8592	0.106782226	0.998868988	20540.71094
2	2.657290913	738.8592	0.106782226	0.999011513	23085.46289
2	2.657290913	738.8592	0.106782226	0.999100663	25944.74219
2	2.657290913	738.8592	0.106782226	0.999201017	29158.61133
2	2.657290913	738.8592	0.106782226	0.999350448	32770.13672
2	2.657290913	738.8592	0.106782226	0.999439457	36827.54297
2	2.657290913	738.8592	0.106782226	0.999593066	41384.50391
2	2.657290913	738.8592	0.106782226	0.999750968	46501.85938
2	2.657290913	738.8592	0.106782226	1	58733.45313

APPENDIX-B
(Results from Methods # 1- 5 technique)

B1. Artificial neural network

Uni-modal capillary pressure curve

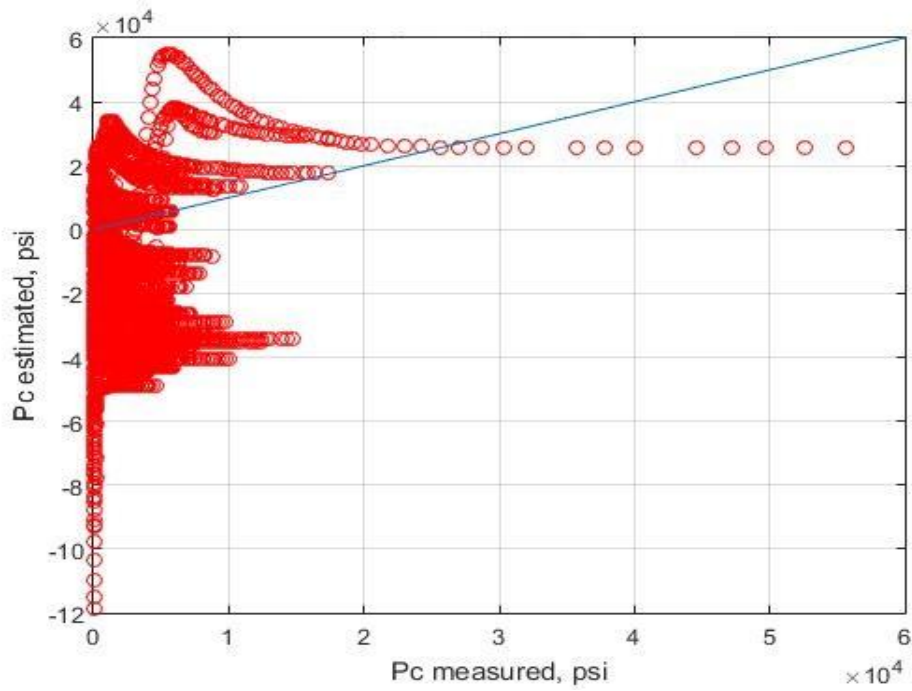


Figure 109: Predicted vs. measured values using ANN – trainb algorithm (Training).

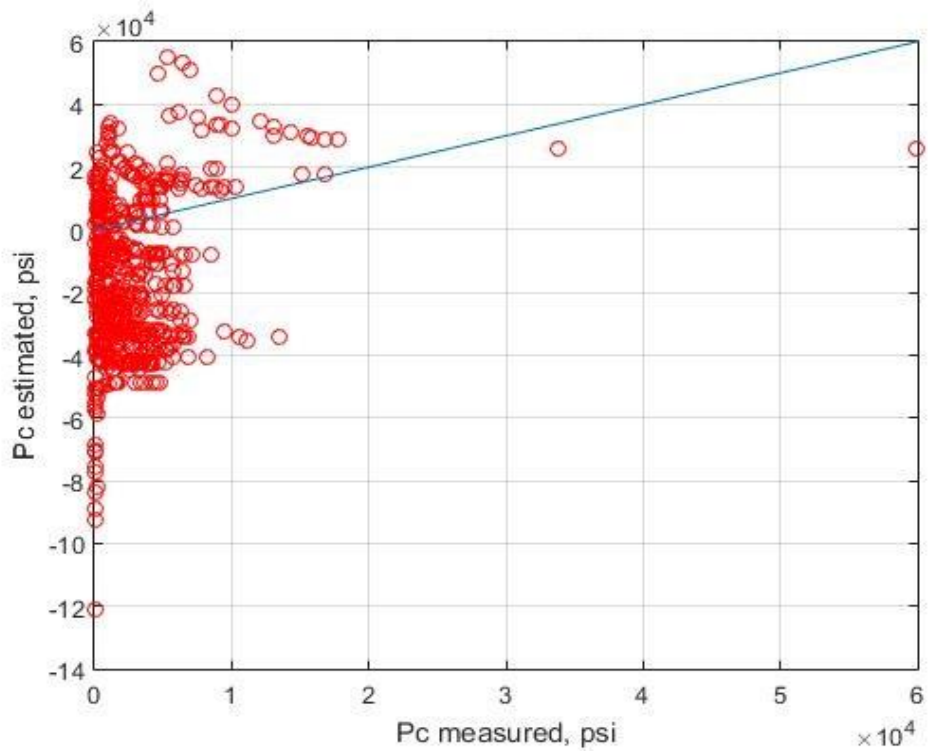


Figure 110. Predicted vs. measured values using ANN – trainb algorithm (Testing).

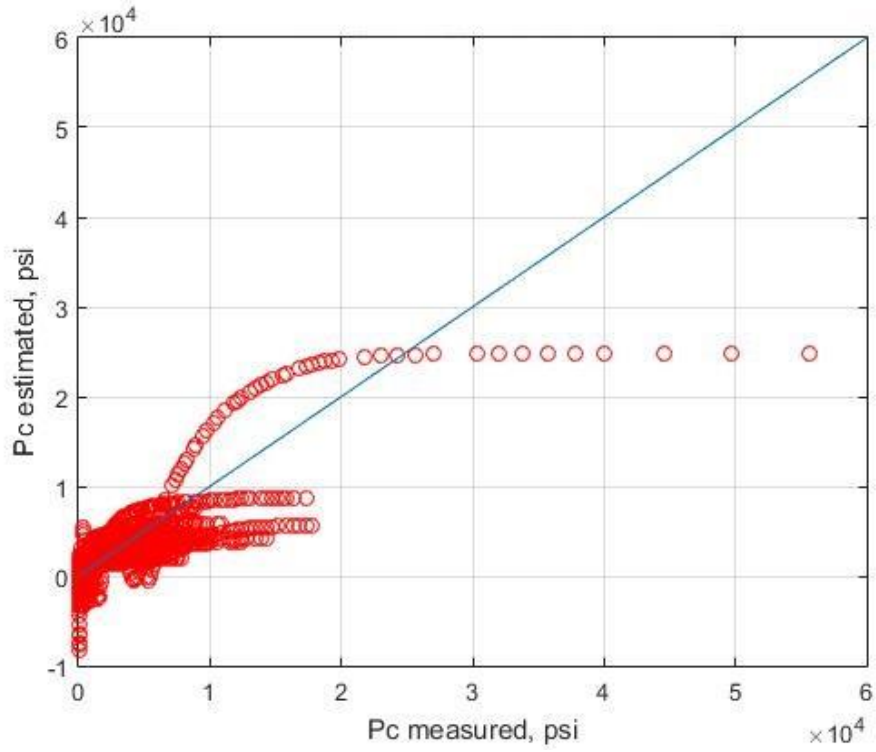


Figure 111. Predicted vs. measured values using ANN – trainbfg algorithm (Training).

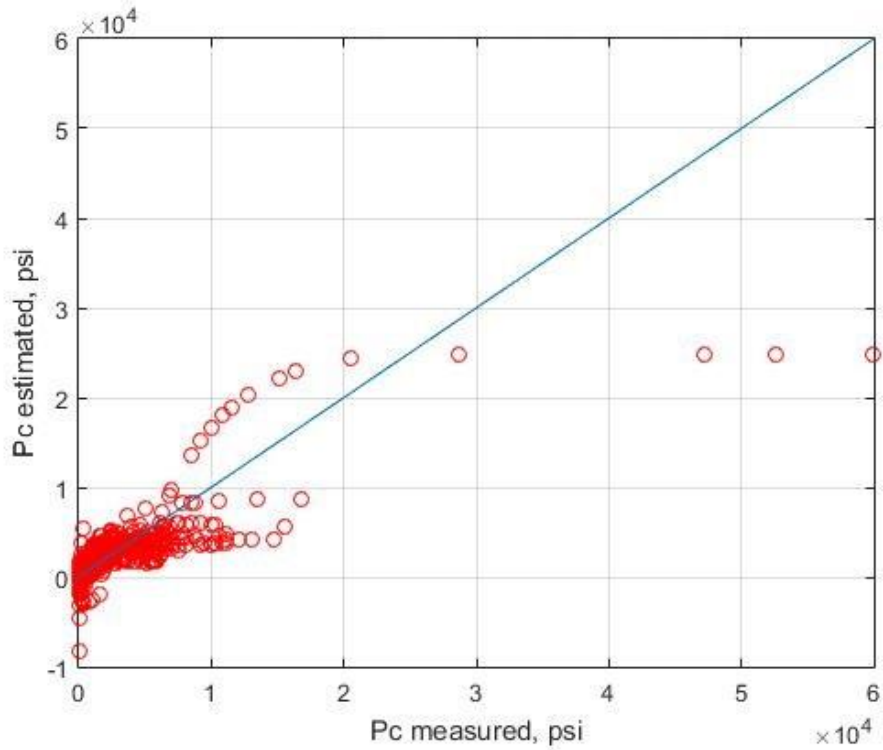


Figure 112. Predicted vs. measured values using ANN – trainbfg algorithm (Testing).

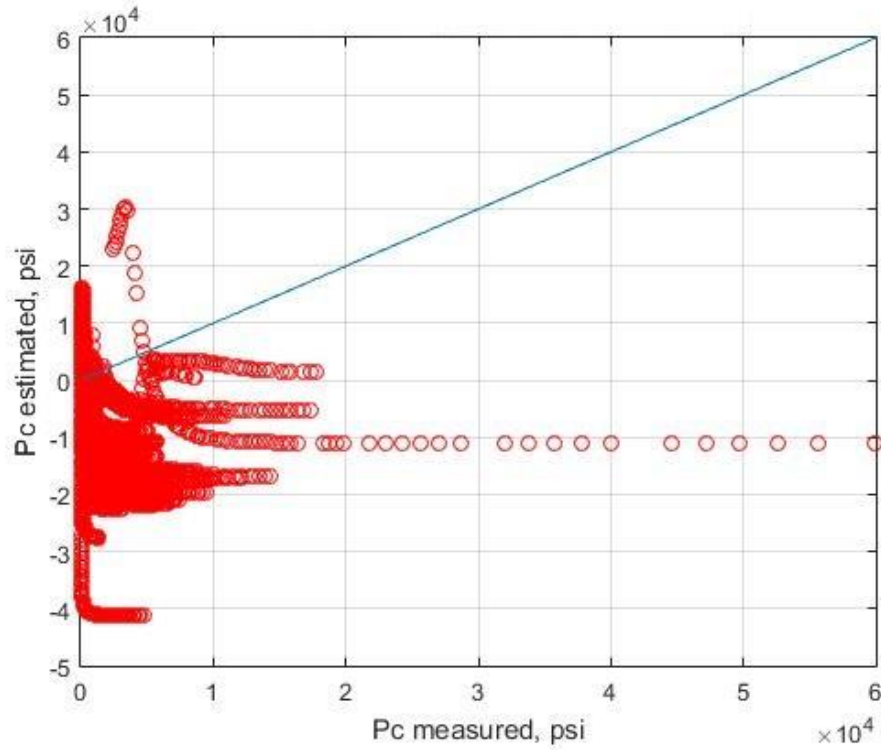


Figure 113. Predicted vs. measured values using ANN – traingd algorithm (Training).

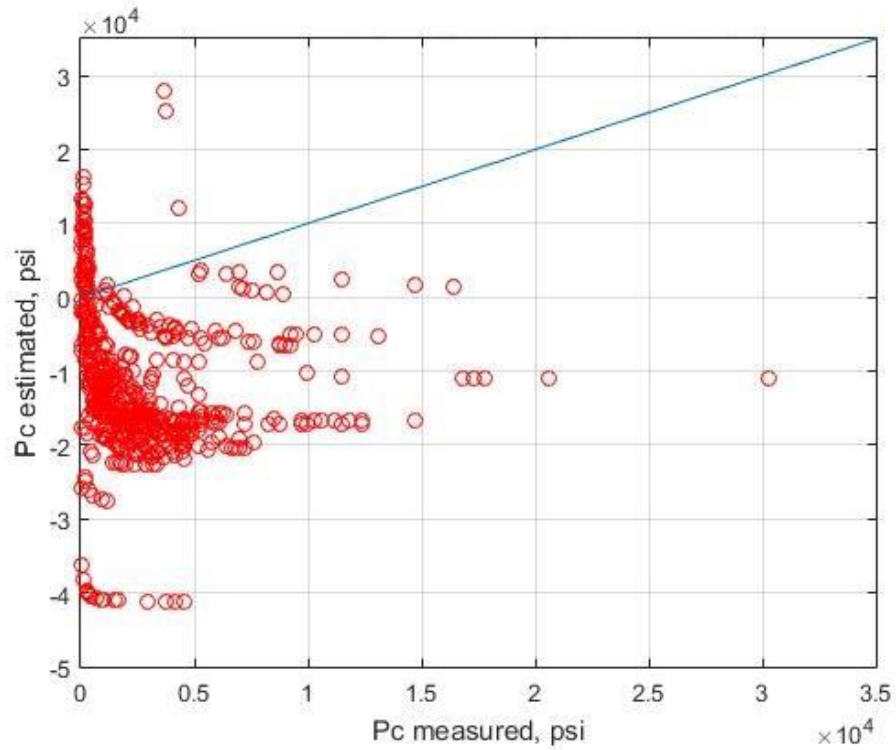


Figure 114. Predicted vs. measured values using ANN – traingd algorithm (Testing).

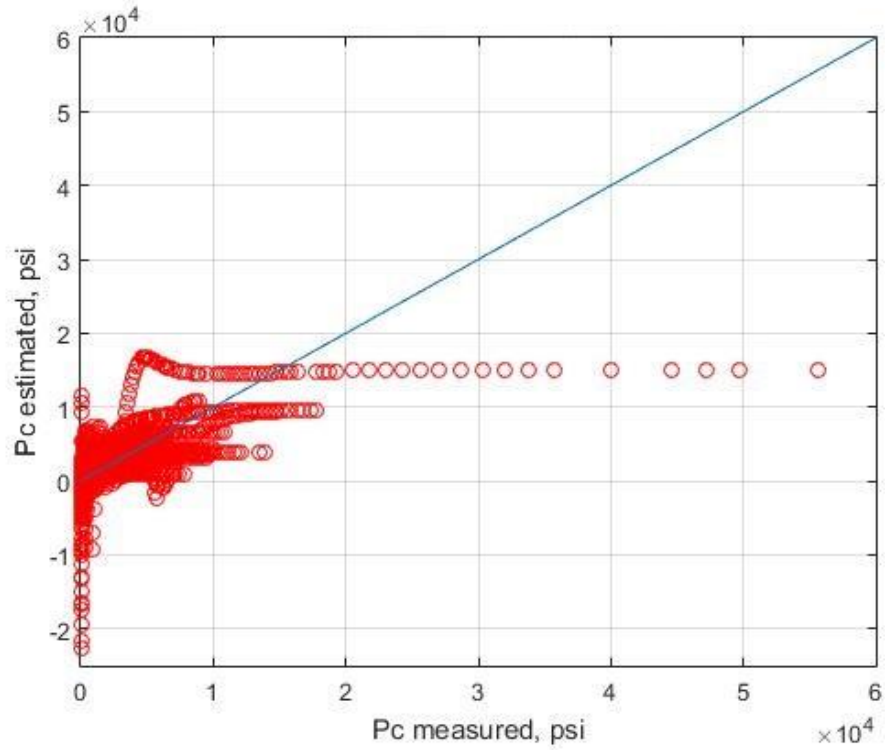


Figure 115. Predicted vs. measured values using ANN – traingdx algorithm (Training).

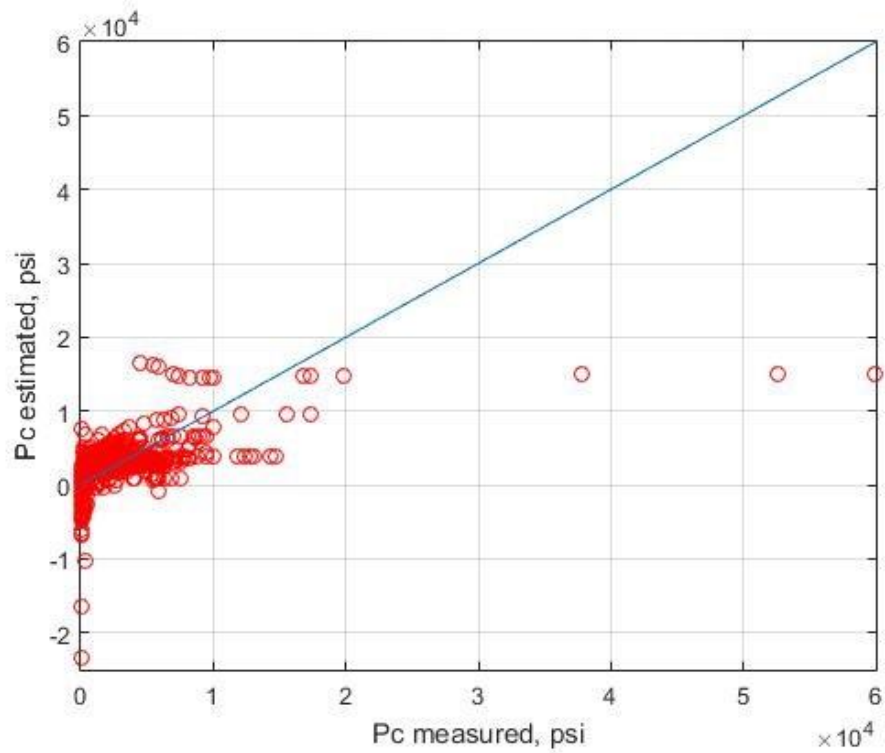


Figure 116. Predicted vs. measured values using ANN – traingdx algorithm (Testing).

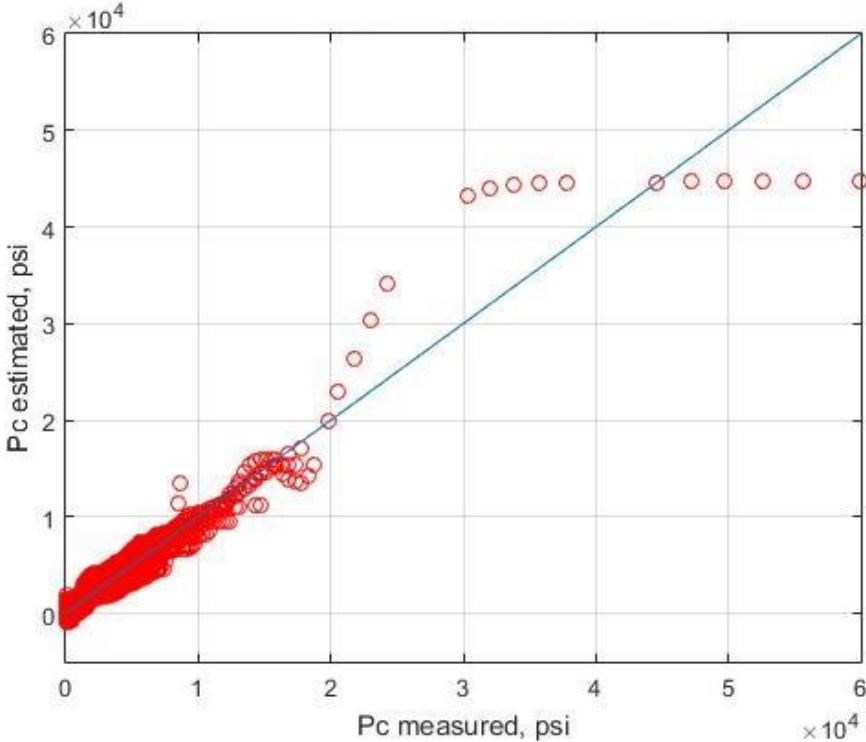


Figure 117. Predicted vs. measured values using ANN – trainlm algorithm (Training).

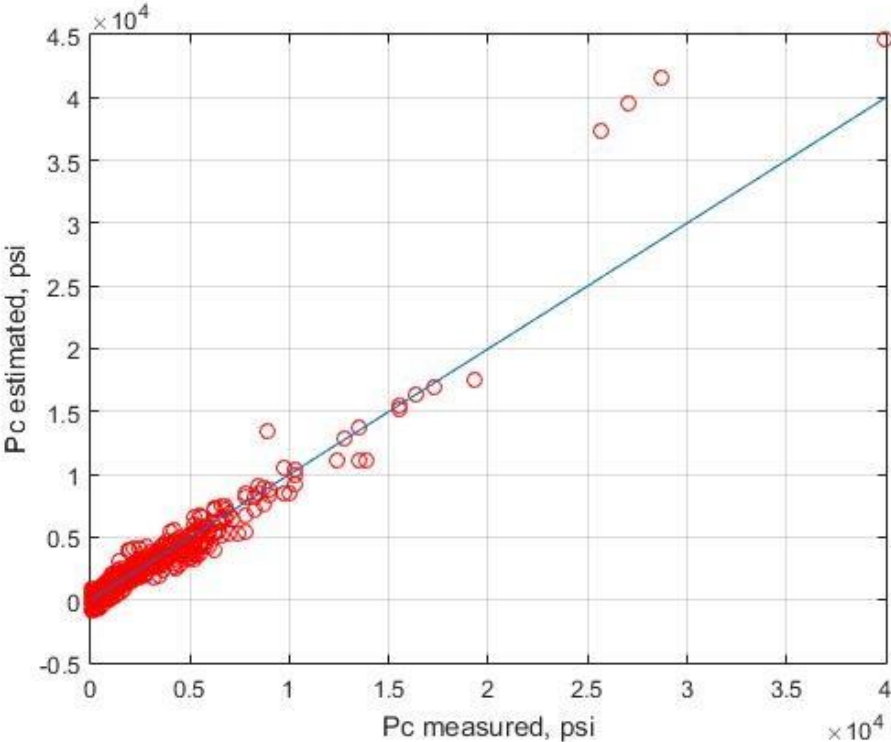


Figure 118. Predicted vs. measured values using ANN – trainlm algorithm (Testing).

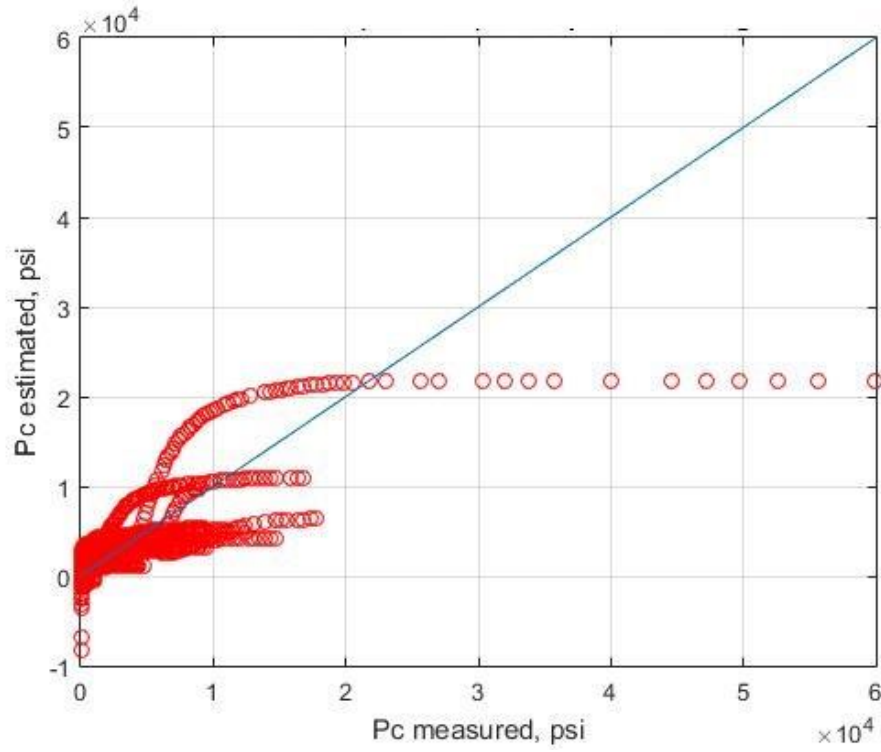


Figure 119. Predicted vs. measured values using ANN – trainoss algorithm (Training).

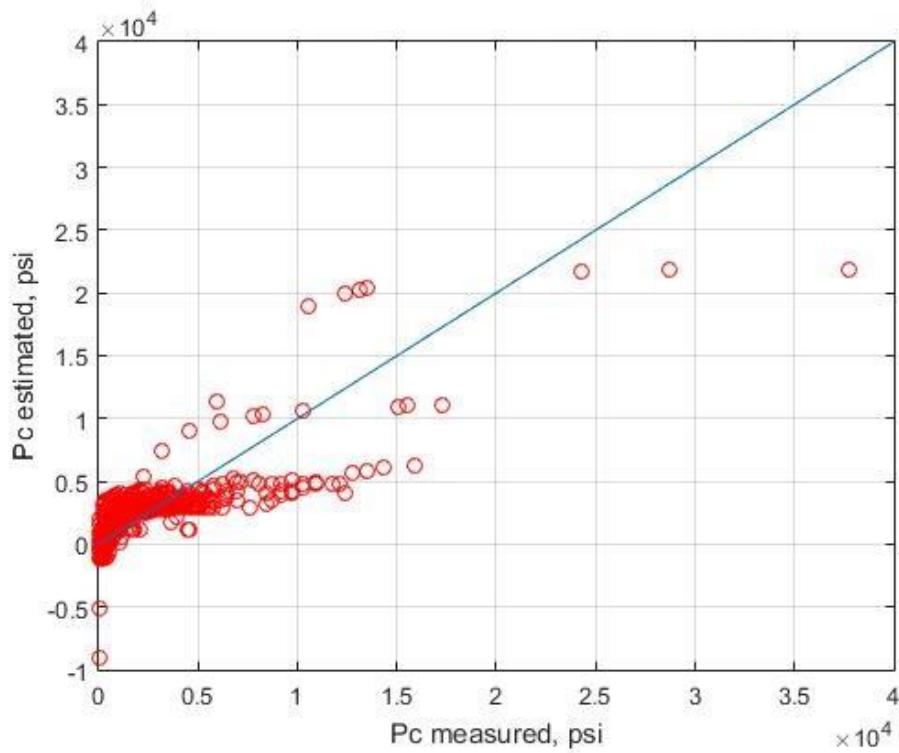


Figure 120. Predicted vs. measured values using ANN – trainoss algorithm (Testing).

Bi-modal capillary pressure curve

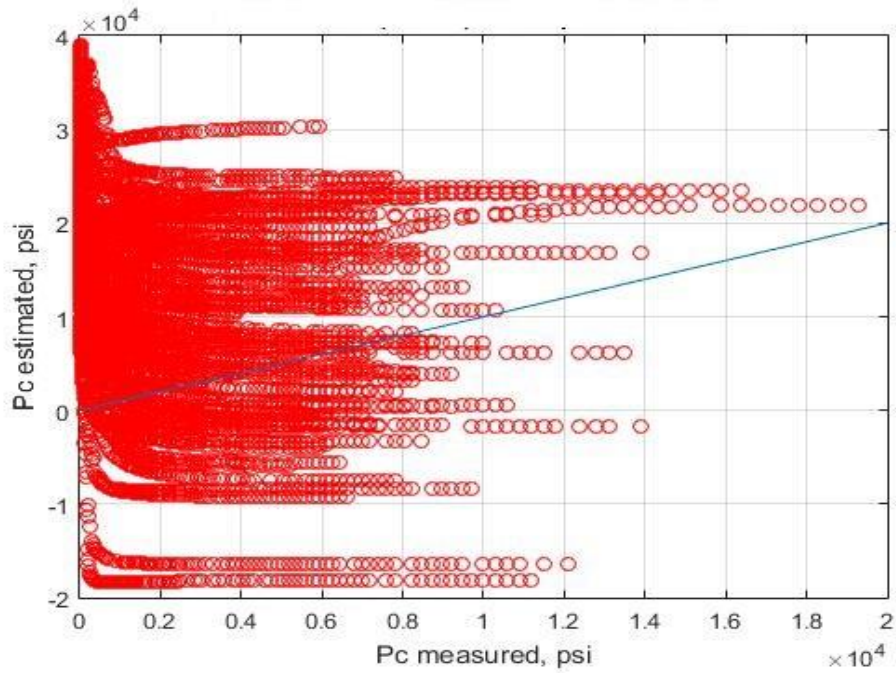


Figure 121. Predicted vs. measured values using ANN – trainb algorithm (Training).

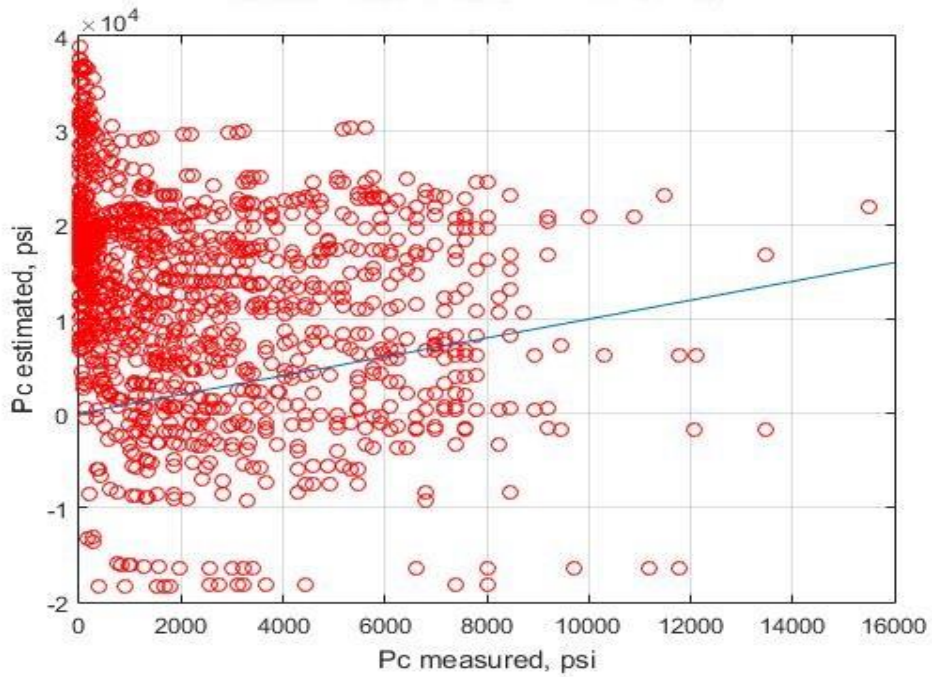


Figure 122. Predicted vs. measured values using ANN – trainb algorithm (Testing).

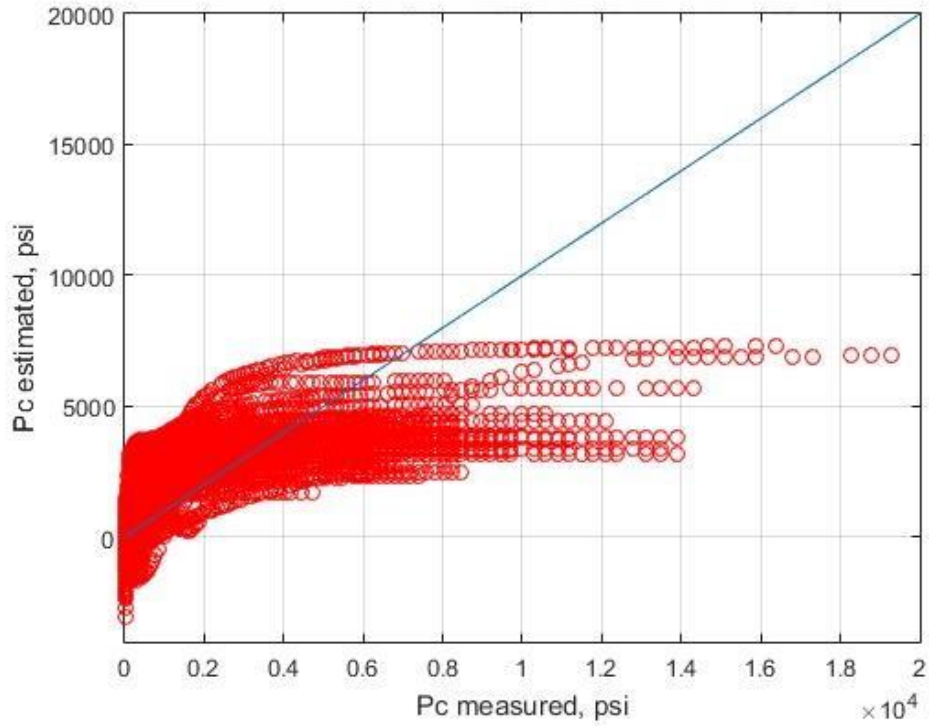


Figure 123. Predicted vs. measured values using ANN – trainbfg algorithm (Training).

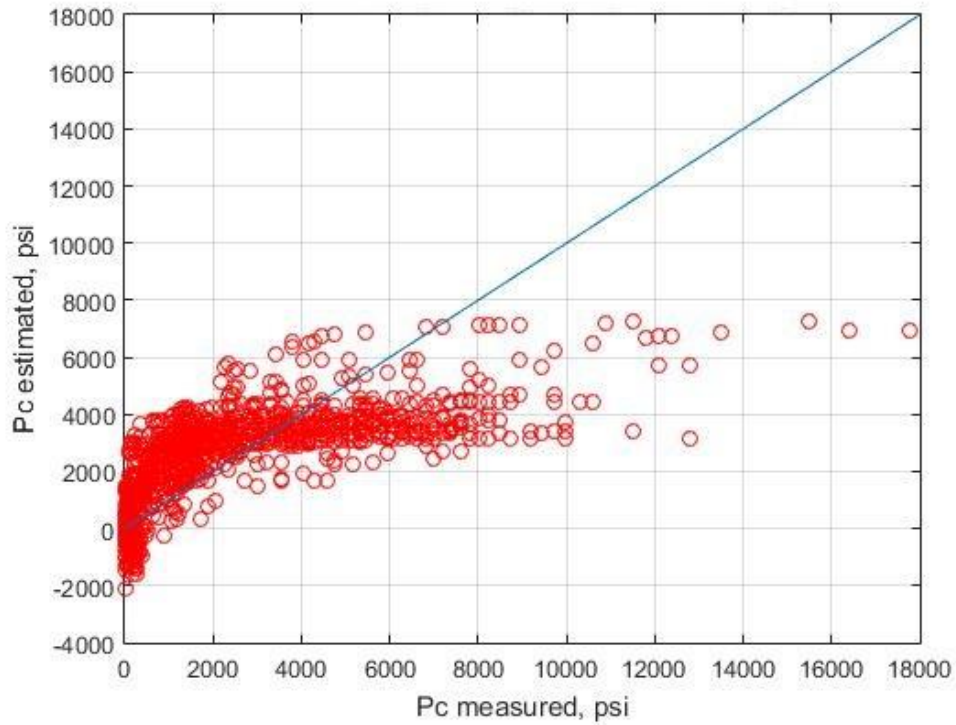


Figure 124. Predicted vs. measured values using ANN – trainbfg algorithm (Testing).

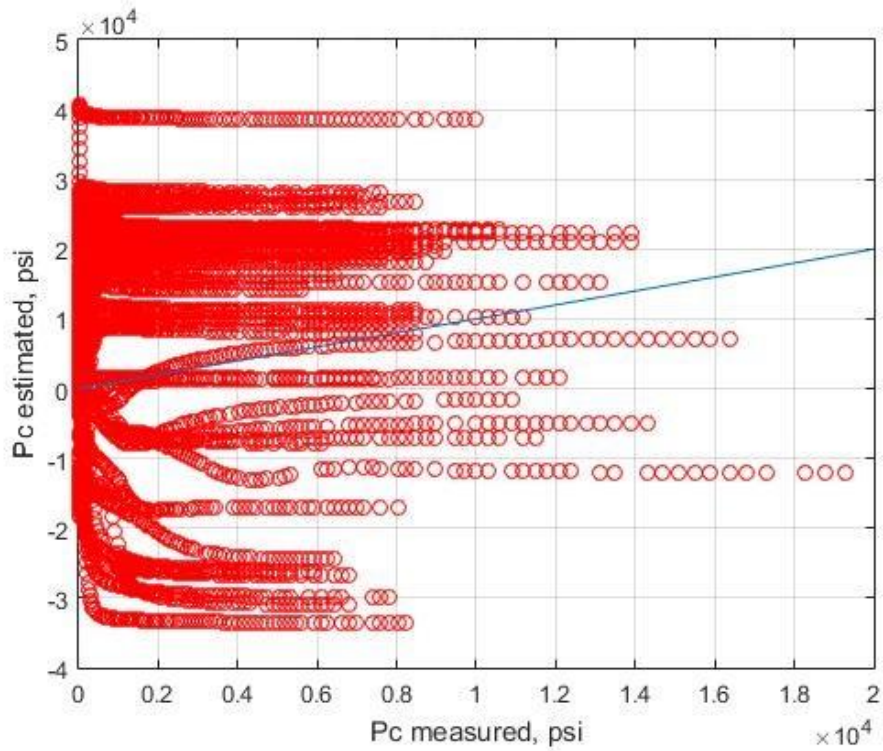


Figure 125. Predicted vs. measured values using ANN – traingd algorithm (Training).

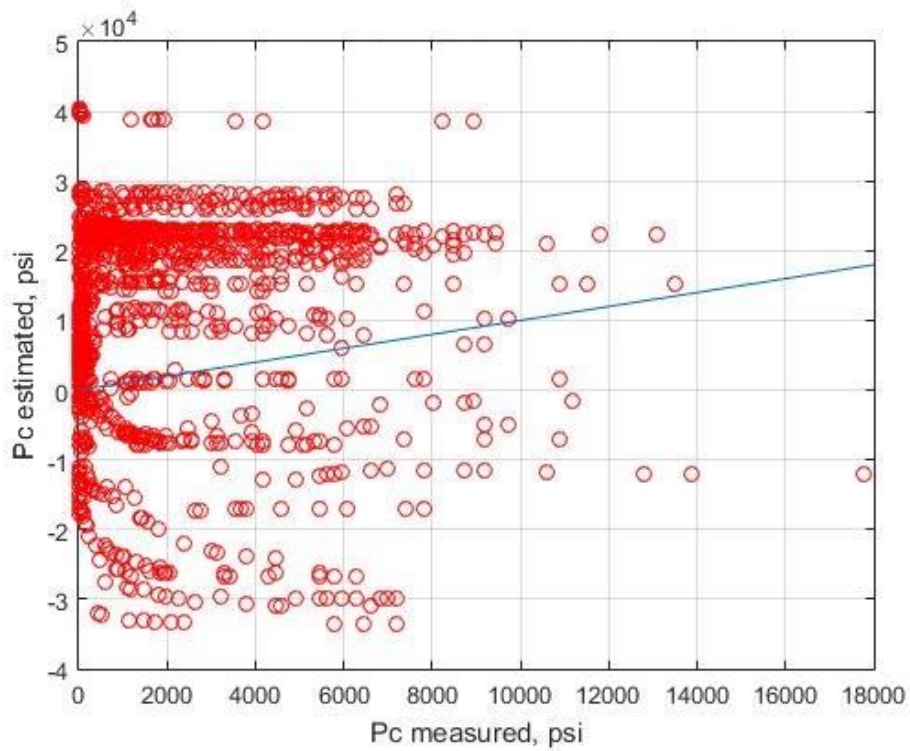


Figure 126. Predicted vs. measured values using ANN – traingd algorithm (Testing).

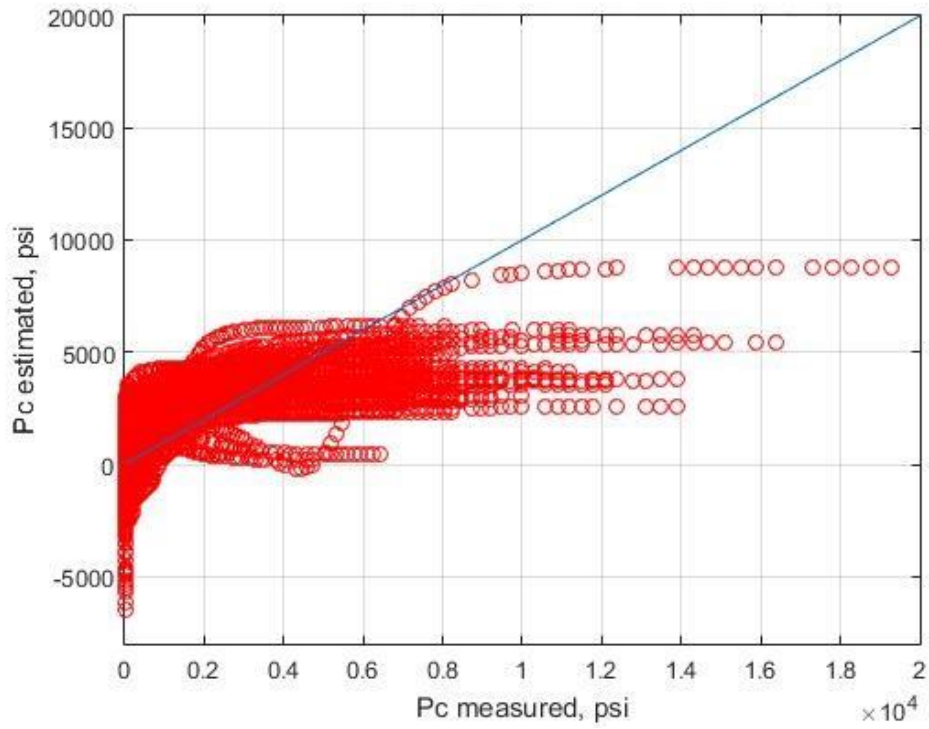


Figure 127. Predicted vs. measured values using ANN – traingdx algorithm (Training).

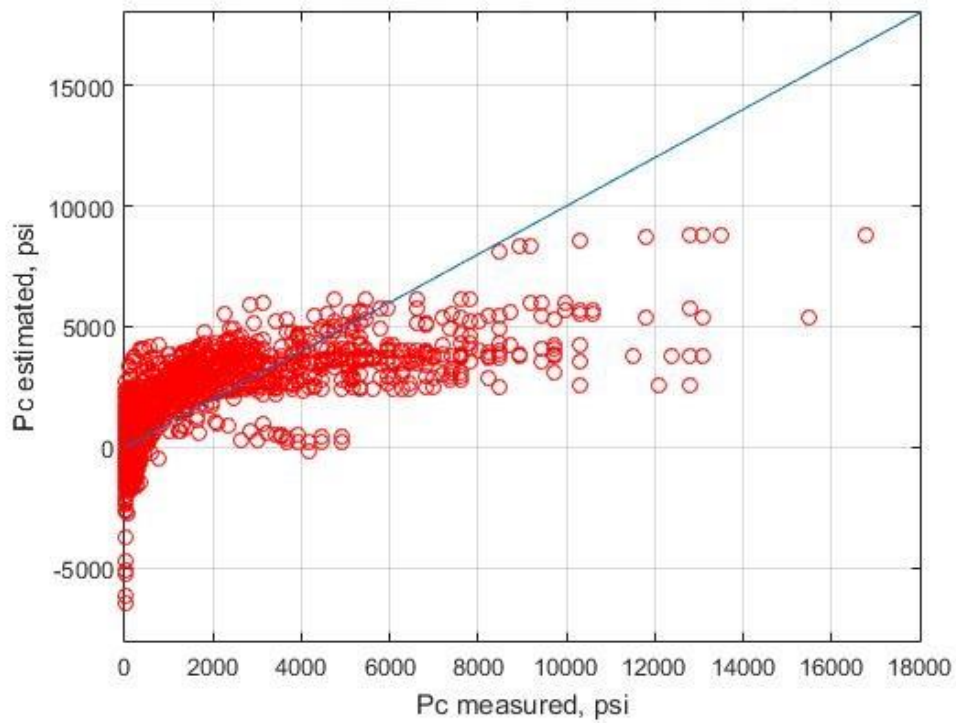


Figure 128. Predicted vs. measured values using ANN – traingdx algorithm (Testing).

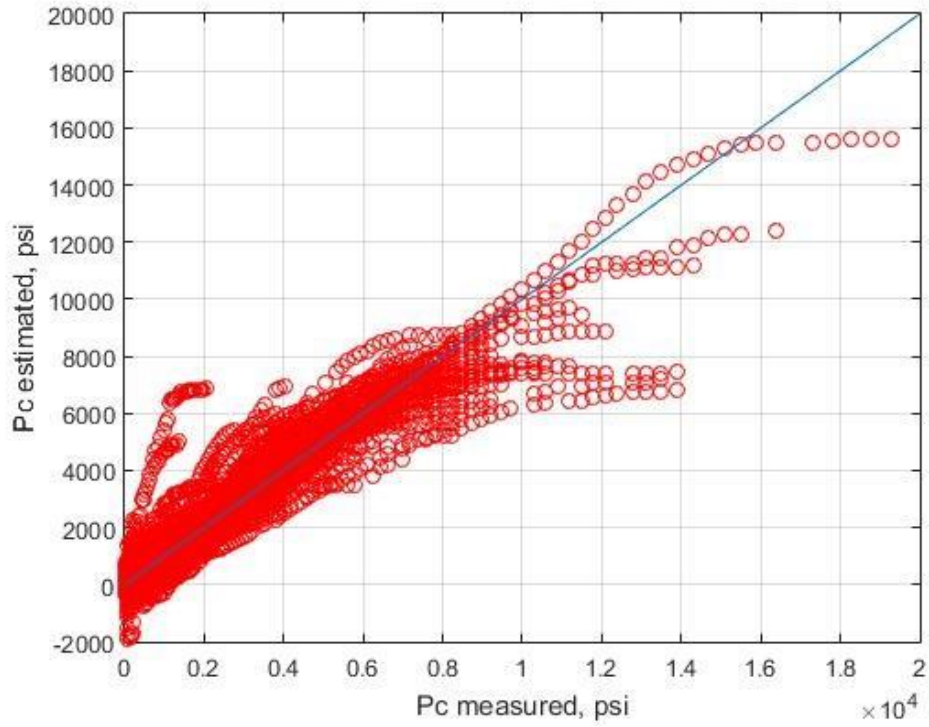


Figure 129. Predicted vs. measured values using ANN – trainlm algorithm (Training).

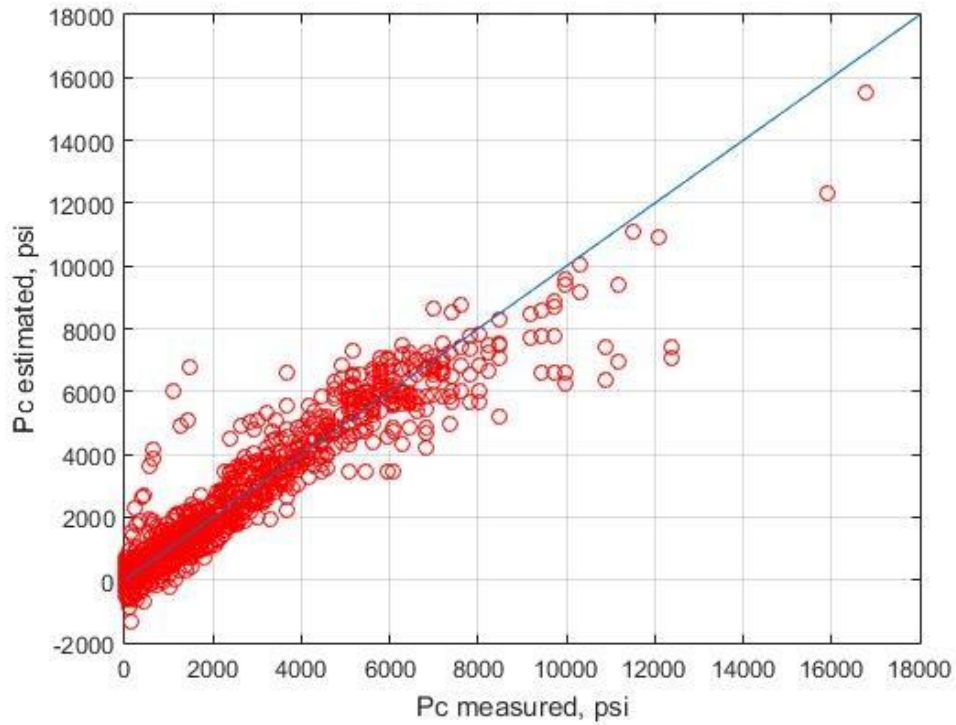


Figure 130. Predicted vs. measured values using ANN – trainlm algorithm (Testing).

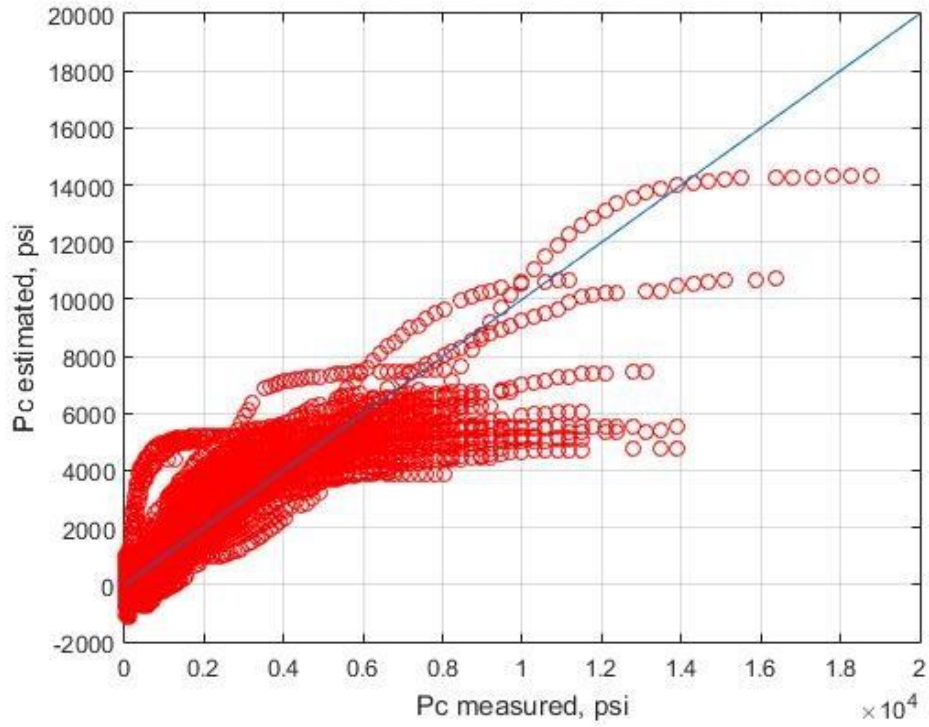


Figure 131. Predicted vs. measured values using ANN – trainoss algorithm (Training).

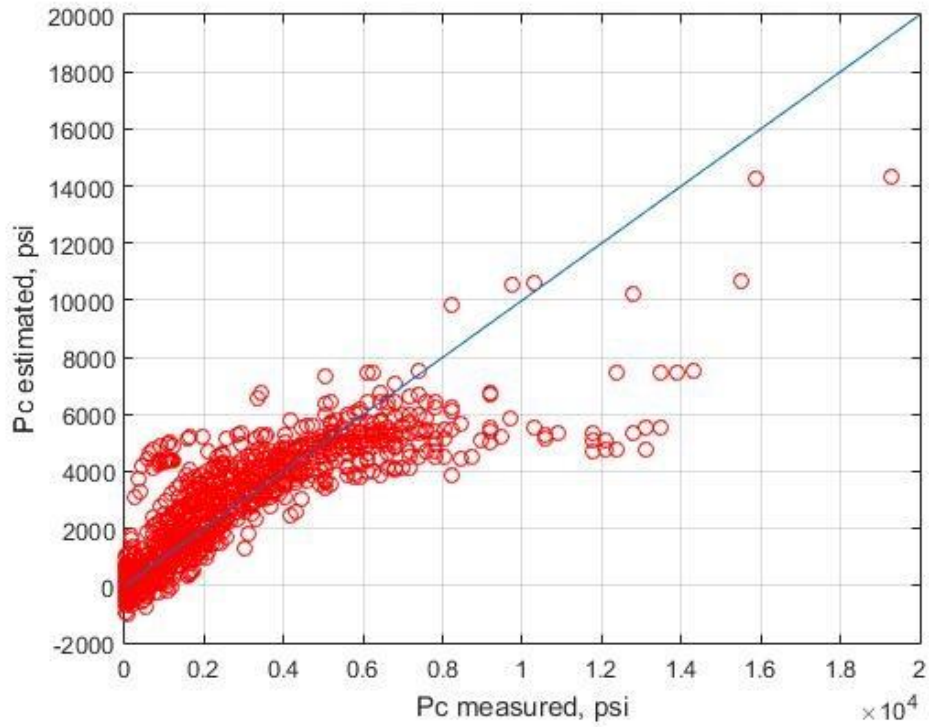


Figure 132. Predicted vs. measured values using ANN – trainoss algorithm (Testing).

Combined modals capillary pressure curve

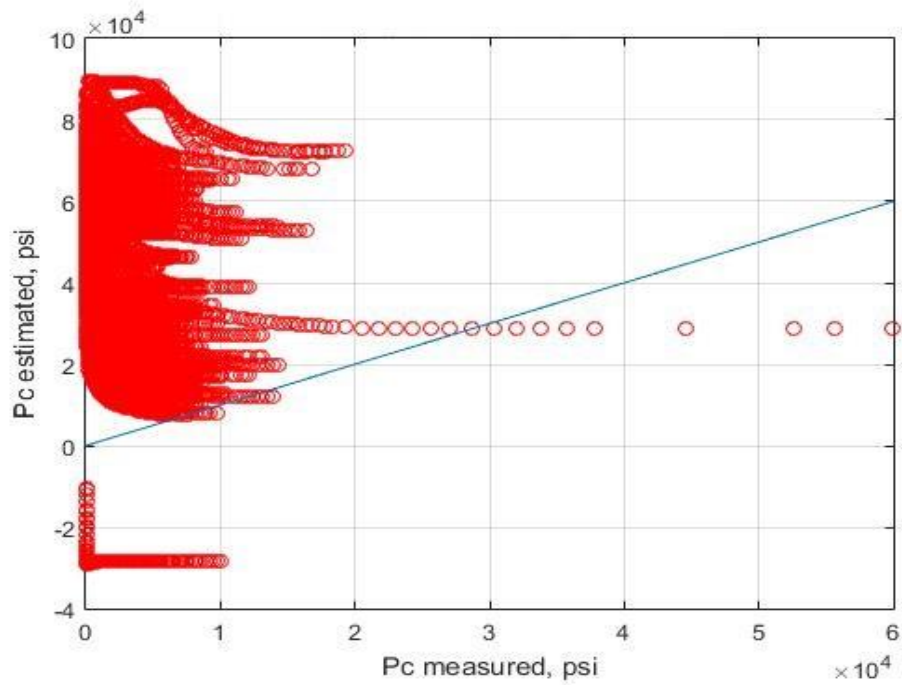


Figure 133. Predicted vs. measured values using ANN – trainb algorithm (Training).

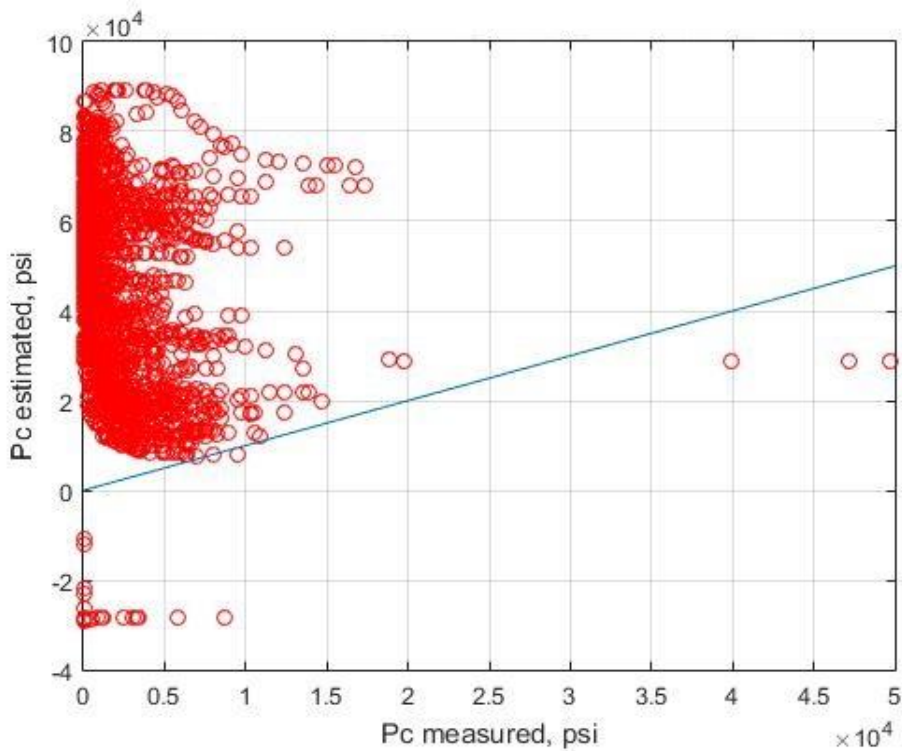


Figure 134. Predicted vs. measured values using ANN – trainb algorithm (Testing).

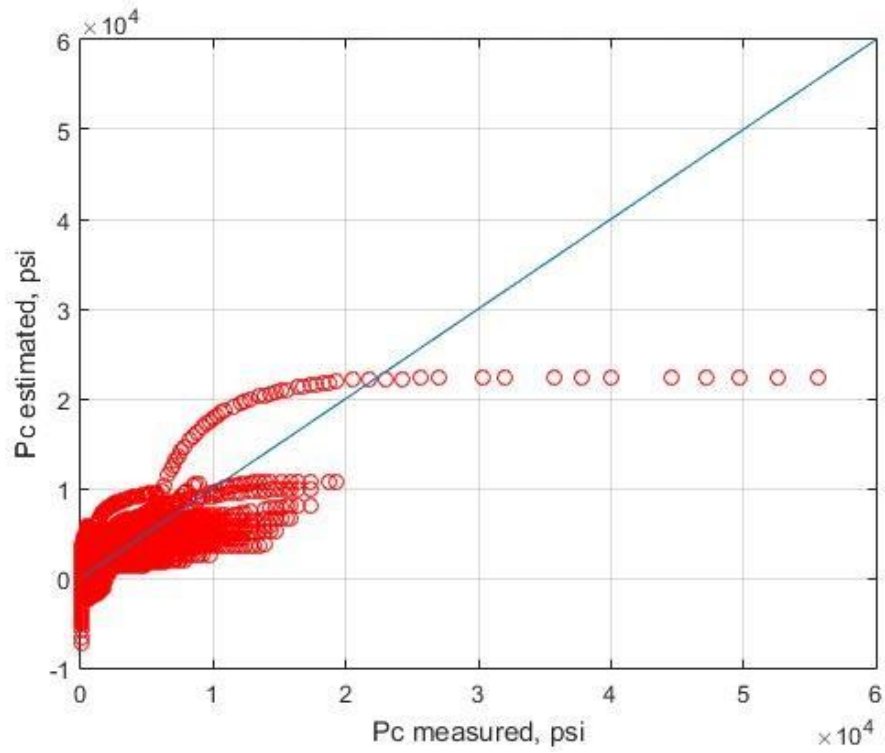


Figure 135. Predicted vs. measured values using ANN – trainbfg algorithm (Training).

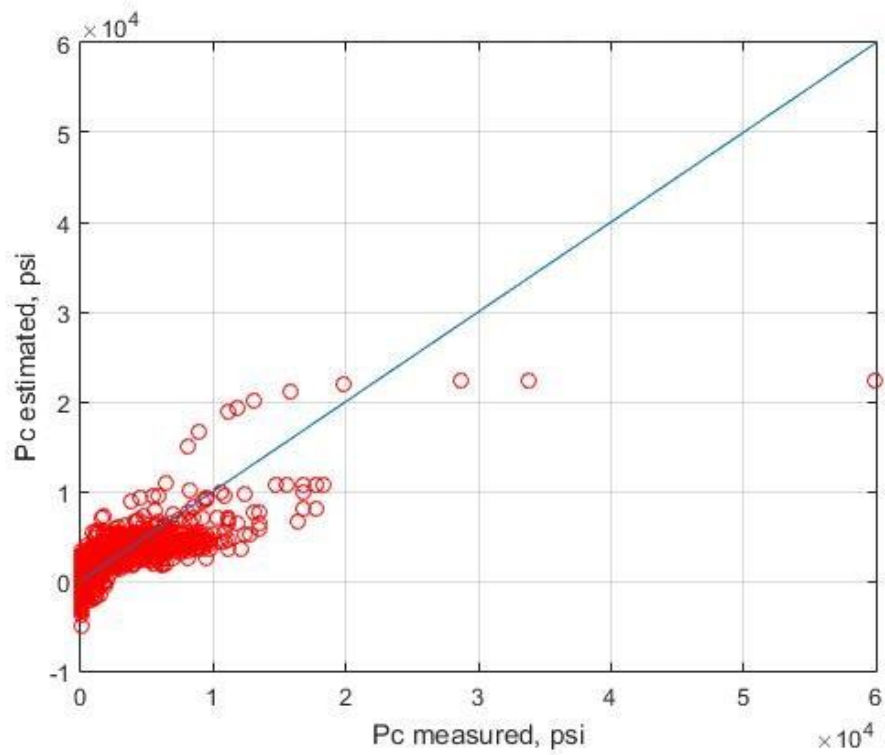


Figure 136. Predicted vs. measured values using ANN – trainbfg algorithm (Testing).

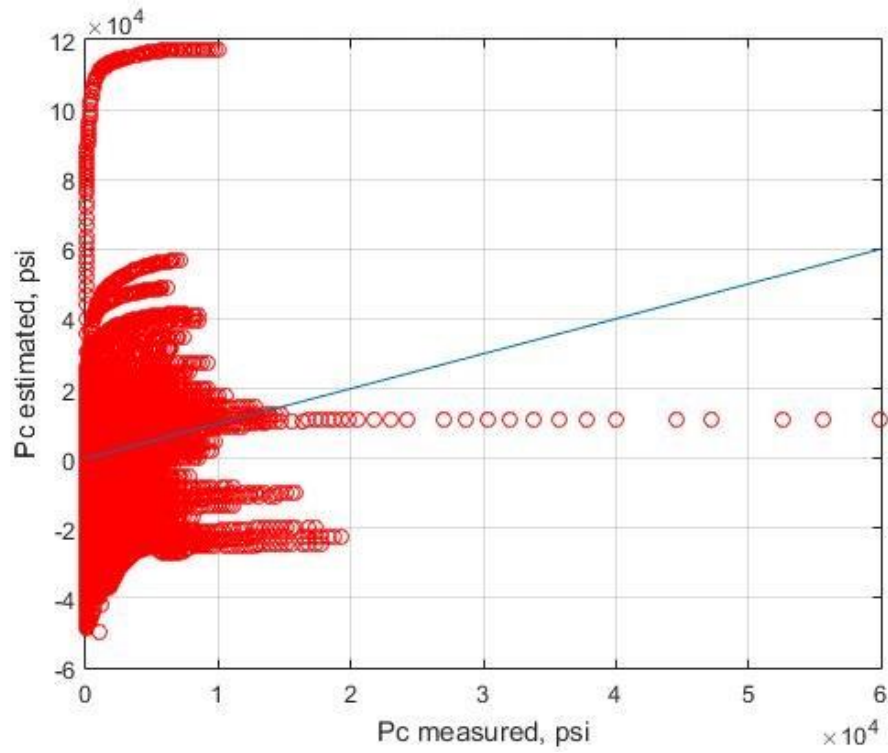


Figure 137. Predicted vs. measured values using ANN – traingd algorithm (Training).

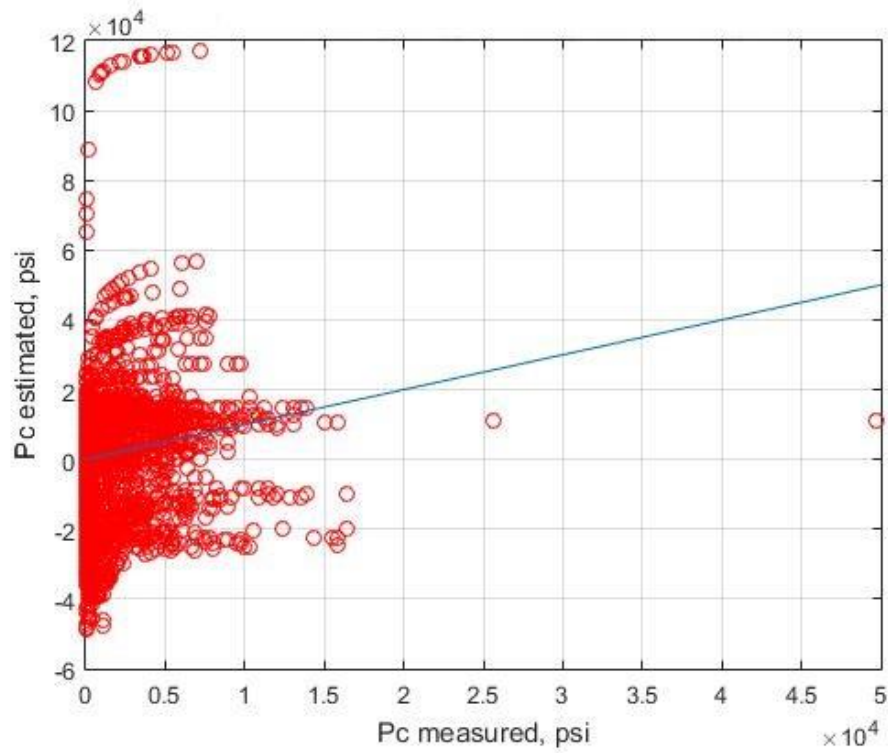


Figure 138. Predicted vs. measured values using ANN – traingd algorithm (Testing).

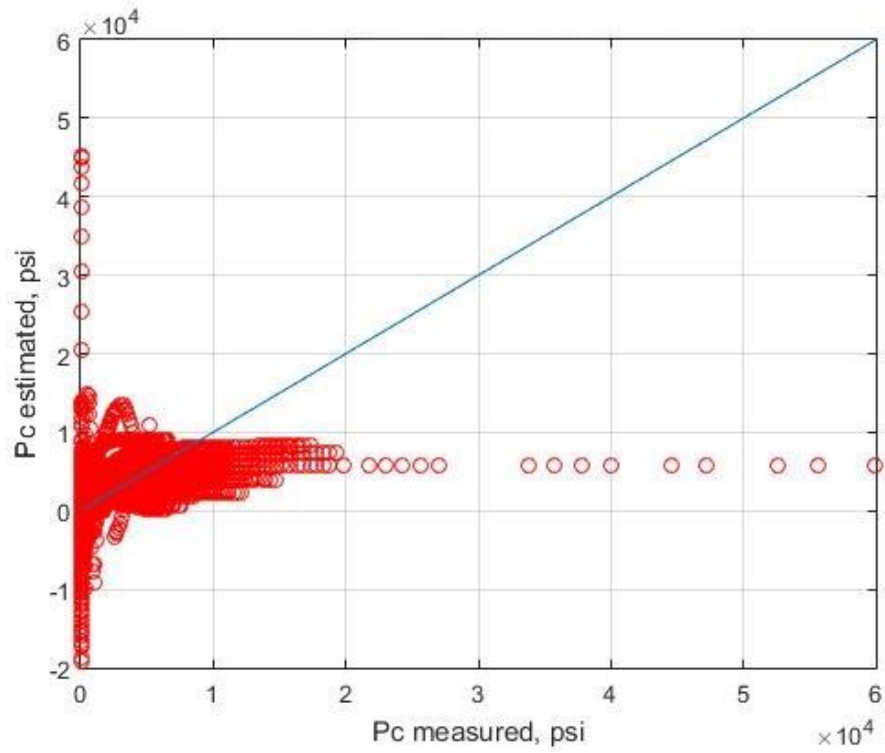


Figure 139. Predicted vs. measured values using ANN – traingdx algorithm (Training).

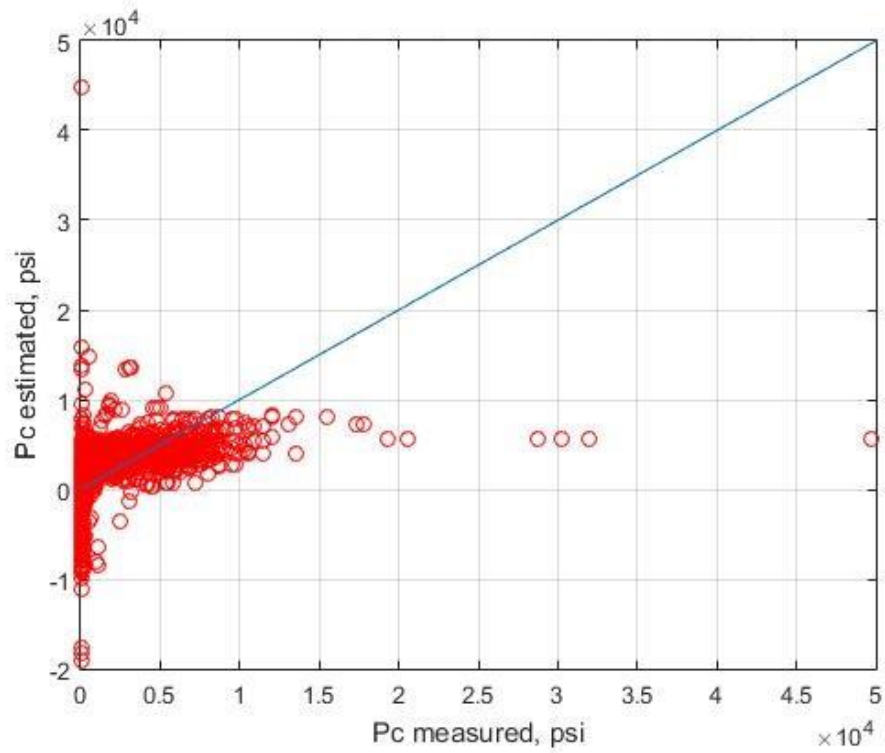


Figure 140. Predicted vs. measured values using ANN – traingdx algorithm (Testing).

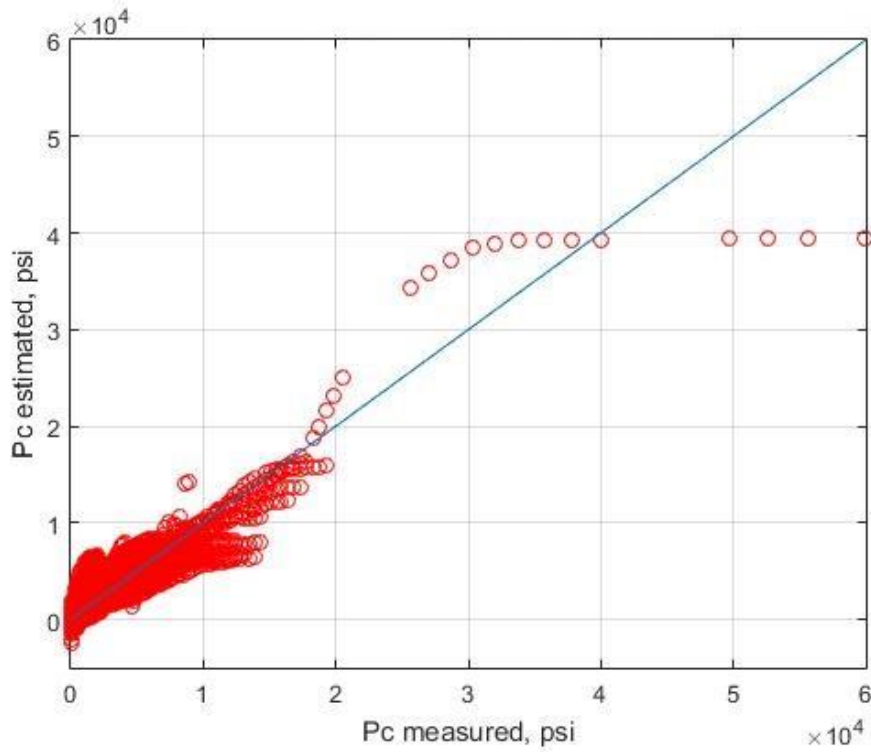


Figure 141. Predicted vs. measured values using ANN – trainlm algorithm (Training).

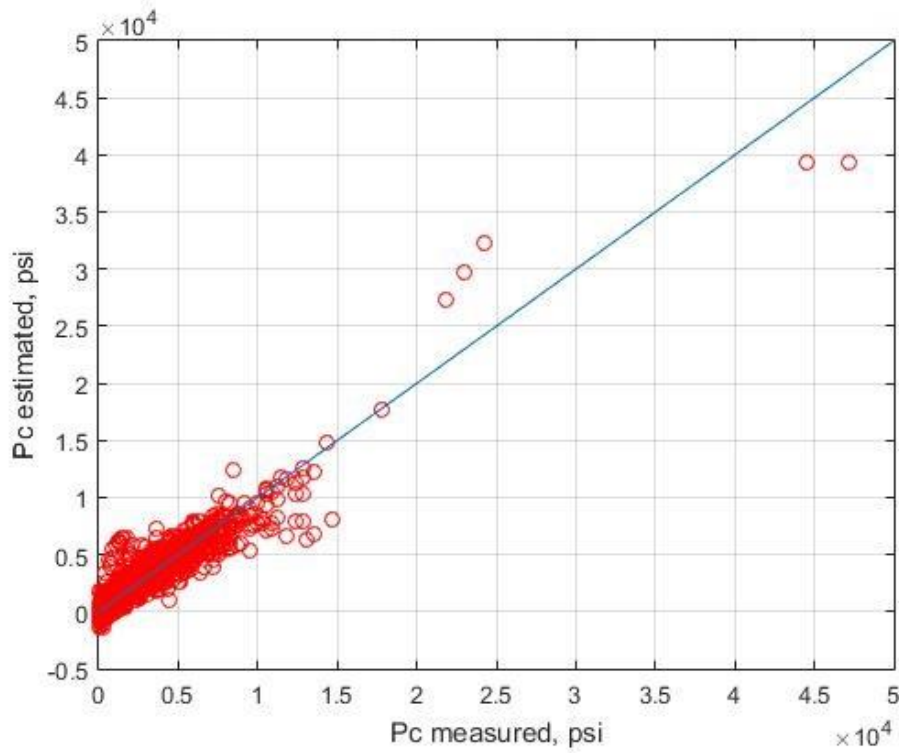


Figure 142. Predicted vs. measured values using ANN – trainlm algorithm (Testing).

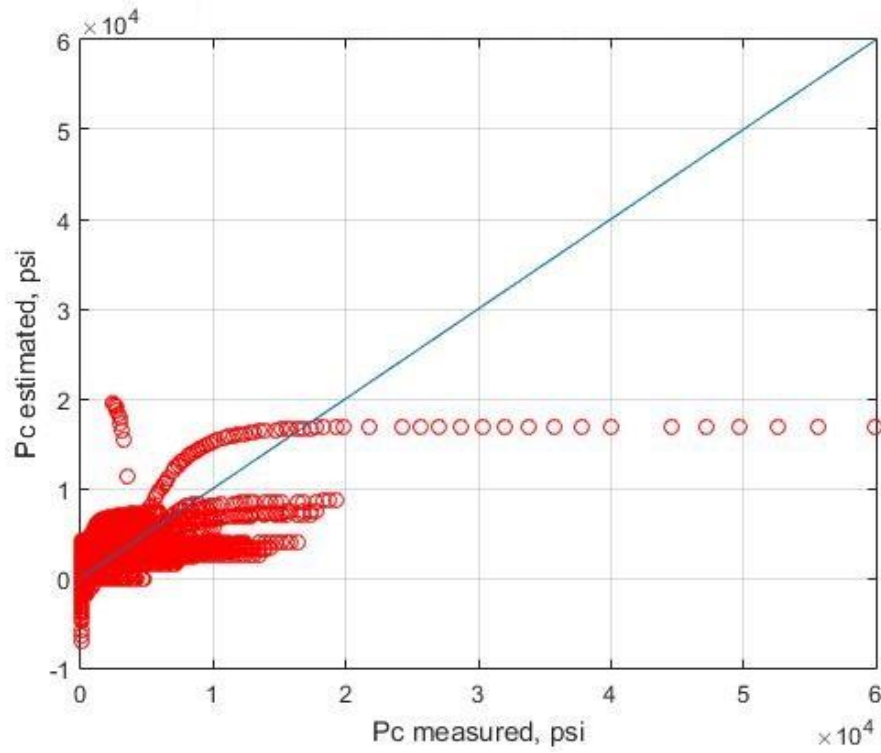


Figure 143. Predicted vs. measured values using ANN – trainoss algorithm (Training).

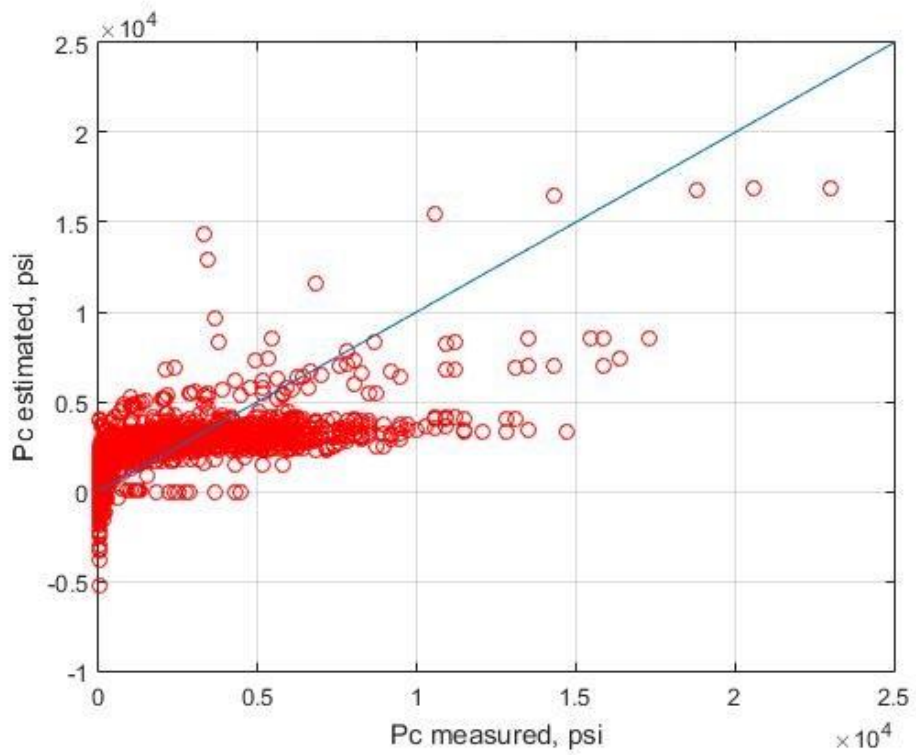


Figure 144. Predicted vs. measured values using ANN – trainoss algorithm (Testing).

B2. Fuzzy logic

Uni-modal capillary pressure curve

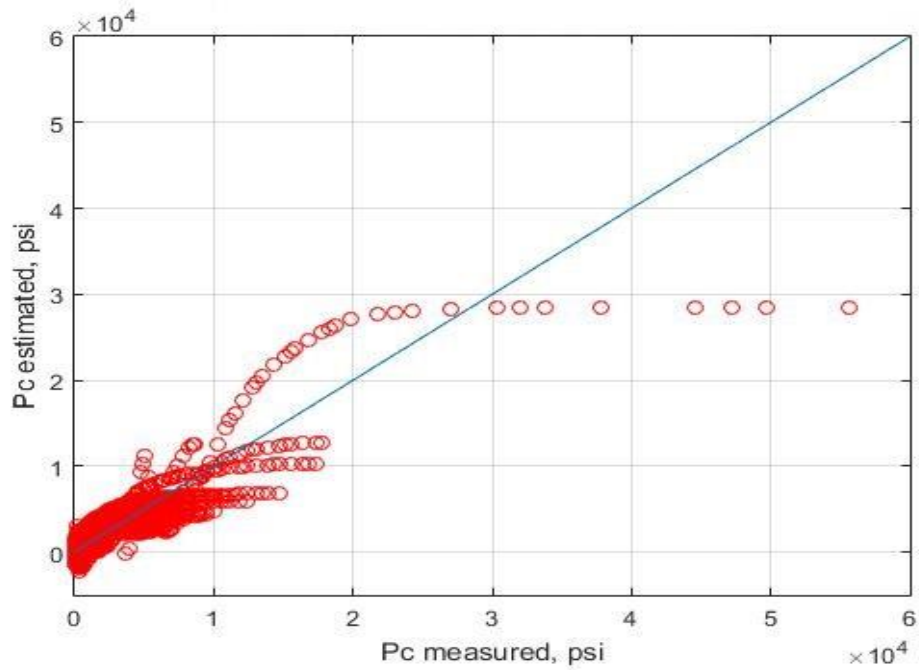


Figure 145. Predicted vs. measured values using Fuzzy Logic – Grid Partitioning algorithm (Training).

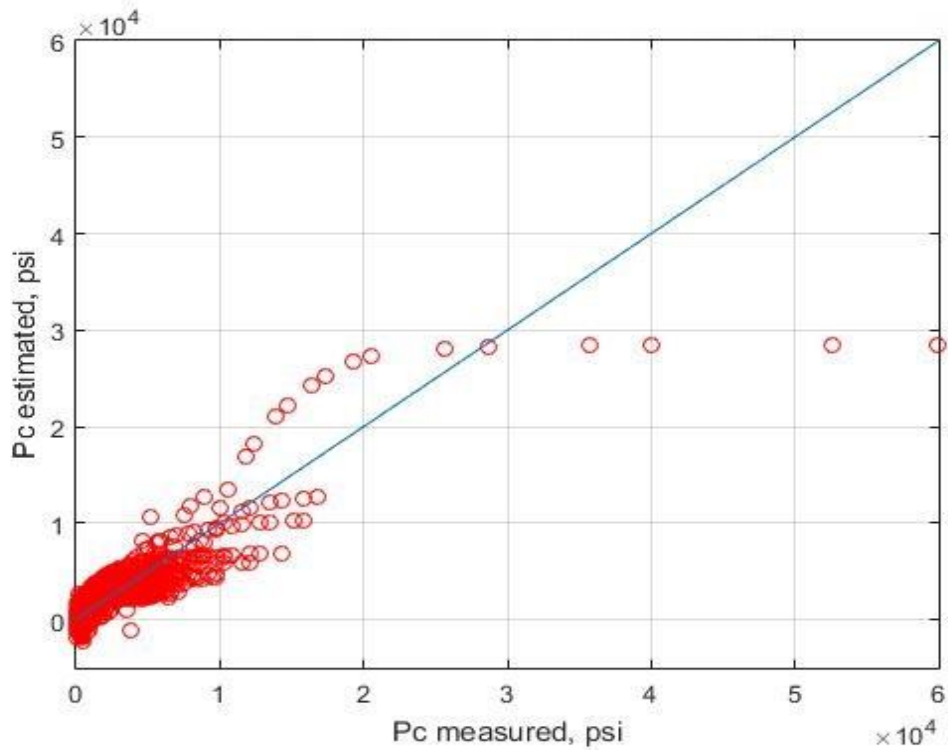


Figure 146. Predicted vs. measured values using Fuzzy Logic – Grid Partitioning algorithm (Testing).

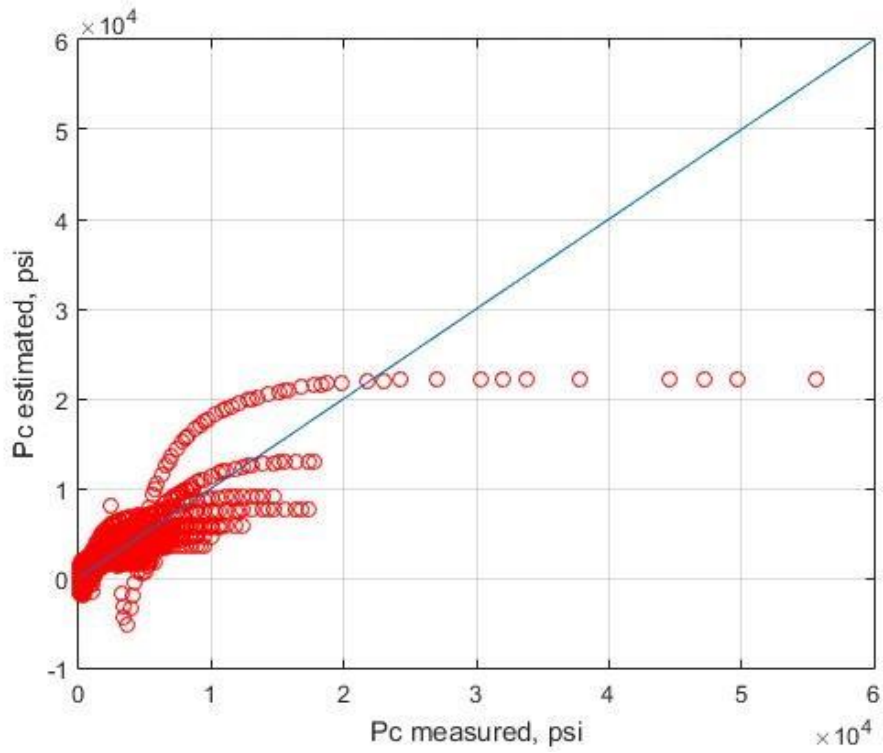


Figure 147. Predicted vs. measured values using Fuzzy Logic – Cluster Radius algorithm (Training).

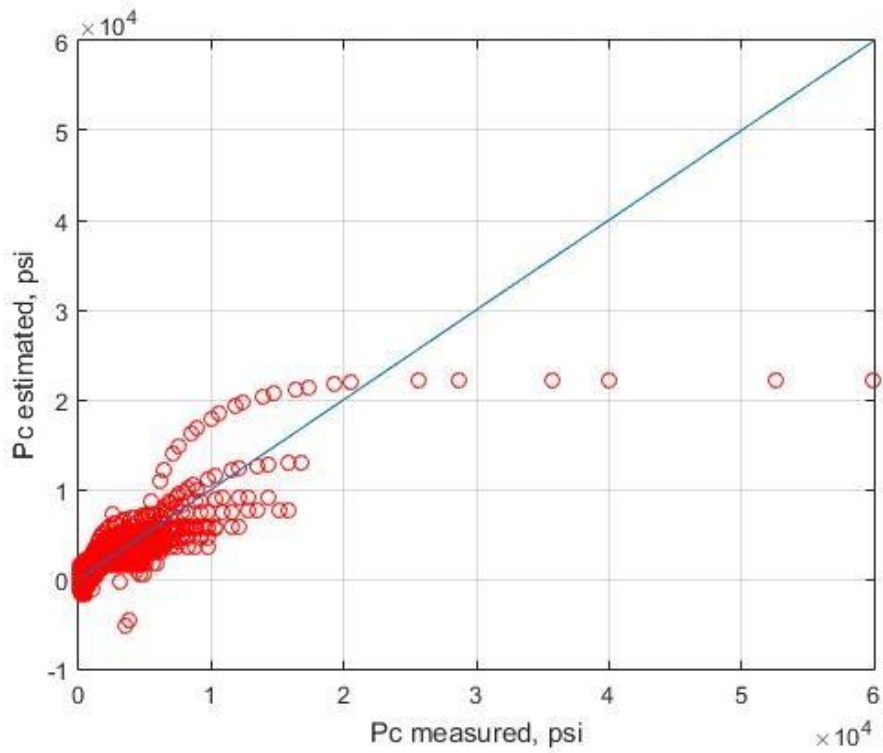


Figure 148. Predicted vs. measured values using Fuzzy Logic – Cluster Radius algorithm (Testing).

Bi-modal capillary pressure curve

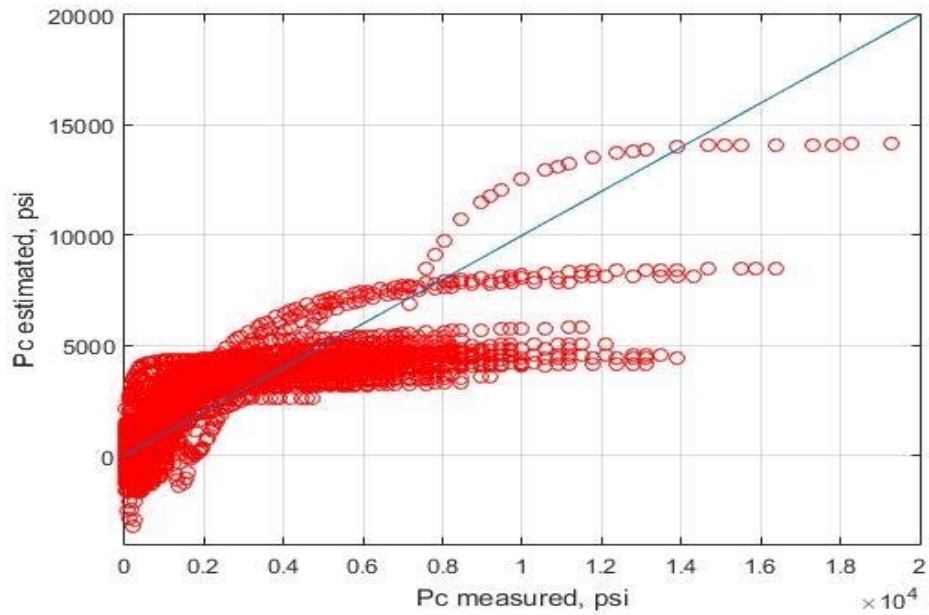


Figure 149.1 Predicted vs. measured values using Fuzzy Logic – Grid Partitioning algorithm (Training).

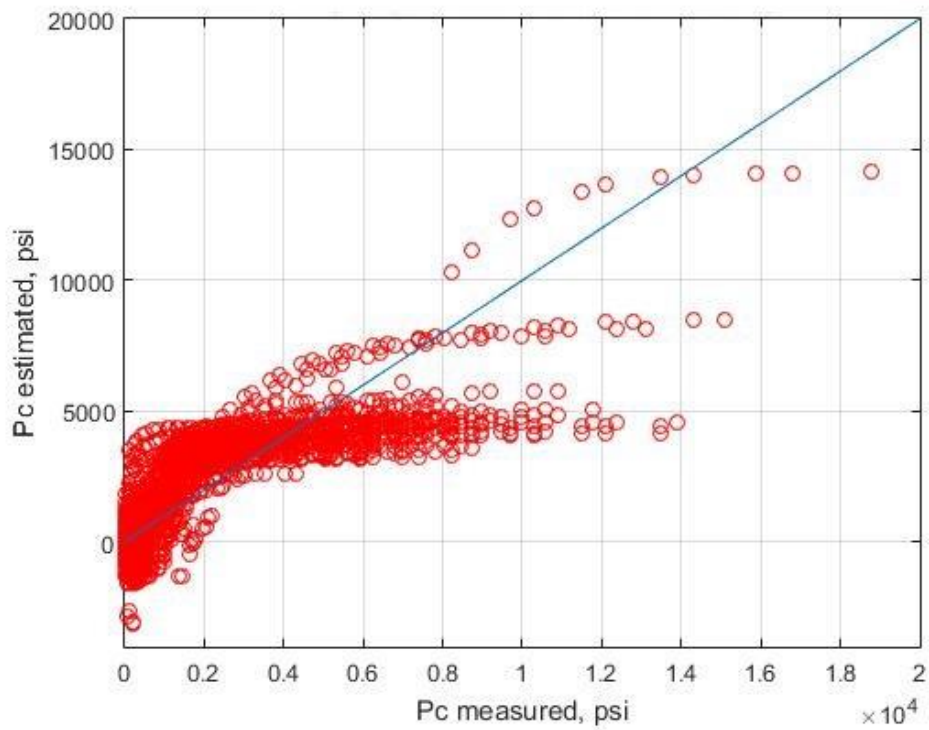


Figure 150. Predicted vs. measured values using Fuzzy Logic – Grid Partitioning algorithm (Testing).

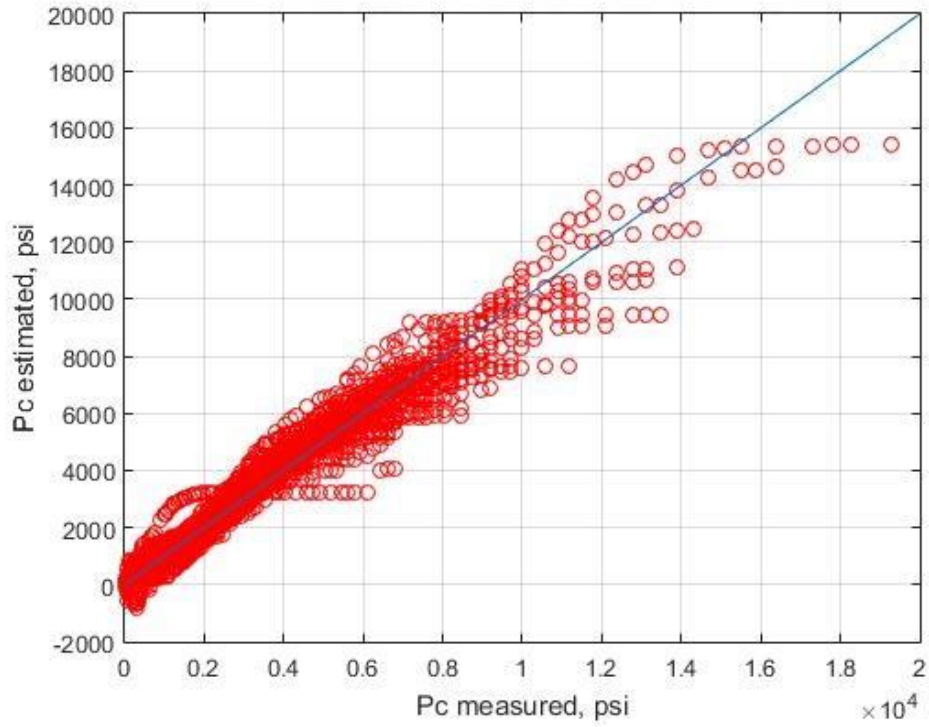


Figure 151. Predicted vs. measured values using Fuzzy Logic – Cluster Radius algorithm (Training).

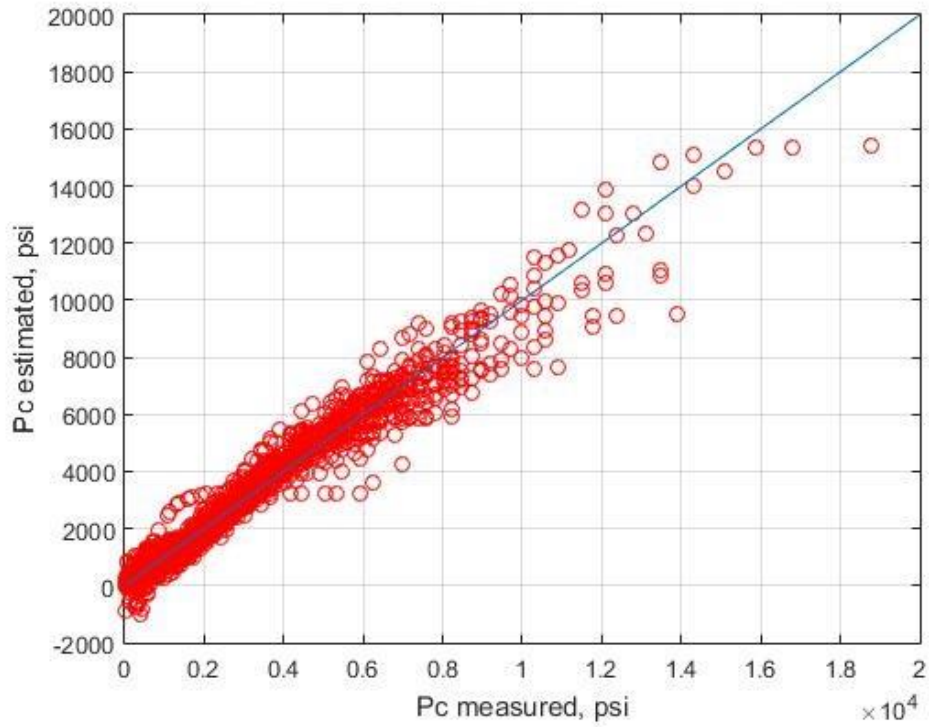


Figure 152. Predicted vs. measured values using Fuzzy Logic – Cluster Radius algorithm (Testing).

Combined modals capillary pressure curve

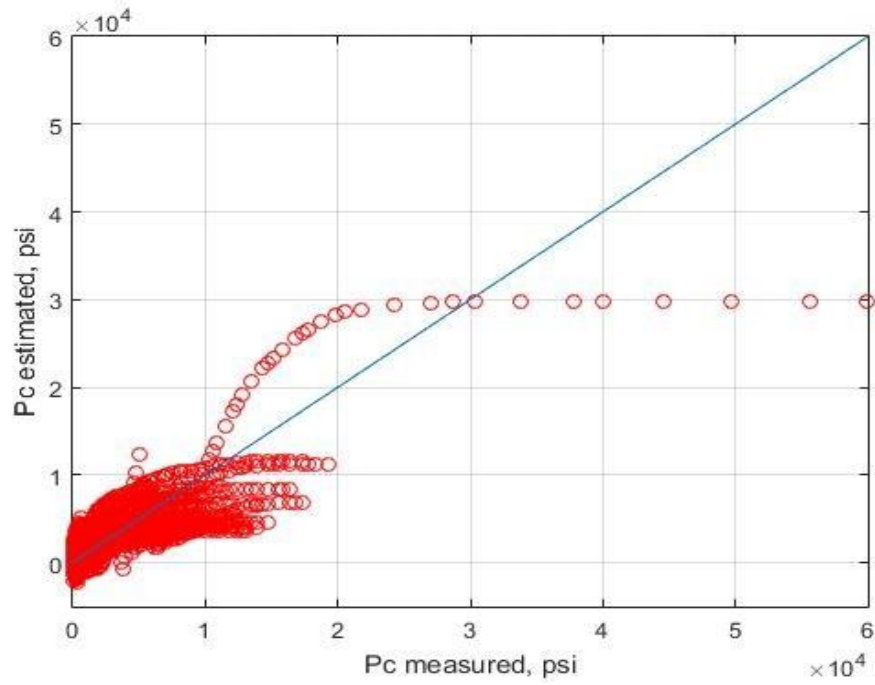


Figure 153: Predicted vs. measured values using Fuzzy Logic – Grid Partitioning algorithm (Training).

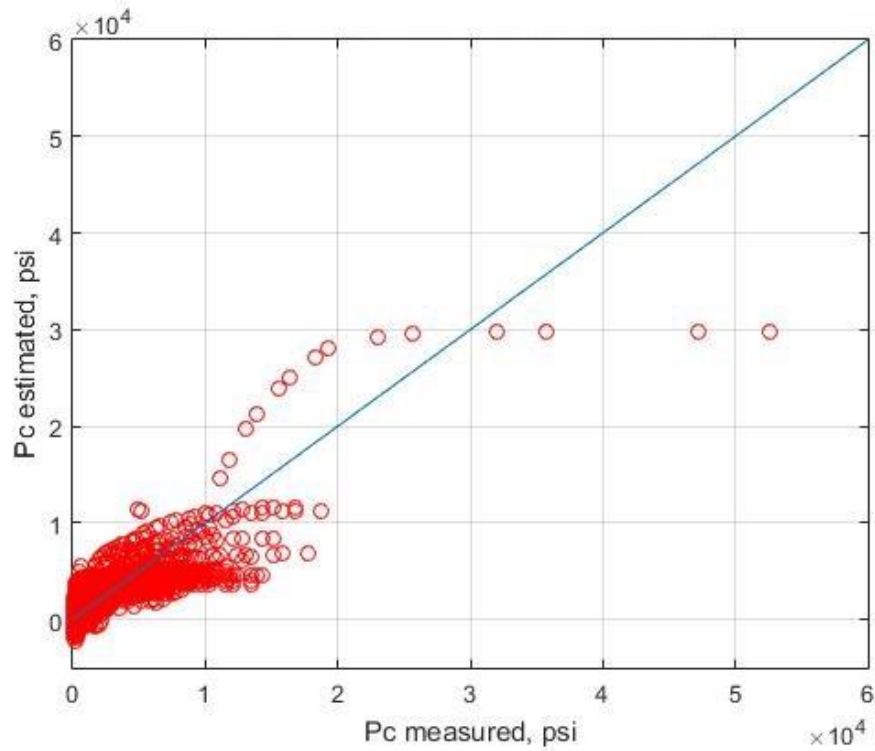


Figure 154. Predicted vs. measured values using Fuzzy Logic – Grid Partitioning algorithm (Testing).

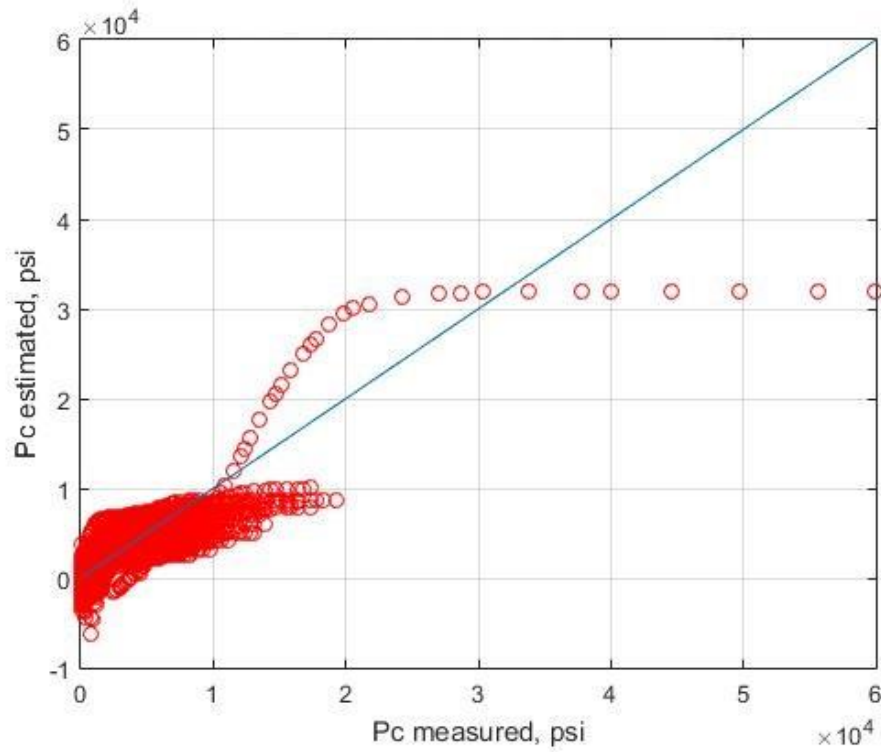


Figure 155. Predicted vs. measured values using Fuzzy Logic – Cluster Radius algorithm (Training).

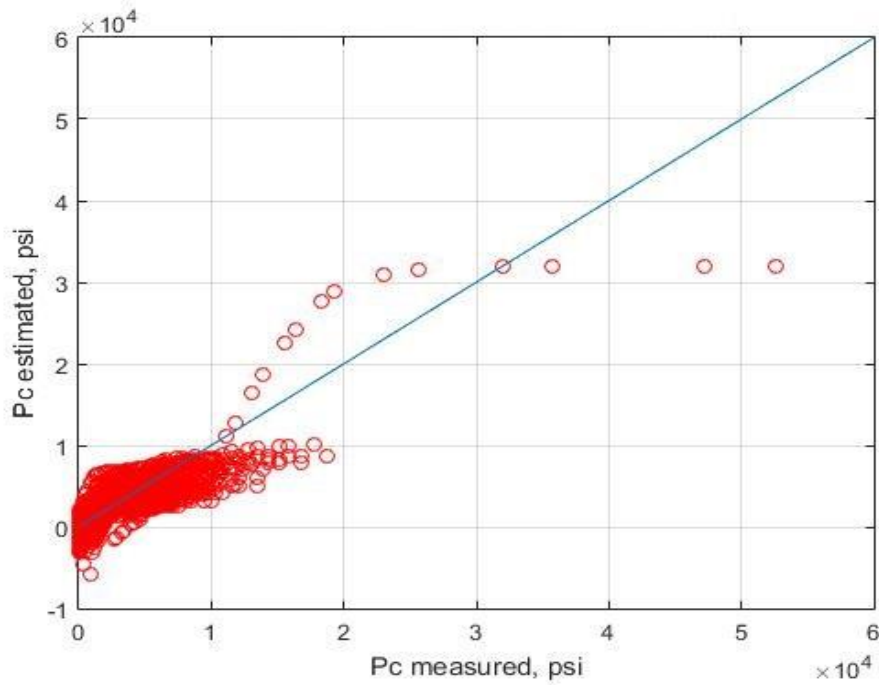


Figure 156. Predicted vs. measured values using Fuzzy Logic – Cluster Radius algorithm (Testing).

B3. Fuzzy logic type-2

Uni-modal capillary pressure curve

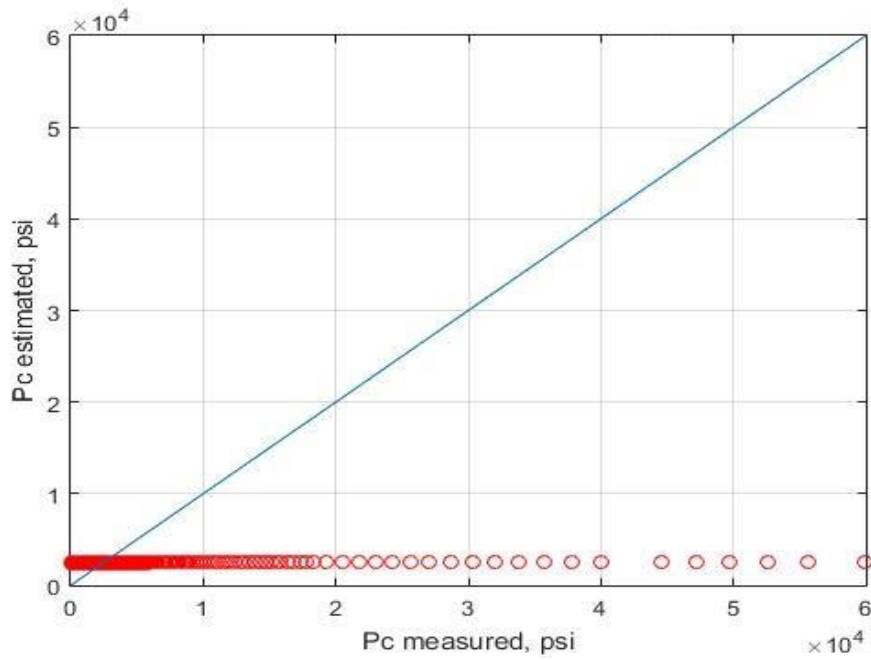


Figure 157. Predicted vs. measured values using Fuzzy Logic type-2 algorithm (Training).

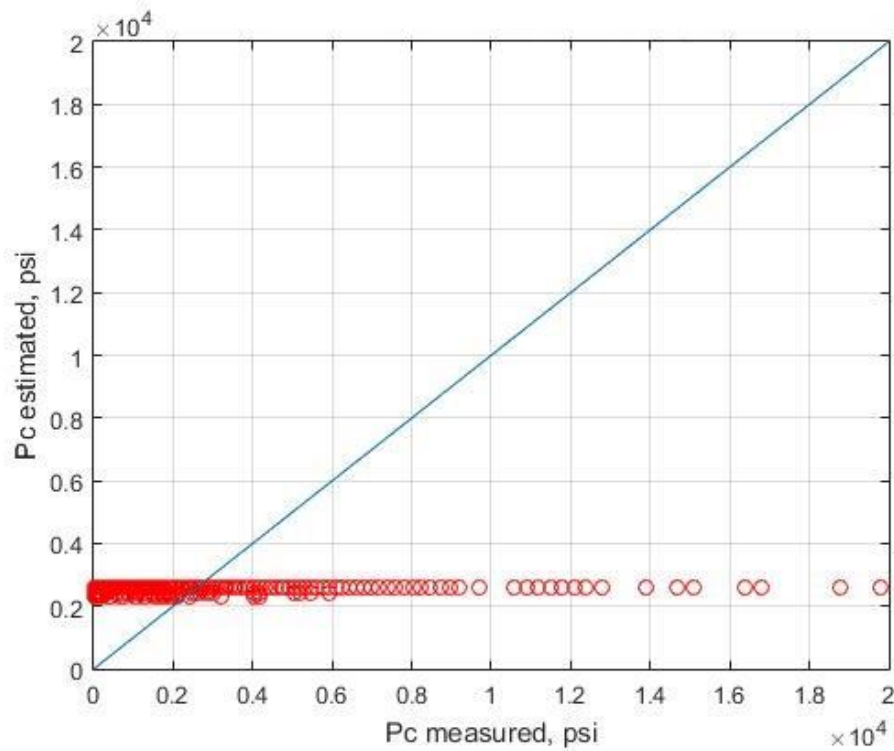


Figure 158. Predicted vs. measured values using Fuzzy Logic type-2 algorithm (Testing).

Bi-modal capillary pressure curve

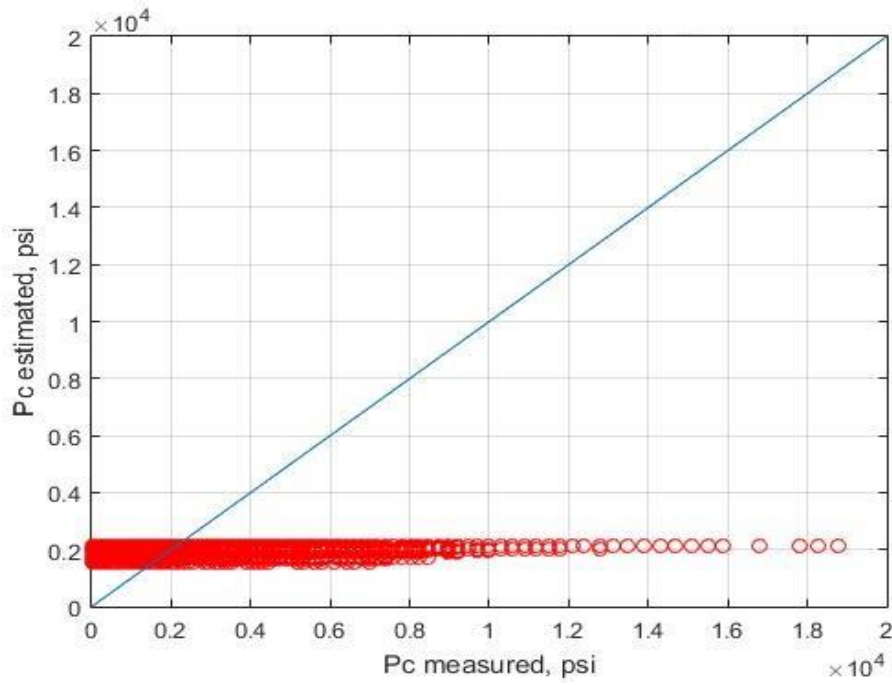


Figure 159. Predicted vs. measured values using Fuzzy Logic type-2 algorithm (Training).

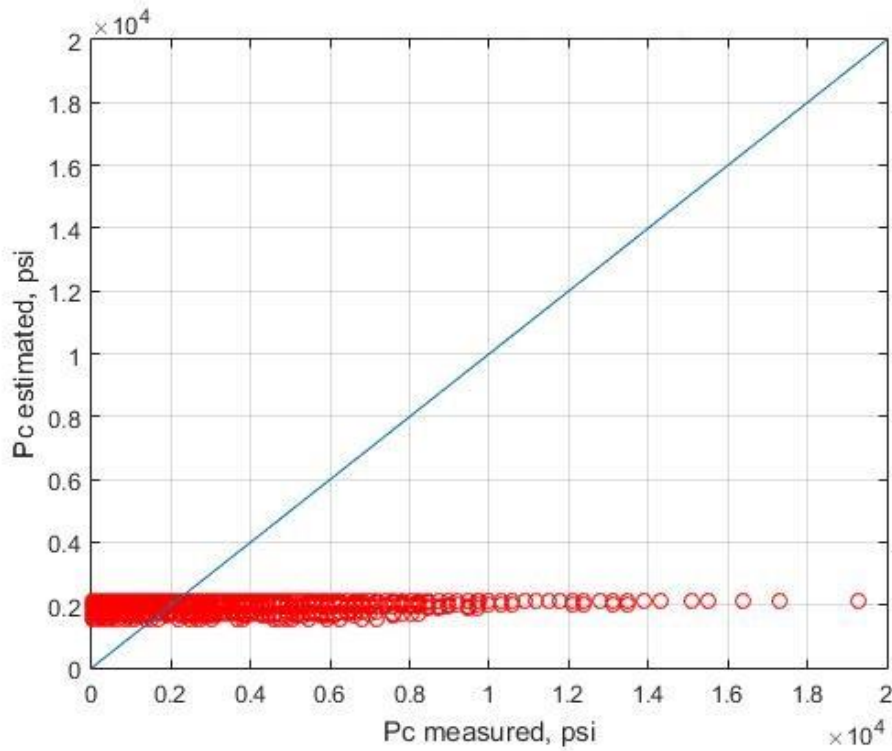


Figure 160. Predicted vs. measured values using Fuzzy Logic type-2 algorithm (Testing).

Combined modals capillary pressure curve

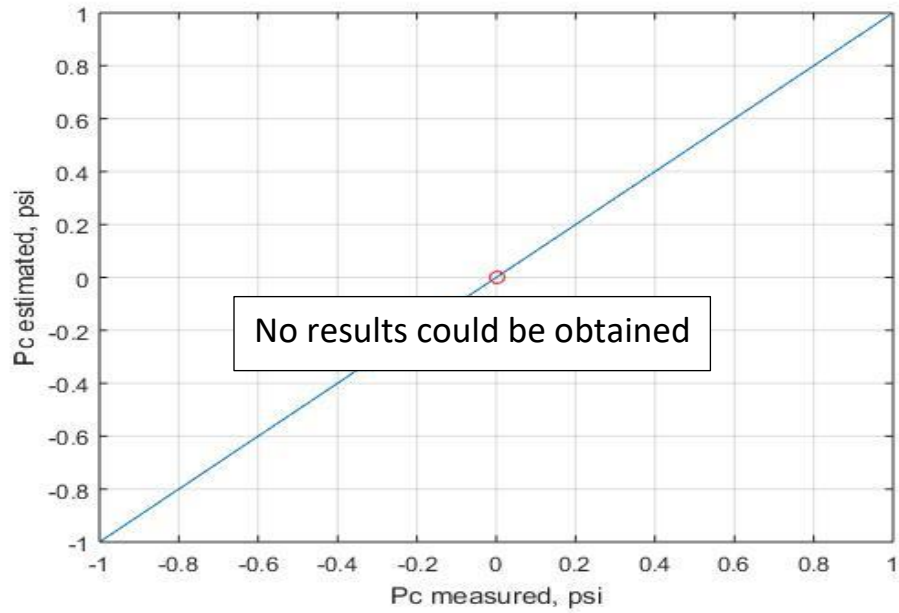


Figure 161. Predicted vs. measured values using Fuzzy Logic type-2 algorithm (Training).

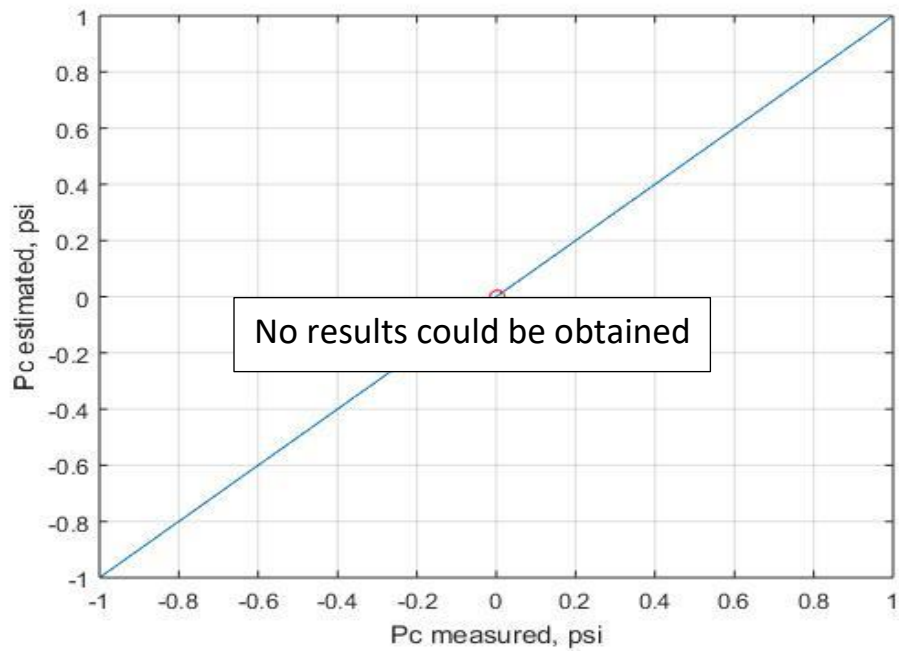


Figure 162. Predicted vs. measured values using Fuzzy Logic type-2 algorithm (Testing).

B4. Support vector machine

Uni-modal capillary pressure curve

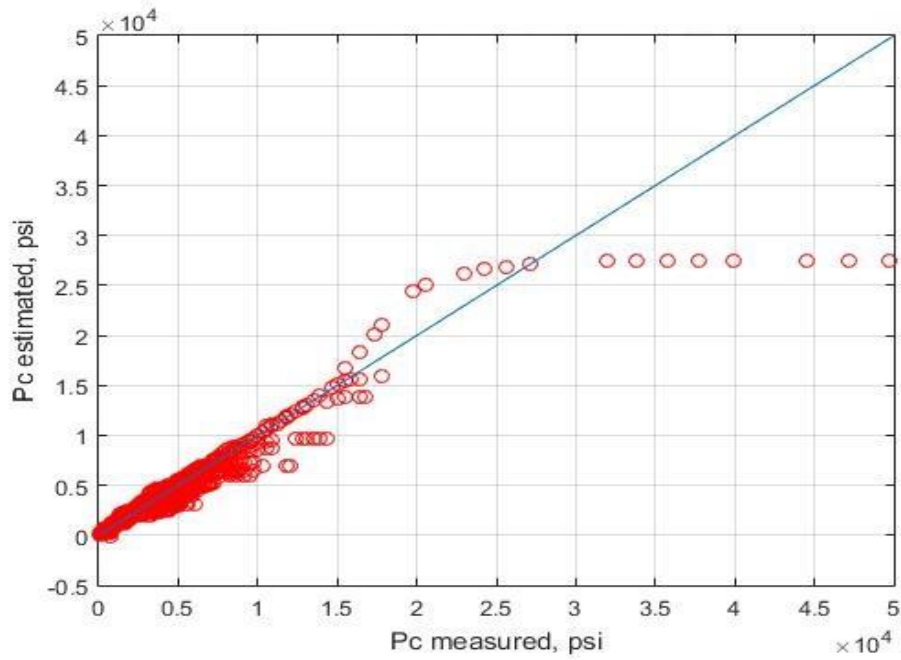


Figure 163. Predicted vs. measured values using support vector machine algorithm (Training).

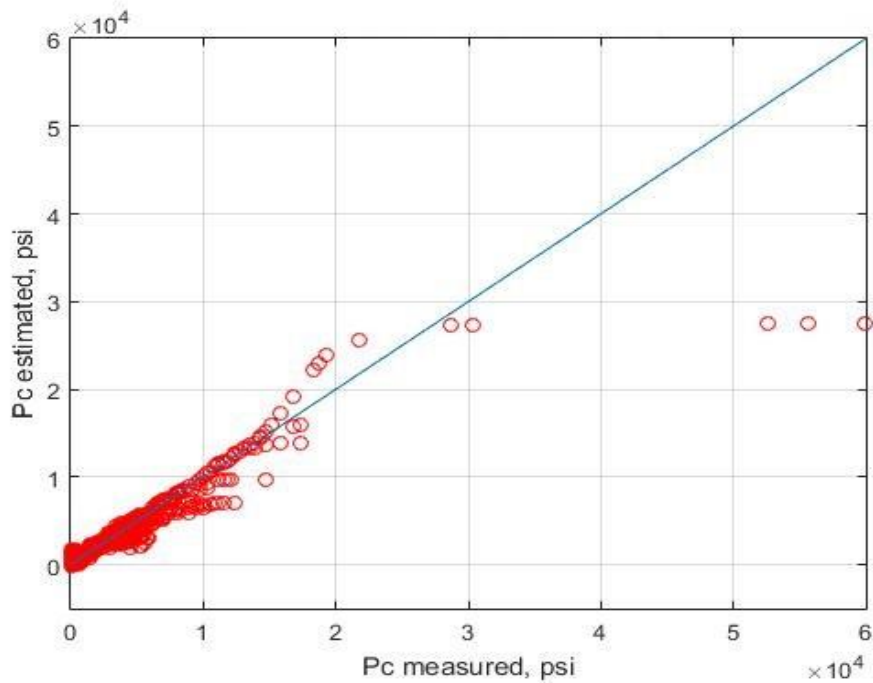


Figure 164. Predicted vs. measured values using support vector machine algorithm (Testing).

Bi-modal capillary pressure curve

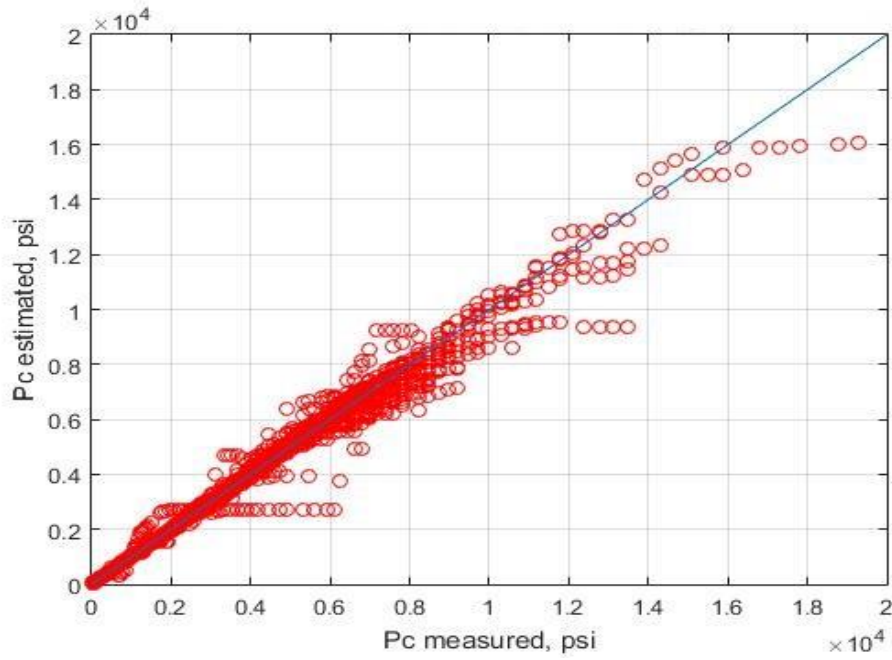


Figure 165. Predicted vs. measured values using support vector machine algorithm (Training).

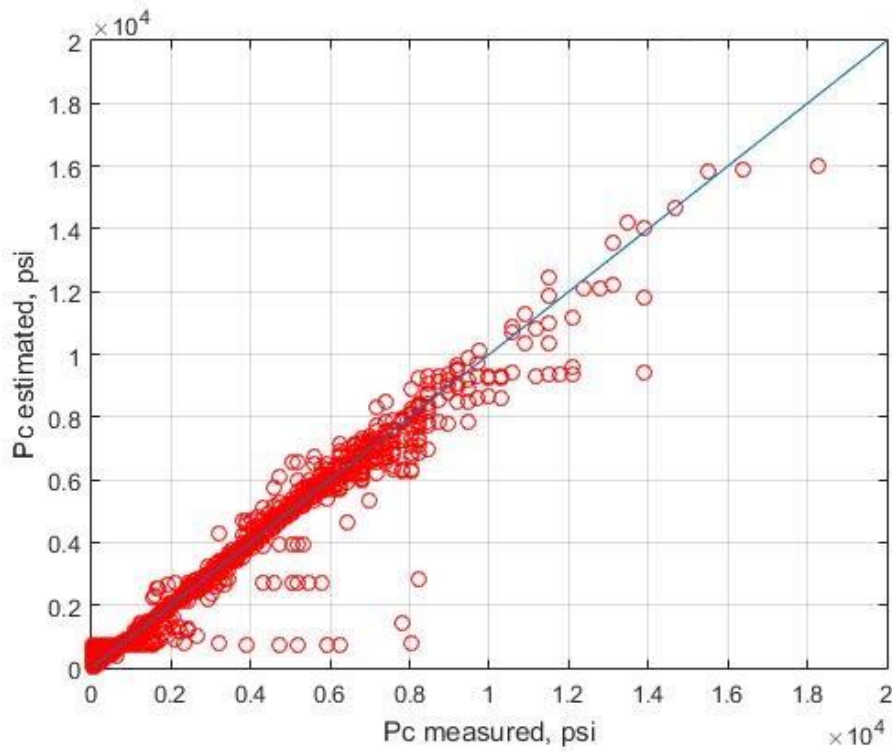


Figure 166. Predicted vs. measured values using support vector machine algorithm (Testing).

Combined modals capillary pressure curve

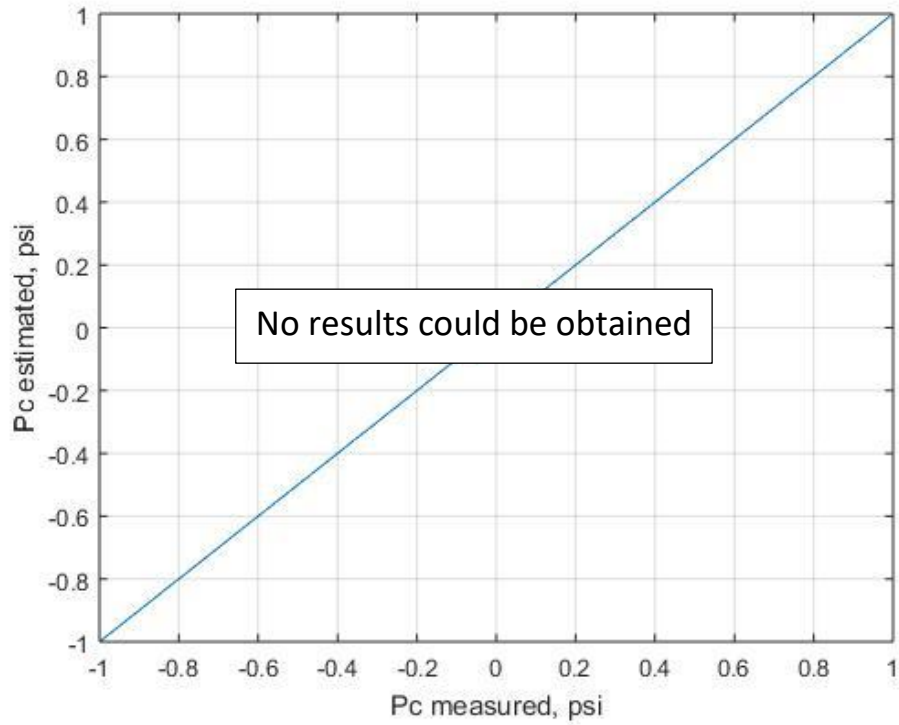


Figure 167. Predicted vs. measured values using support vector machine algorithm (Training).

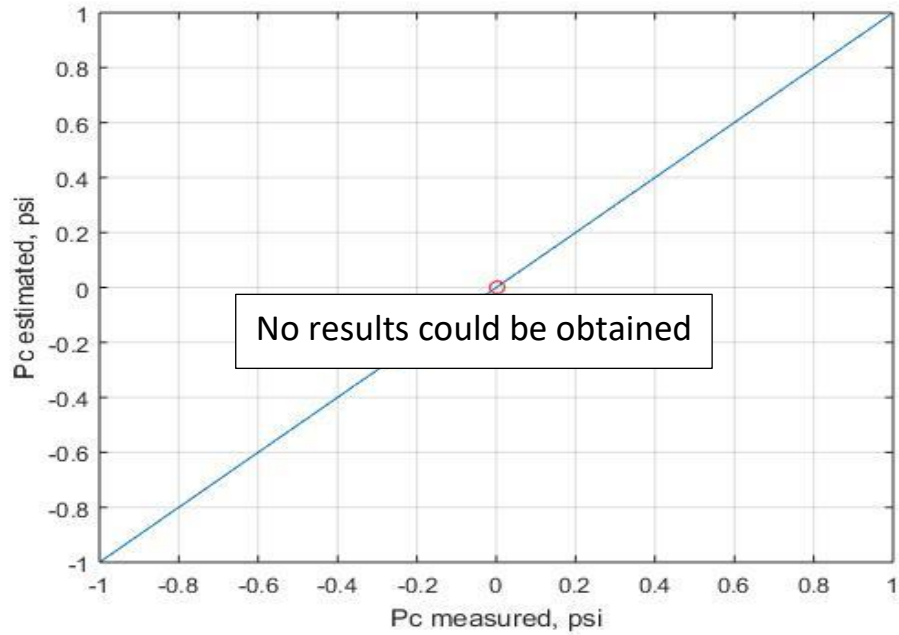


Figure 168. Predicted vs. measured values using support vector machine algorithm (Testing).

B5. Functional Network

Uni-modal capillary pressure curve

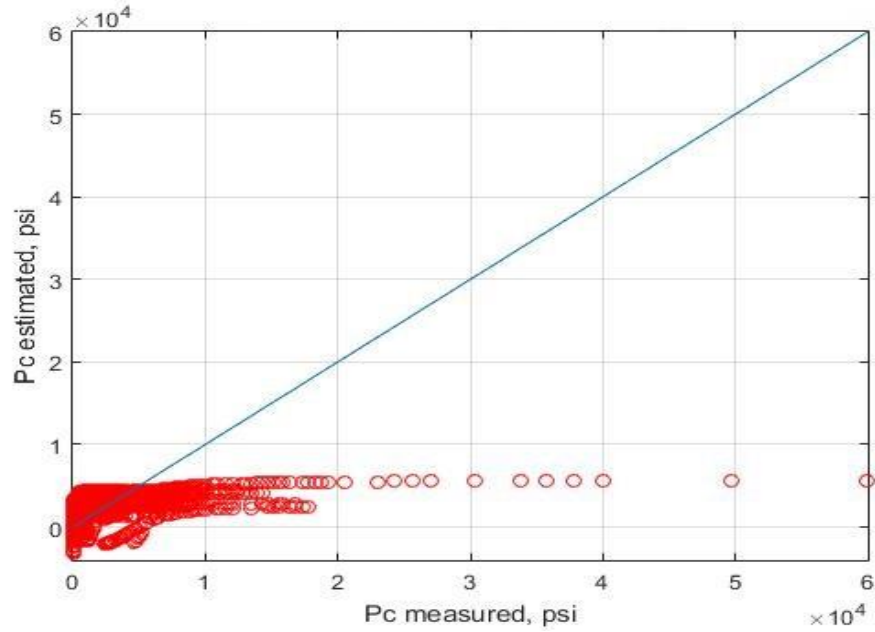


Figure 169. Predicted vs. measured values using functional network algorithm (Training).

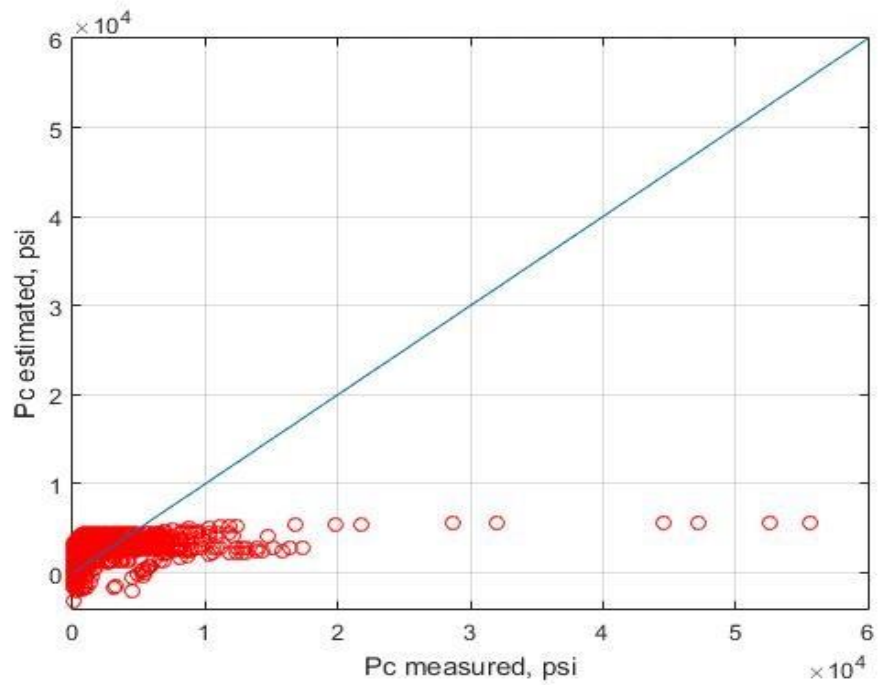


Figure 170. Predicted vs. measured values using functional network algorithm (Testing).

Bi-modal capillary pressure curve

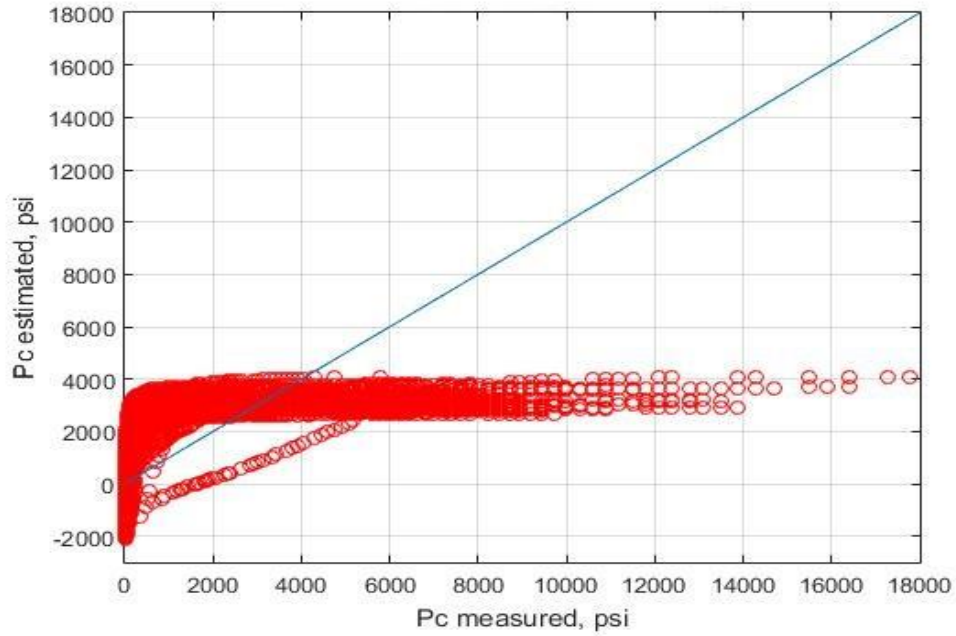


Figure 171. Predicted vs. measured values using functional network algorithm (Training).

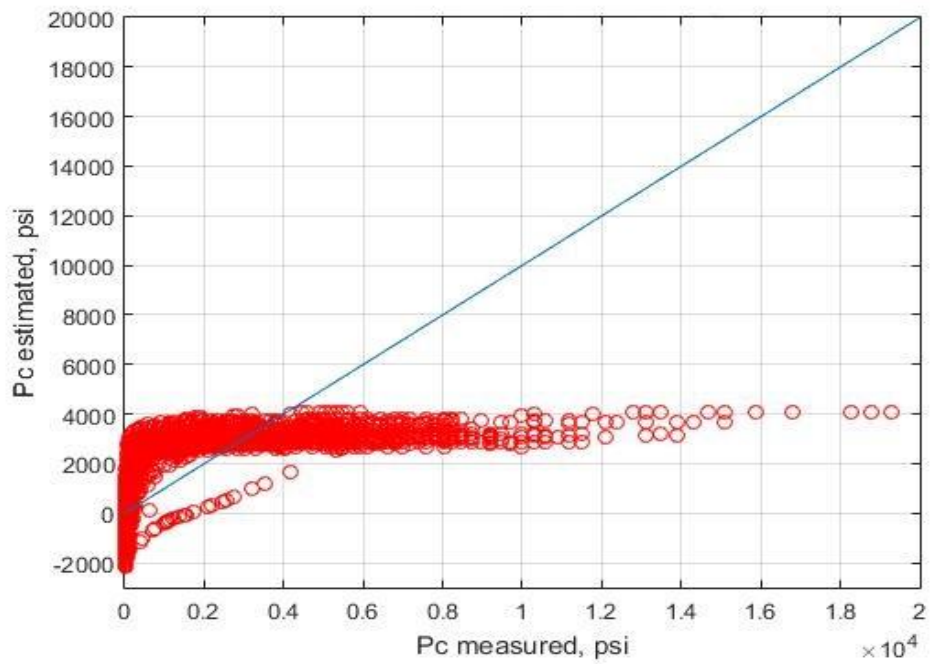


Figure 172. Predicted vs. measured values using functional network algorithm (Testing).

Combined modals capillary pressure curve

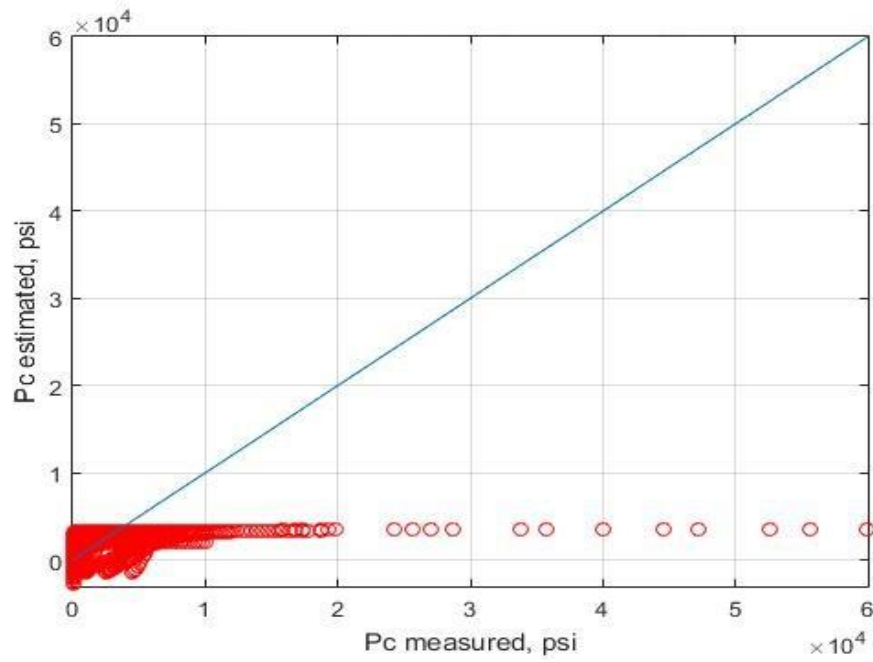


Figure 173. Predicted vs. measured values using functional network algorithm (Training).

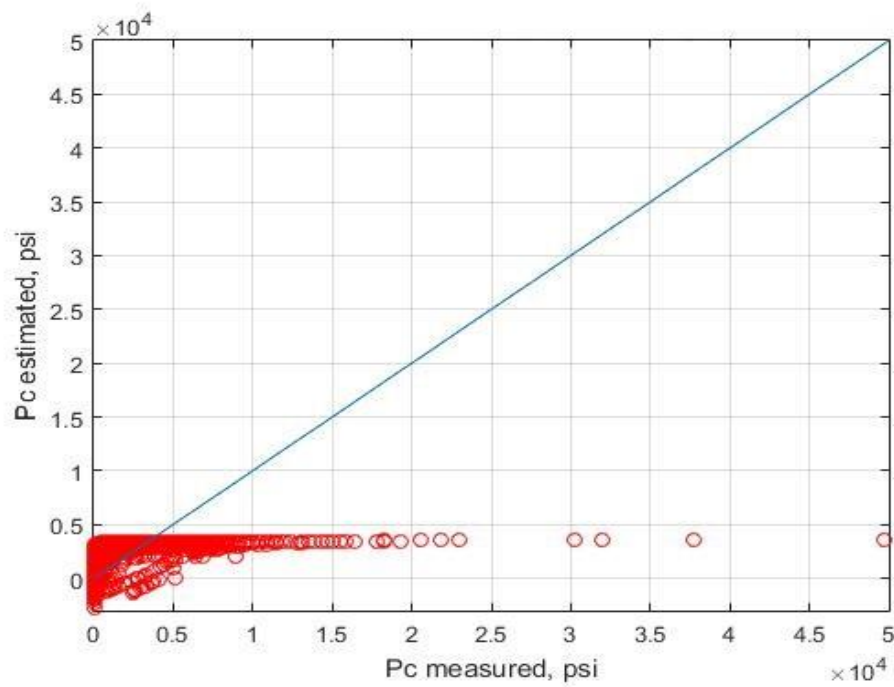


Figure 174. Predicted vs. measured values using functional network algorithm (Testing).

CURRICULUM VITAE

Name: Yasser Ridha BuSaleh

Nationality: Saudi

E-mail: yasser.busaleh@hotmail.com

Address: Post Office Box # 1084
Dhahran 31311
Eastern Province, Saudi Arabia



Education: Bachelor of Science in Petroleum Engineering, 2009
King Fahd University of Petroleum & Minerals,
Dhahran 31261, Saudi Arabia.

Master of Science in Petroleum Engineering, 2017
King Fahd University of Petroleum & Minerals
Dhahran 31261, Saudi Arabia.

Areas of Interest: Well Performance, Reservoir Engineering

Professional Affiliations: Society of Petroleum Engineers (SPE)

Experience: Nine years' experience in oil and gas focusing on reservoir management, reservoir simulation and reservoir technology and software evaluation and support. Nine years involvement and volunteering in SPE – Saudi Arabia Section. Looking for broader reservoir engineering opportunities locally and internationally, seeking to contribute to the growth of global energy and also expand my organizational, leadership and social skills.

Extra Activities: Worked as a production engineer in summer 2005 and as a production facility engineer in summer 2006. Also worked as a part time employee at Jarir bookstore while pursuing my bachelor degree in 2008.

Publications:

Author of “Prediction of Capillary Pressure for Arabian Carbonate Reservoirs using Artificial Intelligence”, MS Thesis, 2017.

Author of SPE paper titled “Capillary Pressure Prediction using Artificial Intelligence”, SPE-182173-MS.

Co-authored SPE paper titled “Assisted History Matching and Uncertainty Analysis by Geologically Consistent Sampling” SPE-182749-MS.

Co-authored SPE paper titled “Estimating Dew Point Pressure Using Artificial Intelligence” SPE-160919-MS.

Awards:

Century Club Award, SPE international

GRMD Service Award and Employee Recognition, internal award